Extraction of Electrocardiography Artefacts from Surface Electromyography Signals using Continuous Wavelet Transform

Anein Deney Simon

A thesis submitted to Auckland University of Technology
in fulfilment for the degree of Master of Engineering

March 2019

Abstract

The study of biosignals such as Electromyography (EMG) and Electrocardiography (ECG) signals is significant within the physiological and medical field for diagnosis and rehabilitation purposes. The extraction of features from these signals by analysing them can be used to understand the possibilities of health and physiological status further. The presence of ECG contamination within surface Electromyography signal (sEMG) has been a problem when analysing the muscle activity. It has been shown that ECG contamination of the EMG signal in muscles of the trunk can influence time-based (amplitude) and frequency-based measures of the EMG signal. This has important implications when interpreting the amount of muscle recruitment and the level of fatigue of trunk musculature. To date, there is little information showing the degree of contamination of the ECG when the trunk musculature is contracting at different intensities. There is no clear information regarding whether the ECG signal can be effectively extracted from the EMG to detect other physiological variables such as heart rate and heart rate variability when the trunk muscles are contracting at different intensities. The significance of the presence of ECG artefacts within sEMG signals at various levels of muscular activity is seen to be diminishing as the intensity of EMG signals increases as the activity across the muscle increases. The different levels of EMG activity are measured by monitoring the degree of Maximum Voluntary Contractions (MVIC) of the muscle.

This research involved the investigation of the ECG artefacts within sEMG signals that were obtained from the lower and upper lumbar erector spinae (ES) muscles of the back. This research involved the extraction of the ECG artefacts from sEMG signals using Continuous Wavelet Transforms (CWT) with thresholding. This technique was applied to sEMG signals obtained from the lower lumbar erector spinae muscles during different levels of static contractions, spanning from 5%-50% of Maximum Voluntary Isometric Contraction (MVIC) at 5% intervals. Surface EMG signals collected across a group of healthy participants within the age bracket of 18-35 with no previous history of back injury or surgeries within the last year.

This research explored the difference in signal properties before and after extracting the ECG signals from the sEMG signals using the CWT. The CWT provides a scalogram plot that indicates the power intensity at each scale for the extracted signal within the time domain. The CWT scalogram can be replotted to show the corresponding pseudo-

frequency-time based spectrum plot. These plots were used to provide the scale values most suitable for the ECG extraction from the sEMG signals.

Using the selected CWT scales, thresholding of these wavelet coefficients was performed prior to the reconstruction of the extracted information to diminish the presence of EMG signals within the reconstructed ECG signals. This technique was used due to the similarity in nature of EMG signals to that of white Gaussian noise. The reconstructed ECG signal is cross verified with an independent 3-lead ECG recording that was collected simultaneously from the same participant during the EMG data collection.

The significance of the ECG signal before and after extracting the ECG signal from the sEMG signal was validated using Fourier power spectrums and finding the median frequencies within the selected time segment. The ECG extraction from sEMG signals using the CWT technique with thresholding was shown to have been successful at lower percentages (5%-20% of MVIC) and was able to have extracted ECG components significantly lowering the median frequency of the EMG signal after the removal of ECG signal. The research showed results demonstrating the extraction of ECG signals from sEMG signals collected from the back muscles at low values of MVIC.

Attestation of Authorship

‘I hereby declare that this submission is my own work and that, to the best of my knowledge and belief, it contains no material previously published or written by another person nor material which to a substantial extent has been accepted for qualification of any other degree or diploma of a university or other institution of higher learning, except where due acknowledgement is made in the acknowledgements.’

Anein Deney Simon

March 2019

Acknowledgements

I wish to express my gratitude to my supervisor, Dr Jeff Kilby, for his patience, support, guidance and advice throughout this research. I also greatly appreciate the assistance given by Dr Grant Mawston from the Physical and Rehabilitation Research Centre at North Shore Campus of Auckland University of Technology for imparting professional knowledge, and information regarding muscle and heart signals.

I would like to thank my family, my parents and my brother for their support, patience and love in the process of completing this work.

Sincere thanks are also extended to helpful friends, participants, data collectors, and all staff of the School of Engineering for their kindness and encouragement during my studying period at the Auckland University of Technology.

Table of Contents

List of Figures

List of Tables

Chapter 1
Introduction

1.1 Statement of the Problem

Biomedical signals are generated by the human body in response to either a voluntary or involuntary event. These are measurable signals which are generated at the site of the respective muscle or organ, along with other forms of interference from other nearby muscles or organs. An example is biomedical signals collected from the upper and lower lumbar (back) muscles, which are likely to contain electromyography (EMG) signals from the muscular activity and interference from electrocardiography (ECG) signals from the heart [1]. The ECG signal might hamper the extraction of information from the EMG signals for monitoring and analysing muscle activity.

Extraction of useful information from biomedical signals is a significant feature in the field of health and rehabilitation research. The properties of EMG signals collected from the body in a region near the heart may have ECG signals embedded within them, which is often difficult to analyse. Due to the complexity of the interference of the individual components in the EMG signals, digital signal processing techniques can be adapted to extract and separate the EMG and ECG signals [2-4] from these signals.

Digital signal processing techniques have been used to extract useful information for quantifying the signal in the study of biomedical signals. There are limitations to the digital signal processing methods and hence, the quality of result attainable. This is mainly evident during the analysis of biomedical signals, which requires further research on these techniques.

1.2 Purpose of the Study

The overall aim of this research was focussed on separating the ECG and EMG components from biomedical signals collected from the lower lumbar erector spinae muscles of the participants at different levels of static Maximum Voluntary Isometric Contractions as a measure to the muscle activity output, applying Wavelet Transform with Thresholding to the Wavelet Coefficients. Wavelet Transform is a digital signal processing technique used for performing analysis of a signal when its frequency varies over time.

1.3 Significance of the Problem

The study of biomedical signals with digital signal-processing techniques in order to extract information and characteristics quantifying the signal is an area of research where engineering and clinical expertise overlap. The advancements in digital signal processing techniques have improved the quality of results of biomedical signals now outweighed those provided by analogue filtering of the signals.

Digital signal processing techniques provide signal filtering, which is related to theoretical parameters, as compared to analogue filtering techniques that operate within constraints of the hardware device parameters and rounding compromises. Analogue filter designs developed are based on magnitude and pulse response for ECG detection, which is required to be optimised through multiple stages while accounting for the limitations of the design [5]. Digital signal processing also provides the advantage of analysing the signal at different stages of implementations of the technique or algorithms, providing a better view of quantifying and truncating any possible errors, and providing efficient information extraction [6].

There has been limited research that has focussed on the extraction of the ECG signals and EMG signals from biomedical signals, or the filtering of either component. These researches have concentrated primarily on signals that have been collected close to the heart in case of ECG, with minor EMG artefacts [3, 7-10]. Other researchers have used EMG signals collected from muscles and have simulated or added ECG components to these signals, to study the effectiveness of the signal-processing techniques in extracting the ECG from the EMG component [1, 11, 12]. This research primarily focusses on the ability and quality of the ECG extraction from the biomedical signals, collected at different levels of maximum voluntary static contraction.

1.4 Structure of the Thesis

The general background of the thesis is structured in accordance with the research and its purpose described in chapter 1. Chapter 2 presents the literature review that describes the background information associated with the muscles, its structure and information related to ECG and EMG signals. This chapter also gives a brief overview of the recent developments associated with the extraction of either component and the techniques using signal-processing and analysis of ECG and EMG signals. Chapter 3 provides a brief theoretical overview of the Continuous Wavelet Analysis and Thresholding applied to the

Wavelet Coefficients used in this research, along with the software development related to these techniques. Chapter 4 presents the data acquisition, along with an overview of the protocols, equipment and the procedures implemented for the collection of the biomedical signals used for this research. The results of the research obtained from the implementation of the Continuous Wavelet Transform with Thresholding on the acquired signals using the developed program are presented in Chapter 5. Chapter 6 presents the conclusion and recommendations for future work related to this research.

Chapter 2
Literature Review

2.1 Introduction

This chapter presents the history and relevant literature related to this research for biosignals such as Electromyography (EMG) and Electrocardiography (ECG) signals, these signals are used in the study of muscular and cardiac activities respectively. Biosignals means a collective electrical signal that is acquired from an organ that represents a physical variable of interest [13]. This signal is usually a function of time and is describable in terms of its amplitude, frequency and phase [13].

Emil du Bois-Reymond in 1849 proposed the possibility of being able to record electrical activity during any form of voluntary activity [14]. However, it was in 1890 that the first recording of the activity was made by Marey, who also termed this activity as electrogram [15]. It was in 1922 that Gasser and Erlanger were able to present electromyography in the form of electrical signals using an oscilloscope, and the research involving these electrical signals has been a vital focus of study within the biomedical area of research [16].

The first electrocardiogram was recorded by Willem Eindhoven, using a string galvanometer that he invented in 1903 [17]. Advancements have followed this discovery detailing the electrical response and the nature of the activity of the heart muscles to identify and diagnose physiological conditions and responses to both medical and physiotherapy procedures.

2.2 Literature Search

An extensive literature search was carried out to find relevant information and resources related to 'electrocardiography' and 'electromyography'. When using the word electrocardiography, other search terms such as 'ECG' and 'QRS' were used. The term QRS was included as it is the primary component of the ECG signal that distinguishes the ECG signal from EMG signals. For information relating to electromyography, the other search term used was 'EMG'.

The search terms used for obtaining the information for the research on digital signal processing were 'wavelet' and 'thresholding'. These terms were used to collect any information detailing these techniques being applied to ECG and EMG signals or other biomedical signals within the signal extraction context.

The literature search comprised of journal articles related to information using the key terms mentioned above and was focused on the articles dated from 2007 and later. This ensured that the information obtained during the research was contemporary. The literature review consisted of 12 articles involving the study of various techniques for the separation of ECG and EMG signals. These articles were limited to sEMG signals obtained from healthy individuals and any research studying a particular medical condition, or physical ailments were excluded. The resources used for the literature search were obtained from peer-reviewed literature databases such as ScienceDirect, Scopus and IEEE, and were accessed through the Auckland University of Technology library website.

The following section in this chapter discusses the background of muscle structure and signals relevant to this research.

2.3 Muscles, Electromyography and Electrocardiography

The muscular system enables the voluntary and involuntary functions and/or movement of the human body. Muscular contractions facilitating these mechanisms has been a primary focus of research and development within the biomedical sector today. This section focusses on the striated muscles found within the human body that generate the ECG and EMG biomedical signals.

2.3.1 Muscle Classification

The muscles within the human body are classified based on their structure and are primarily classified as striated muscles and non-striated muscles. Striated muscles are mainly responsible for the voluntary movement functions of the body except for cardiac muscles that are involuntary. Non-striated muscles are responsible for the involuntary movement functions within the body.

2.3.2 Striated Muscles

Striated muscles are cylindrical multinucleated cells consisting of cylindrical structures known as myofibrils. The myofibrils are composed of myofilaments that are thick and thin filaments of protein such as actin, myosin and titin, shown in Figure 2-1 [18]. The myofibrils are bundled and maintained within the parallel structure by sarcomeres, which are the functional units responsible for maintaining the muscle structure in striated muscles [18].

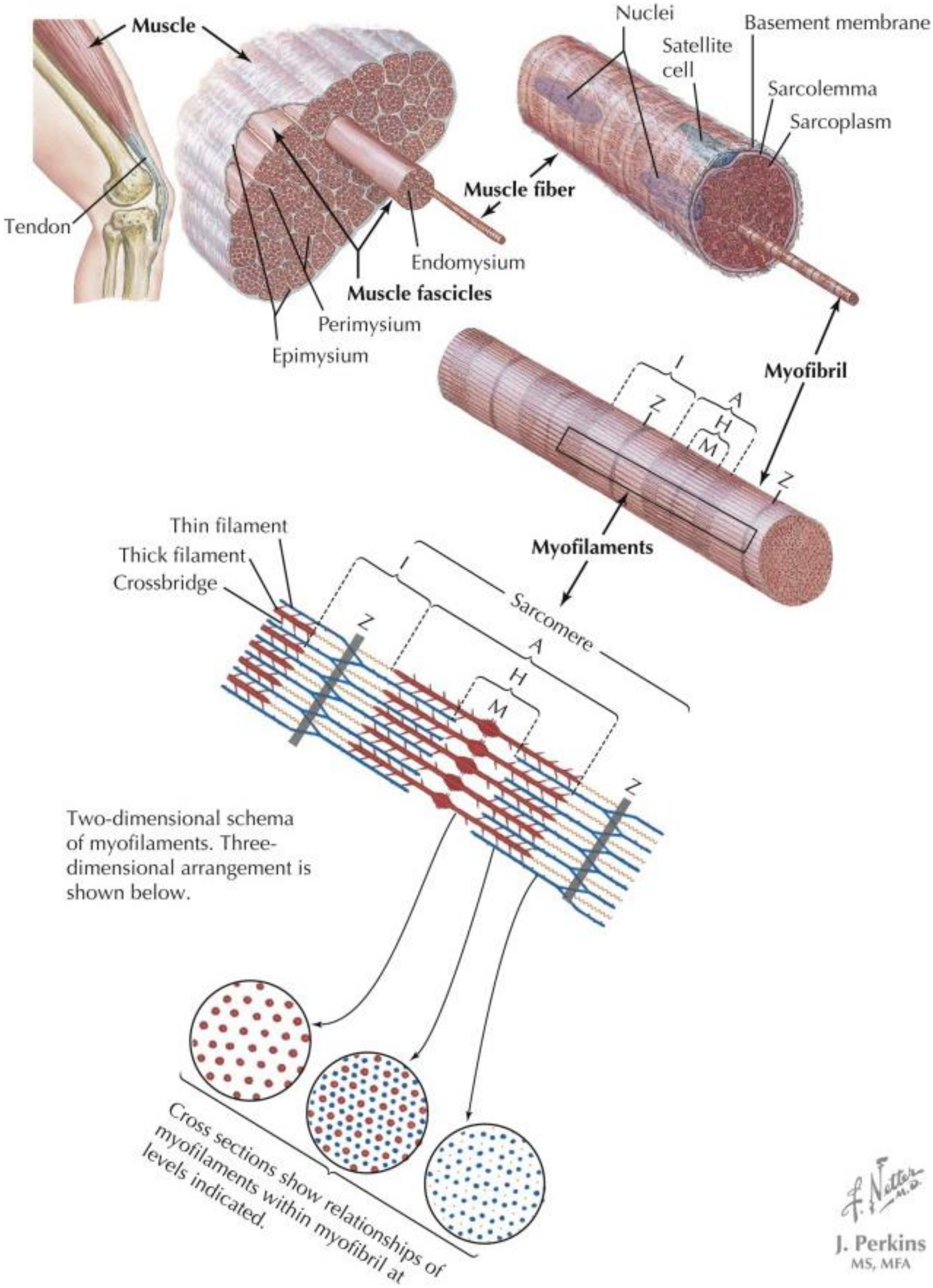

Figure 2-1: Structure of the Skeletal Muscle [18]

The sarcomere shows overlapping arrays of thick and thin filaments. The thin filaments are anchored perpendicularly to the Z lines, which are located on the two sides of the longitudinal axis of the sarcomere [19]. The thick filaments, with the myosin heads toward the Z lines, arise from both sides of a perpendicular line, named M line, at the centre of the sarcomere [19]. During contraction, the myosin heads form cross-bridges with actins and pull the thin filaments toward the M line [19]. Such an arrangement of the thick filaments is known as bipolar geometry, shown in Figure 2-2 [19].

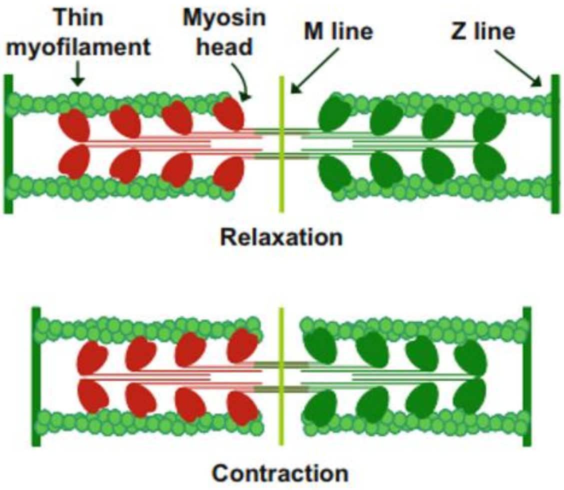

Figure 2-2: Bipolar geometry structure of striated muscles, when they are in (a) state of relaxation and (b) state of contraction (bottom) [19].

The contraction of striated muscles in response to neural impulses has been a focus of study to observe the EMG signals. Striated muscles are classified into skeletal muscles, which facilitate the voluntary movements of the human body and the cardiac muscles that facilitate the functioning of the heart.

Skeletal muscles are attached to the human skeleton and are responsible for the reflexive. postural and voluntary responses of the human body. The skeletal muscles are comprised of a number of motor units (a motor neuron and all the muscle fibres it innervates). A motor neuron sends electrical signals (action potentials) to the neuromuscular junction that, will, in turn, induce impulses to muscles, to initiate the contraction of the muscle cells to facilitate the voluntary movement or response. The motor neurons attached to the muscles are the primary factors that control the force produced by a muscle. The bioelectrical signals generated at the skeletal muscles by the muscle cells during skeletal muscle contraction can be detected using electromyography signals.

Cardiac muscles are striated in structure. Unlike skeletal muscles, they are involuntary in their functional behaviour]. The functioning of the cardiac muscles (heartbeat) during the circulation of blood is controlled by the autonomic nervous system via the sinoatrial node. The human heart has four chambers consisting of cardiac muscles that facilitate the functioning of the heart. The contraction of the cardiac muscles makes the heart circulate blood throughout the body. The bioelectrical signals generated in the heart is the response to the cardiac muscle activity are referred to as electrocardiography signals that represent electrical signal transmission across the atria (P-wave) and ventricles (QRS complex and T wave).

2.3.3 Non-Striated Muscles

Non-striated muscles (commonly known as smooth muscles) are made of thin and thick filaments. The thin filaments of non-striated muscles are made of actin monomer double helixes, and the thick filaments of non-striated muscles are made of type 2 myosin that can interact with the actin and hydrolyse adenosine triphosphate (ATP) for muscle contraction.

In smooth muscle, thin and thick filaments are arranged less orderly, so there is no clear appearance of the existence of sarcomere [19]. The myosin heads of the smooth muscle on one side of the thick filament face in one direction with myosin heads on the opposite side facing in the opposite direction [19]. Such an arrangement, termed side polar geometry, would enable a thin filament to slide unimpeded along a thick filament "side" until the end of the thin filament is reached, shown in Figure 2-3 [19].

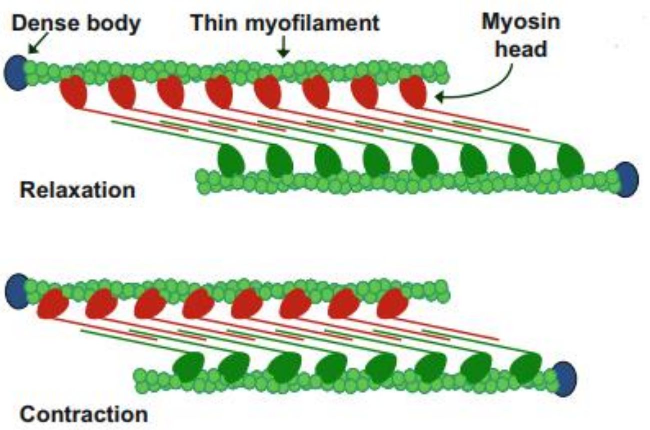

Figure 2-3: Polar geometry structure of non-striated muscles or smooth muscles, when they are in (a) state of relaxation (top) and (b) state of contraction (bottom) [19].

The non-striated muscles are mainly in the vascular walls of the blood vessels, gastrointestinal tract and airways. These vascular smooth muscles are responsible for the circulation of blood within the human body by muscular contractions, and they are a significant influencer of the blood pressure.

2.3.4 Electromyography

Electromyography studies signals that measure the electrical current generated in muscles during contraction [13]. Electromyography provides information on the muscle activity and can be classified into two types (Surface EMG and fine-wire EMG), based on the type of electrode and procedure followed for the extraction of the EMG signals [20]. Surface electromyography (sEMG) signals are collected using surface electrodes placed on the skin and can provide the EMG signal from a collection of muscle fibres (motor units) within the muscle below the site of electrode placement [20]. On the other hand, fine-wire or intramuscular, EMG detects the electrical signal of the muscle fibres of motor units located close to the end of a wire(s) inserted into the muscle [20].

Skeletal muscle signals typically contain electrical activity from multiple motor units that are responsible for the contraction of the muscle shown in Figure 2-4 [18]. The electrical response of a combination of these motor units known as compound motor action potentials (CMAP's) that are collectively attained by the surface electrodes to be recorded as sEMG [20].

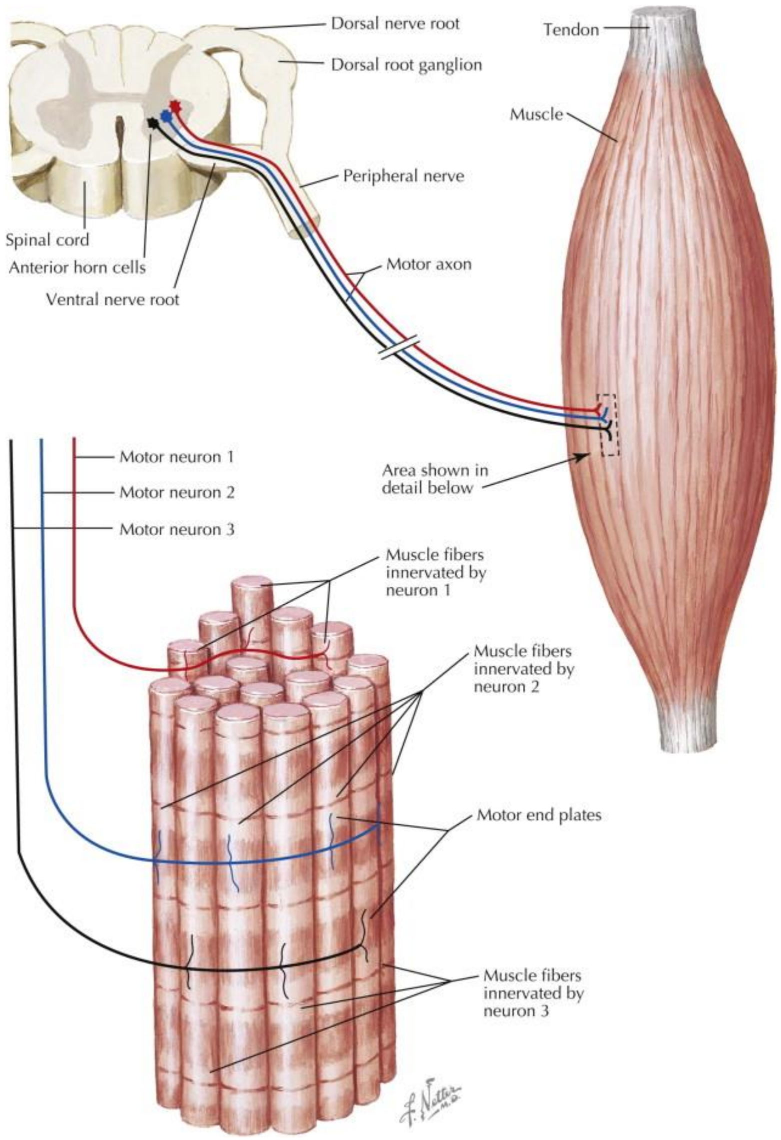

Figure 2-4: Motor Unit consisting of a single motor neuron and the muscle fibres it innervates [18]

The surface electromyography signals emitted by the muscles are weak, ranging from 0.1 to 5 mV with a frequency spectrum of 0 to 1000 Hz [18, 20]. The frequency band of the EMG signals is primarily within the 10 ~ 500 Hz range, with 50 ~ 150 Hz being the dominant frequency band of the EMG power spectrum [20]. The individual motor unit action potentials (MUAPs) that collectively comprise the recorded sEMG signal vary within the frequency spectrum [20].

The sEMG signal provides information of the muscular activity but also contains other artefacts that are obtained from the skin and subcutaneous tissues, electrical noise and movement artefact, and in the trunk, electrical activity of the heart [21].

The frequency components of the electromyography signal generated by the muscles have been used to study the fatigue of muscles, and both amplitude and frequency analysis can be used to detect muscular response during different intensities of muscular contractions [10, 22]. For example, patients with chronic low back pain show lower activation levels of lumbar back muscles when compared to those with no low back pain. This patient groups also exhibit altered patterns of back muscle fatigue when compared to healthy subjects. The MUAPs extracted from the electromyography signals may be used for classifying neuromuscular disorders and diseases. For example, the dominant MUAPs from the EMG signal has been analysed using signal processing and disease classifying techniques to identify and analyse neuromuscular disorders [23]. Neuropathy and myopathy are common neuromuscular disorders that have been previously researched based on information extracted from the EMG signals [24, 25].

The study of electromyography signals has been integrated into movement control of artificial or robotic and prosthetic body parts [26-28]. The MUAPs pertaining to a single motor unit or the collecting MUAPs for multiple motor units have been a focus of study to decode and recreate the function or movement. The EMG signals are used to identify the dominant MUAP to recognise the muscular movement or contraction that is required to be induced, as well as the underlying responses of other body parts or systems associated with it.

2.3.5 Electrocardiography

Electrocardiography studies signal that measure of the bioelectrical properties generated by the heart during cardiac muscle contraction, while it circulates the blood throughout the body. These contraction cycles classified as beats are triggered by electrical impulses from the sinoatrial node. The signals pertaining to the activation of the cardiac muscles are described as ECG signals. ECG signals are important in diagnosis, as they comprise vital information relating to arrhythmias, ischemia, and myocardial infarction.

The most common ECG recording procedure involves the use of 12 electrode leads consisting of three bipolar limb leads (I, II and III), 3 augmented limb leads (aVR, aVL, and aVF), and 6 chest leads (V_1 to V_6), shown in Figure 2-5.

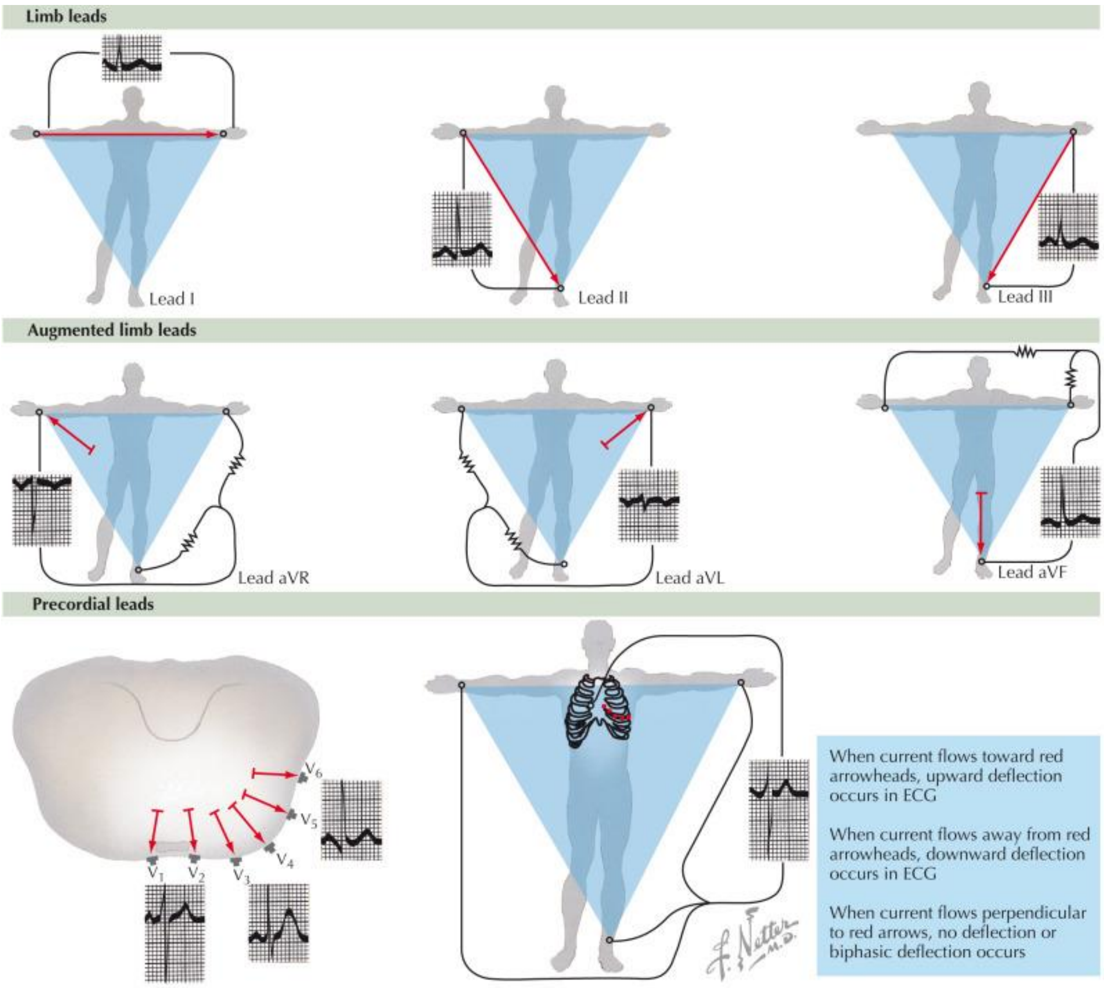

Figure 2-5: ECG signal and electrode placement [29]

The placement of these electrode leads defines the structure of the ECG signal. The chest leads provide the surface ECG signals which are referenced close to the heart. Therefore the placement and spacing of these electrodes on the torso influences the structure of the recorded ECG signal [29]. ECG signals can be decomposed as waves, segments or intervals. Waves are the characteristic points of the ECG signal that can be defined as deviations from the isoelectric line, i.e. having or involving no net electric charge or difference in electrical potential. These points are named successfully P, Q, R, S, T, U. Segments are the isoelectric line periods between waves. Intervals are the period between characteristic points of waves.

2.3.5.1 Waves

The waves present in the ECG signal relate to the underlying action potentials of various cardiac tissues during polarisation and depolarisation [29]. The waves are denoted by the letters P, Q, R, S, and T were assigned by Willem Eindhoven [17]. The cardiac activity triggered by the depolarisation of the sinus node is minuscule, so it does not significantly affect the ECG signal recorded from the skin surface by clinically-used ECG machines [29, 30], shown in Figure 2-6 are:

- P wave is the current generated by the sequential depolarisation of the atrial cells of the right and left atria.
- Q wave represents the first downward deflection of the ventricular depolarisation.
- R wave represents the first upward deflection of the ventricular depolarisation.
- S wave the second downward deflection of the ventricular depolarisation.
- T wave represents the ventricular repolarisation following the depolarisation during the QRS complex.
- U wave represents a small upward deflection following the T wave. The exact reason for the U wave is still uncertain and is seldom visible in ECG.

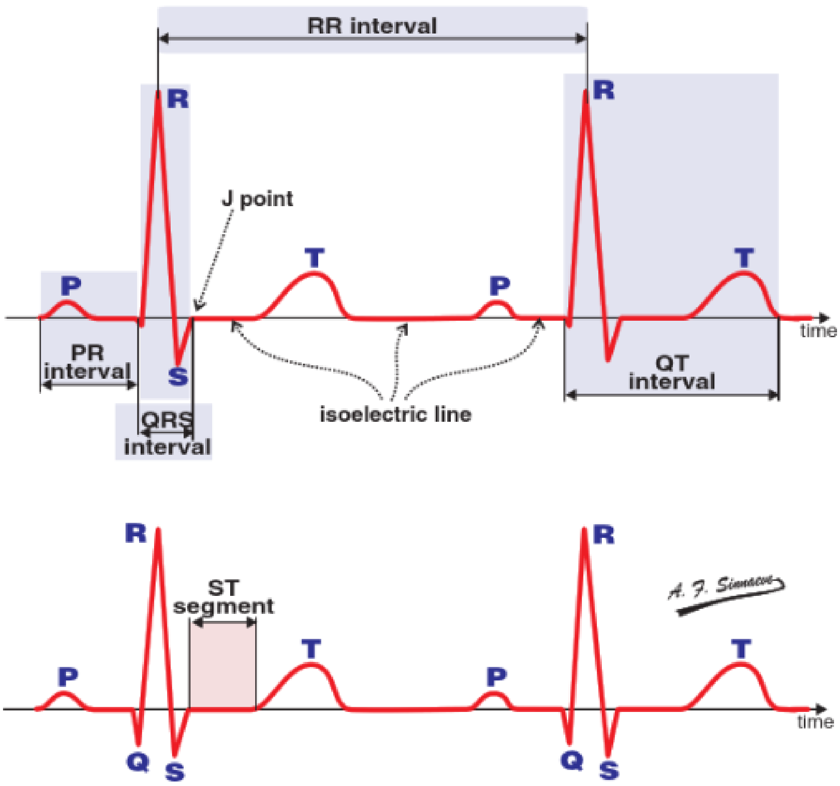

Figure 2-6: Characteristic points, Intervals and Segments of an ECG signal [30].

2.3.5.2 Segments

The segments are periods between waves within the ECG signal in the heart are isoelectric shown in Figure 2-6. The most commonly documented segment is the S-T segment, which represents the period between the S wave and the T wave during which the atria are relaxed, and the ventricles are contracted. However, there is no electrical activity recorded during this period. The length of the ST segment is inversely affected by the heart rate [30]. Intervals

The intervals within the ECG signals denotes the period between the characteristic points of the signal, including the waves and any complexes, shown in Figure 2-6 are:

- PR interval lies between the onset of the P wave and the onset of the Q wave. The PR interval denotes the time taken for the cardiac impulse from the sinus node and the right atrium to the ventricles.
- RR interval denotes the period between the peaks of consecutive R waves. The RR interval is commonly used for the computation of the heart rate.
- QRS complex denotes the period of ventricular depolarisation. The QRS complex lies between the onset of the Q wave and the end of the S wave. The QRS complex is the most dominant feature within the ECG signal, due to the larger muscle mass of the ventricles in comparison to the atria.
- QT interval denotes the period between the depolarisation and repolarisation of the ventricles. The QT interval lies between the onset of the Q wave and the end of the T wave.

2.4 Back Muscle Anatomy

The back muscles are vital to maintaining the posture of the human body and can be defined as the muscles on the posterior part of the trunk extending from the neck to the pelvis [31]. The major group of back muscles are the back extensors and consist of the upper and lower erector spinae and multifidus. The back muscles provide support to the spine by being attached to the ribs, vertebrae and their lateral and posterior processes [31, 32]. The back muscles are divided into two groups:

1. Extrinsic muscles assist with the movement of the limbs and respiration [32].
2. Intrinsic muscles assist with the movement of the spine and posture maintenance [32].

2.4.1 Erector Spinae Muscles

The erector spinae muscles are the largest group of back muscles. They are responsible for maintaining posture, extending the spine (or resisting flexion), and laterally bending the spine [33]. They are the most active trunk muscle during functional activities involving manual handling (lifting and lowering). These muscles are the area of interest related to the collection of the biosignals used for this research, shown in Figure 2-7.

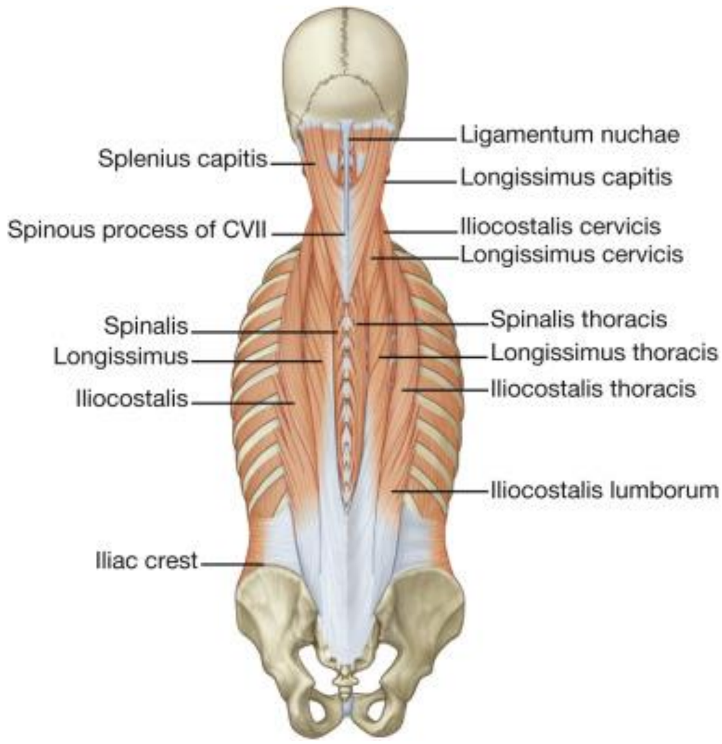

Figure 2-7: Erector spinae muscles [33]

The upper erector spinae consists of the upper fibres of longissimus and iliocostalis lumborum, which originate from the thoracic transverse processes and lower seven ribs and form an aponeurosis that attaches to the posterior pelvis and sacrum (MacIntosh). Fibres tend to run parallel to the spine and SEMG of this muscle is typically recorded approximately 4-5 cm from the spinous process of T9 [34]. The lower erector spinae consists of the fascicles of longissimus thoracis and iliocostalis, and EMG data is typically recorded from electrodes located three cm lateral to the L3 spinous process [34]. Further detail information of the erector spinae group of back muscles is found in Appendix A of this thesis.

2.5 Review of Recent Signal Processing Developments

The extraction of ECG artefacts from EMG signals focuses on the signal acquisition procedures, surface electrodes, muscle activity and signal processing techniques. This research focuses on the use of Continuous Wavelet Transform (CWT) for the extraction of ECG artefacts from EMG signals. This section discusses the recent research and developments of using the CWT technique for extraction of ECG features from the EMG signal.

The research surrounding the extraction of ECG or EMG signals from sEMG signals focusses on an array of processing techniques. Hashim et al. [3] have developed techniques for cancelling EMG artefacts from ECG signals by using modified normalized least mean square (NLMS) adaptive filters proving successful in mitigating the EMG artefacts of the ECG signal. The implementation of least mean square (LMS) adaptive filtering on sEMG signals collected from the back muscles has been developed by Yaohang et al. [1] to remove the ECG contamination from the sEMG signals from the right lower erector spinae muscle contraction of a single subject. This research has also incorporated an adaptive powerline interference canceller alongside the LMS filter. The ECG signal from the chest was used as a reference in the filter design for the extraction of the ECG contamination [1].

Taelman et al. [35] applied the concept of wavelet transform and Independent Component Analysis (ICA) on sEMG signals of shoulder muscles combining both these procedures, to overcome the overlapping frequency spectrum and lack of redundancy in a number of channels. The results of this research were successful in eliminating the ECG contamination within the sEMG signal at lower levels of muscle activity. However, during this research it was concluded when using raw ECG signal as raw data for the wavelet Independent Component Analysis (wICA), the results outperformed the results obtained without the inclusion of the ECG as raw data [35]. The use of ICA with complex discrete wavelet transform (CDWT) was proposed by Horihata et al. [36]. This research also attempted the separation of ECG and EMG components from the biosignals analysed. The research concluded that the proposed technique of produced excellent results that satisfied the objective of separating the ECG and EMG signals [36].

The procedure of combining discrete wavelet transforms (DWT), and ICA for removal of ECG signals from sEMG signals extracted from the thoracic back muscles was undertaken by Nougarou et al. [11]. This research applied a combination of these procedures to localize and cancel the ECG within the sEMG signals. It involved the use of the DWT and ICA for the localization of ECG and the cancellation of this ECG signal, based on the electrode signals and the estimated cardiac pulses position. The results concluded that it was able to provide better results in terms of relative error and coherence mean, compared to simulated methods aimed at direct cancellation of the ECG signal [11].

The research done by Smital et al. [37] focusing on the reduction of EMG in ECG signals using adaptive wavelet wiener filtering was implemented using an artificial noise generated to the ECG signal. The noise for the research was generated using white Gaussian noise with the power spectrum being modified to that of EMG signals. This research had concluded that the parameters of the technique for decomposition, filtering and thresholding were vital to improving the results [37].

Chaudhary et al. [38] compared the different wavelets for discrete wavelet transforms (DWT) and the impact of different thresholding methods that would be most effective for de-noising ECG signal. The research compared the effect of ten different wavelets on de-noising ECG in case of powerline interference, baseline drift and EMG noise. The five thresholding methods of hard, soft, semi-soft, Stein and level-dependent threshold estimator based on neighbouring coefficients were applied to the coefficients obtained from the DWT process. This research concluded that the various thresholding techniques were successful in improving the results obtained from the de-noising procedure. The research also found that to denoise EMG signal from ECG signals, semi-soft thresholding is the most effective [38].

The detection of the QRS component has been significant towards ECG denoising and extraction of ECG information. Zhou et al. [9] developed an adaptive threshold algorithm based on wavelets for QRS detection. This research implements the de-noising of the ECG signal from powerline interference, baseline drift and EMG noise prior to the detection of the QRS interval. Zhou used DWT for the decomposition of the signal and applied the thresholding technique to the coefficients for the de-noising of the signal prior to reconstructing the signal for QRS detection. Zhou et al. [9] concluded that there was a significant margin of difference in the signal de-noising quality comparing the hard, soft and adaptive thresholding methods with adaptive thresholding producing far better de-noising results.

The research on the method of ECG de-noising based on improved wavelet packet by Gang et al. [39] followed a similar scheme of de-noising the ECG signal as Zhou et al. [9]. However, Gang et al. [39] focused on decomposing the collected ECG signal using a Dyadic wavelet packet algorithm rather than DWT. The research involved combining the wavelet packet to remove artefacts within the lower frequency range and the thresholding technique to remove the higher frequency noise artefacts. It was concluded that the wavelet transforms have a filtering range in terms of frequency similar to digital filters; however, it proves to be a better ECG de-noising tool within both the time and frequency domain due to the delay of the digital filters. The research also concluded that the implementation of the thresholding with the wavelet packet functions provided better results in terms of removal of the EMG interference within the ECG signals [39].

Verma et al. [8] used the thresholding function conjointly with wavelet decomposition and empirical mode decomposition for de-noising ECG signal. Soft thresholding was used for the filtering purpose that was optimised for minimum distortion by minimising the consecutive mean-square error (CMSE) criterion. This research produced better results in terms of de-noising the ECG signal in comparison to the EMD-based filtering method [8].

The extraction of ECG signals from EMG signals follow the removal of signal components. The reviewed research primarily focuses on the separation of the ECG or EMG signals from sEMG signals collected during minimal activation of the muscles. The signals used during these researches follow a similar pattern of having a dominant element of either the EMG or ECG signal that is sought to be the objective of their study. Investigations involving the use of simulated signals during the examination of signal separation techniques for the extraction of the ECG and EMG signals were also reviewed. The use of simulated signals in these researches involve the generation of signals based on parameters or functions set by the researcher and lacks the implementation of the signal processing techniques proposed on real-world signals and assessing its effectiveness on these signals. The researches reviewed as part of the literature review had provided satisfactory outcomes confirming their conclusions to the studied signal processing technique.

2.6 Objectives and Methodology

This research focused on the extraction of the ECG and EMG signals using sEMG signals collected from the lower and upper erector spinae muscles of the back. The research used the digital signal processing application of continuous wavelet transform, along with thresholding to extract the ECG signal component.

EMG signals, along with ECG signals, were collected from healthy individuals aged between 18 and 35 years of age with no back or neuromuscular injuries. Bipolar surface electrodes (Nortrode) were placed on the skin surface superficial to the right upper erector spinae (5 cm lateral to the T9 spinous process) and lower erector spinae (approximately 3 cm lateral to the L3 spinous process). Surface EMG signals were amplified (×500) and band-pass filtered (10-500 Hz) at collected at a sample rate of 1500 Hz. The participants were required to undergo a Maximum Voluntary Isometric Contraction (MVIC) and different levels of contractions, for the data collection used in this research.

The extraction of the ECG artefacts from the sEMG signals for this research used a new signal processing algorithm developed using MATLAB, which utilized the continuous wavelet transform function. The Continuous Wavelet transform used the Morlet mother wavelet to produce a scalogram to show the scales of the wavelet in the time domain with the intensity of the signal generated by the analysis. This information provided a suitable foundation for the selection of the scales and the fine-tuning of the scale parameters for the extraction of the ECG. The thresholding function is applied to the coefficients obtained from the wavelet transform prior to reconstruction to limit the higher frequency components that have a very low or insignificant presence in terms of amplitude within the whole frequency band analysed. These results were compared with the ECG signal that is simultaneously collected from the individuals with the sEMG signals used.

Chapter 3
Digital Signal Processing

3.1 Introduction

This chapter focuses on the digital signal processing techniques used for the analysis of the biosignals collected from the participants, who were part of this research. The theoretical principles of the digital signal processing techniques used are discussed in this chapter, which covers Continuous Wavelet Transform (CWT) with Thresholding. Also covered are the basics of biosignal acquisition and pre-processing of the biosignals used in this research.

A biomedical signal is a phenomenon that carries information related to one or more biological systems involved [40]. Biosignals or biomedical signals are signals that show the bioelectrical activity of one or more biological systems within the body.

3.1.1 Biosignal Classification

Biosignals or Biomedical signals are classified into discrete and continuous signals, based on signal acquisition and processing. Continuous signals are defined within any point of the time domain and are processed using analogue signal processing techniques. The discrete signals are quantised digital signals that are discrete points reflecting the value of the amplitude at the time it is measured [41]. In this research, the signals used are discrete, which were analysed by digital signal processing techniques, using a personal computer.

Signals are classified on the nature of the waveform recorded shown in Figure 3-1, either as:

- Deterministic
- Stochastic

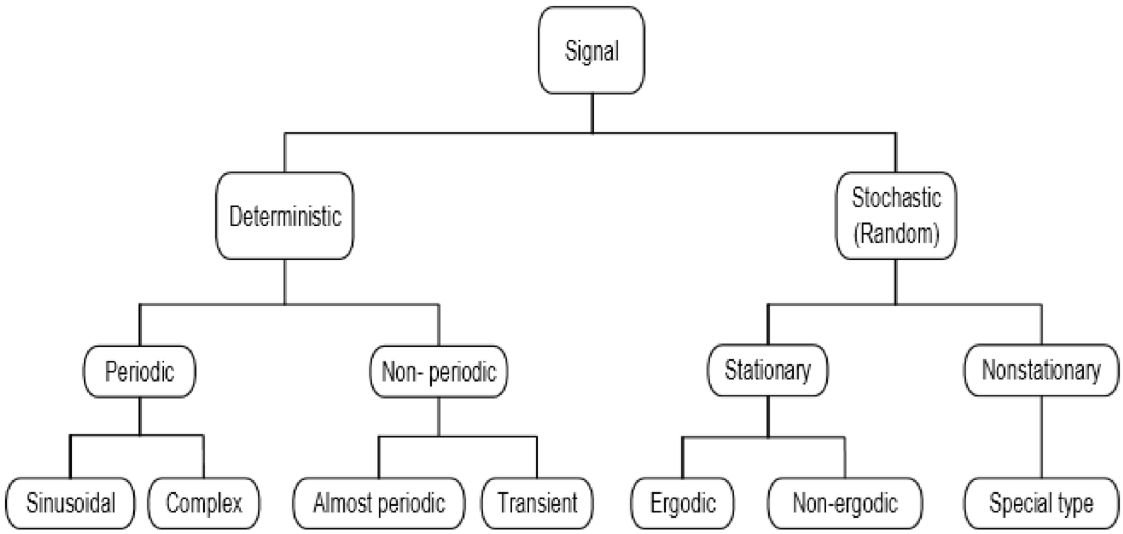

Figure 3-1: Signal Classification [42]

Deterministic signals can be represented by a mathematical expression, and they can be classified as periodic or non-periodic signals. Periodic signals are considered to have repetitions of the waveform within the time domain. These repetitions can be either sinusoidal or complex waveforms, that can contain more than a single waveform that can be represented by a Fourier series. Non-periodic signals are signals that do not repeat themselves but can be represented by a mathematical expression. These non-periodic signals are classified into transients and almost-periodic signals [41].

Stochastic signals have functions that are random in nature and cannot be expressed by using a mathematical expression but can only be expressed in terms of probabilities. The collections of these random processes produced sample functions known as 'ensembles'. These sample functions share the same distribution probabilities, even though they differ from the other in detail. Stochastic signals are classified into stationary and non-stationary [41].

The biosignals are never completely deterministic, and always have an unknown element within them that is stochastic in nature. This is because of the complexity associated with the acquisition of the biosignals and the systems related to the generation of these signals.

3.1.2 Biosignal Acquisition

The acquisition of biosignals is determined by the standards of the equipment available and the technological advancements within the biomedical industry. Biosignals are continuous in nature at the site of the collection of the signal, and they are collected in terms of electric variables which are currents, voltages or field strengths. The bioelectric signals are collected from the site using sensors such as electrodes, and these signals are directly used for further processing.

There are various stages in the acquisition of biosignals from acquiring the analogue signal to converting it to a digital signal for analysis, shown in Figure 3-2.

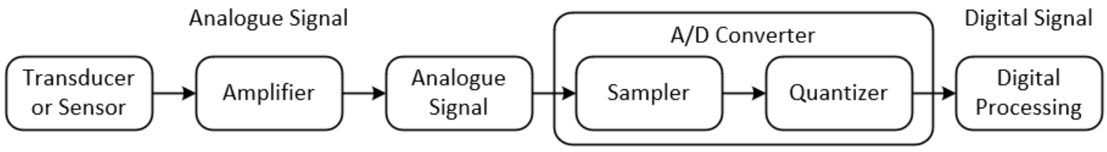

Figure 3-2: Biosignal Acquisition

The data acquisition of the analogue signals has a pre-processing phase that involves the amplification and filtering of the signal. The amplification and analogue filtering of the signals are based on the parameters of the input analogue signal, and the requirement set by the analogue-to-digital converter (A/D) for the digital signal used for processing. The amplification and filtering are used to set the bandwidth limit for the signal prior to analogue-to-digital conversion, to reduce any aliasing while preserving signal information and quality.

The amplification of the signal improves the resolution of the signal for the filtering of the signal. Since the biosignals have a low signal-voltage amplitude, the amplification procedure is vital to avoid excessive filtering and truncating of the signal components. The amplification procedure also changes the amplitude of the continuous-time signal to match the input voltage range required for the analogue-digital converter. The analogue filter's primary objective is to eliminate external noise artefacts such as interference caused by the hardware (electrodes, signal collection cables, etc.), and other external sources such as lights or the movement of the surface and hardware.

The conversion of the analogue signal to a digital signal is an important step in the signal acquisition process for digital processing and analysis. The analogue-to-digital conversion can be classified into signal sampling and quantisation procedures. The signal sampling process converts the continuous signal to discrete points within the time domain that provides elements for quantisation. The quantisation process assigns a value for the amplitude corresponding to the continuous signal at the discrete-time element determined by sampling [43].

The sampling process is determined by the Nyquist-Shannon theorem, which indicates that a continuous-time representation of the signal can be recovered from the discrete-time samples if the sampling rate (f_s) is greater than twice the signal bandwidth (f_b).

$$f_s > 2f_b \tag{3.1}$$

The sampling value is vital to assessing the frequency spectrum and reproducing the information previously held by the original signal. For example, the frequency component of sEMG can be as low as 10-20 Hz and ranges to 400-500 Hz. When the sampling frequency is less than twice the signal bandwidth, the Nyquist-Shannon theorem is not satisfied, and this results in incorrect reconstruction of the signal, and that is known as aliasing. Also, this undersampling of the signal results in some elements within the signal to not be recorded, giving loss of information within the signal [43]. Hence, the sEMG data collected from the trunk muscles are typically collected at a sampling rate of at least 1000 Hz [44].

The quantisation of the signal primarily depends on the resolution of the analogue-to-digital signal. However, the quantization of the signal limits the value that can be assumed by the amplitude of the continuous-time signal, and this process of the signal requires it to be truncated or rounded to the nearest quantisation level [43].

The discrete-time signal generated from the digitisation of the continuous-time signal is used for the extraction of features from the signal. In this research, the sEMG signal obtained from the hardware is sampled at a frequency of 1,500 Hz, to record the components within the frequency bandwidth up to 750Hz. The major sEMG signal frequency components are present up to a value 500Hz [44], which is well within the frequency bandwidth for the sampling frequency at which the signal is acquired.

3.1.3 Biosignal Digital Signal Processing of ECG and EMG

Biosignal digital signal processing involves the extraction of the signal features, signal parameters and evaluation of the extracted information. This is the second phase of the research, which involved taking the entire signal processing and using MathWorks® MATLAB version 2017b.

For this research, the digital signal processing techniques were applied to the sEMG signal to extract the ECG artefacts contained within the sEMG signal. Due to the overlapping amplitude and frequency values of ECG and sEMG signals shown in Figure 3-3, the extraction of ECG signals from sEMG signals is challenging.

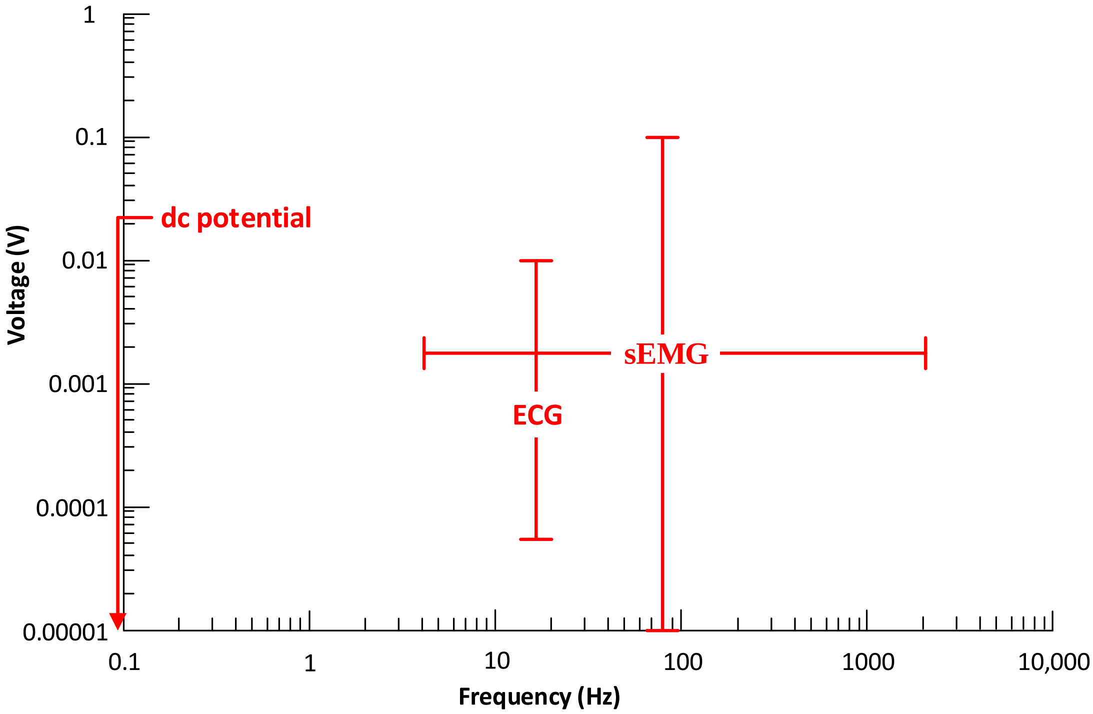

Figure 3-3: Range of amplitude and frequency components of ECG and sEMG signals

3.1.4 EMG and ECG feature extraction

The focus of this research was to be able to extract the ECG component from the sEMG signal for the back muscles at different levels of Maximum Voluntary Isometric Contraction for a predetermined task. The Fourier power spectra of the original biosignal collected that retained sEMG and ECG components were analysed, to investigate the difference between the sEMG component prior and post-removal of the ECG artefact signal.

The extraction of the ECG artefacts from the sEMG signals can be achieved using the wavelet transform techniques. This literature review discusses previous research that has been carried out over the past 10 years for the extraction or separation of ECG and EMG signals, and the removal of one signal from the other using the wavelet transform and Fourier Transform (FT) techniques. The Continuous Wavelet Transform (CWT) and

Discrete Wavelet Transform (DWT) techniques are commonly used for the feature extraction of the ECG and EMG signals. Fourier Transform (FT) is used for analysing the frequency spectrum of the signals. The theoretical overview of both the FT and the CWT are discussed in sections 3.2 and 3.3, along with the concept of thresholding.

3.2 Fourier Transform Analysis

Fourier Transform (FT) is a mathematical technique for representing a signal as the sum of constituent sinusoidal functions with different frequencies. Fourier transforms express the Fourier series in a generalised format using exponentials and complex numbers, in contrast to the Fourier series that express the signal function as the sum of sine and cosine functions at different frequencies.

The Fourier transform $\mathrm{F}(\omega)$ of a time-domain signal $\mathrm{x}(\mathrm{t})$ can be expressed as an integral function given by:

$$\mathrm{F}(\omega) = \int_{-\infty}^{\infty} \mathrm{x}(\mathrm{t})\mathrm{e}^{-\mathrm{j}\omega\mathrm{t}}\mathrm{dt} \qquad (3.2)$$

where the angular frequency $\omega = 2\pi\mathrm{f}$ given using the signal input frequencies f. FT is used for spectral analysis, as it can express all the frequencies and amplitudes of the sinusoidal components of a time-domain signal.

3.2.1 Fourier Transform

The Fourier Transform (FT) can theoretically only be applied to signals of continuous-time and infinite duration. The signals that are acquired and stored on the computer are referred to as ‘discrete’, meaning that the acquired digital signals have data points that are sampled and quantised. Discrete signals have a finite number of data points and are not continuous in nature. This makes the use of the general Fourier Transform expression given in equation (3.2) for spectral analysis unsuitable for discrete signals. So Discrete Fourier Transform (DFT) is used to convert the discrete-time signal from the time domain $\mathrm{x}[\mathrm{n}]$ to the frequency domain signal $\mathrm{X}[\mathrm{k}]$.

$$X[k] = \sum_{n=0}^{N-1} x[n]e^{-j2\pi kt/N} \tag{3.3}$$

The discrete angular frequency 2πk can be calculated using the signal frequency k. The number of samples in both the discrete-time and discrete-frequency domain N is used to set the limits for the discrete Fourier transform function.

The DFT of a discrete signal is found using the MATLAB function ‘fft’. For this research, the sEMG signals were acquired and stored on a computer are discrete-time signals. The Fourier Transform of the sEMG signals were computed using MATLAB, and the frequency response of the discrete-time signal is generated. The raw sEMG signal collected from an isometric contraction at 50% Maximum Voluntary Isometric Contraction (MVIC) of the lower erector spinae muscle group sampled at 1,500 Hz is shown in Figure 3-4 (top plot), with the spectral analysis of the sEMG signal shown in Figure 3-4 (bottom plot). The Fourier Transform shows the dominant frequency, as well as the amplitude of each frequency component present within the signal.

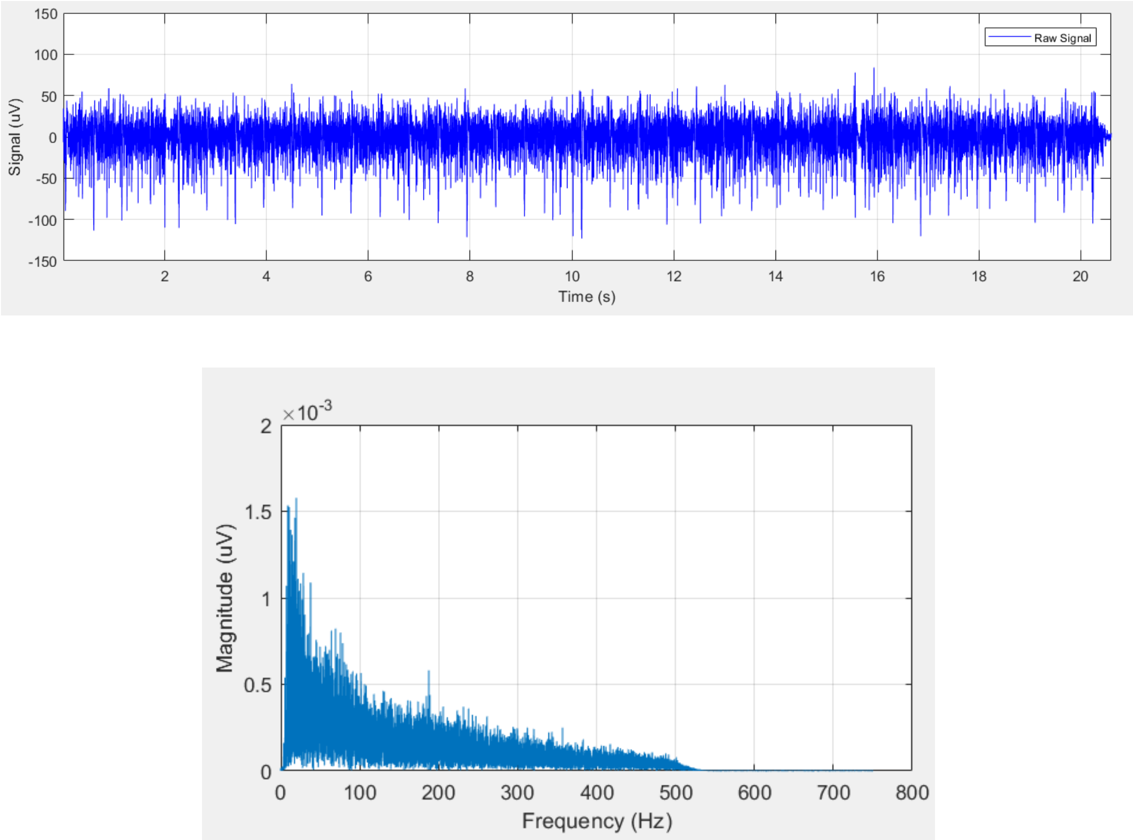

Figure 3-4: Raw sEMG signal (top) from the lower erector spinae muscle at 50% Maximum Voluntary Isometric Contraction (MVIC) and the Fourier Transform plot of the sEMG signal (bottom).

The exact time-localised distribution of the frequency components of the original signal cannot be defined using FT. This is because the FT of the signal provides the power spectra of the signal within the frequency domain. The FT frequency spectrum plot of the signal is a measure of the amplitude of each sinusoidal value at different frequencies. FT transforms the signal from the time domain to the frequency domain, and the signal is assumed to be stationary in nature. This results in the FT not being able to detect non-stationary and transient features, such as any drifts or abrupt changes within the signal. sEMG signals have those characteristics, and they are considered to be important features. FT is not an ideal technique for the extraction of features within sEMG signals. However, FT is ideal for assessing the power spectrum of the signal, and it can be used to observe the amount of power preserved post and pre-filtering of sEMG signals. The time resolution is better for the signal analysed within a narrow window using the Short-Time Fourier Transform (STFT), but it also has a poor frequency resolution. On the other hand, if a wide window is used for STFT, the frequency resolution tends to be better, but the time resolution of the signal is poor.

3.3 Wavelet Transform

The Wavelet Transform (WT) is a technique that is applied for the analysis of heart-activity monitoring, compression of video and medical images and signals. WT is the analysis of signals using localized wavelets with the presence of a time frame. WT is able to preserve the information of the time localisation for each frequency components that are observed to be present in the time-domain of the signal. This information can be used to analyse the instantaneous characteristics and features of the signals such as abrupt changes. The wavelet analysis uses a time-scale analysis that provides a flexible time-frequency resolution. It is not affected by the limitations of the size of window or data like that of time-frequency-based analysis techniques such as Short Time Fourier Transform (STFT) [45].

The WT is an expression of the signal in the form of an infinite series or linear combination set of wavelet functions that are constructed, based on the mother wavelet. The mother wavelet is the original window function that is manipulated to obtain the wavelet functions required for the extraction of signal features shown in Figure 3-5. The mother wavelet can be manipulated using two methods: (a) the first method is the dilation or compression of the mother wavelet known as scaling shown in Figure 3-5 (top plot) and (b) the second method is the movement of the mother wavelet along the time domain of the signal known as translating or shifting shown in Figure 3-5 (bottom plot). The translating and scaling processes of the mother wavelets produce sets of wavelet functions known as daughter wavelets that form the wavelet functions used for the signal analysis [46].

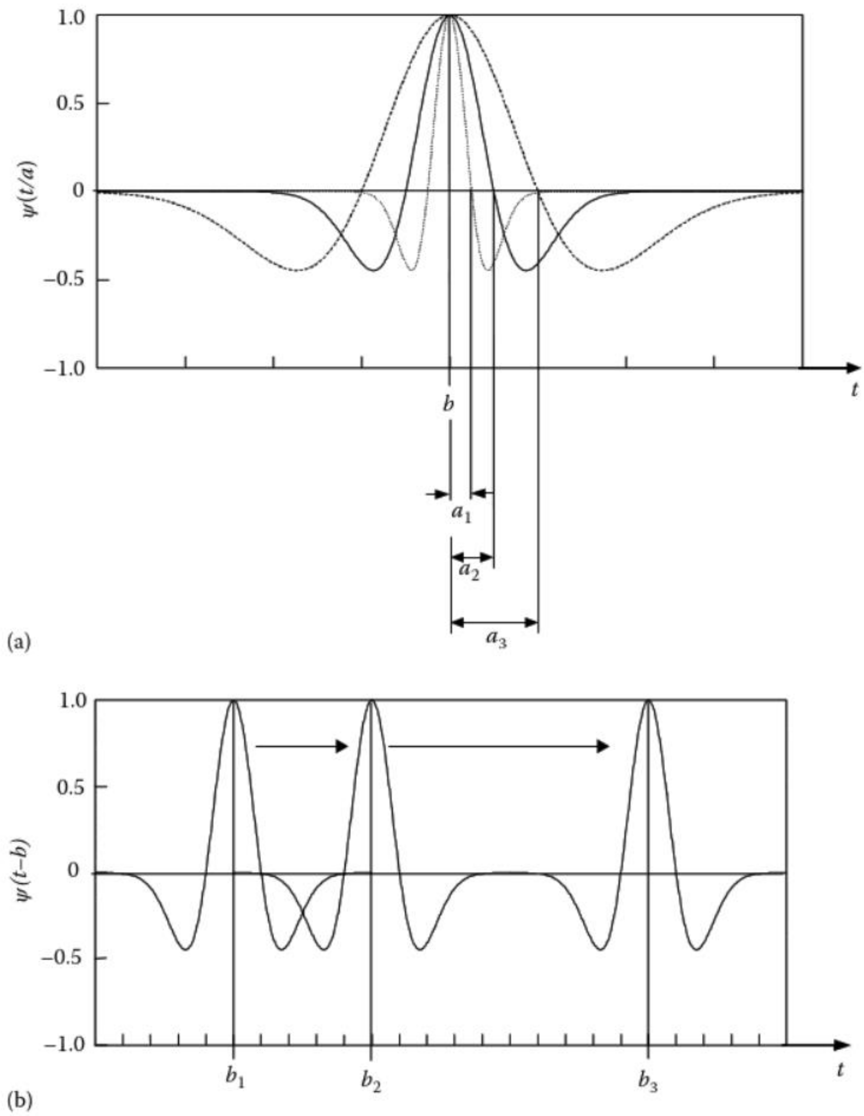

Figure 3-5: 'Wavelet Scaling' - the dilation of the mother wavelet (top) and 'Wavelet Translating' - the wavelet being moved within the time domain (bottom) [47].

The higher scales on the mother wavelet results in the dilation of the mother wavelet producing daughter wavelets with low frequency and the lower scales, on the other hand, compresses the mother wavelet producing daughter wavelets with higher frequency. The scale value for the scaling of the mother wavelet inversely affects the frequency of the daughter wavelets generated using the mother wavelet. The WT uses these daughter wavelets, which are shifted in the time domain as they are superimposed on each other in synchronisation. Mathematically, the interpretation of the wavelet can be identified as the convolution of these daughter wavelets to the original signal to generate a scalogram plot representing the amplitude of the value resulting from the matching of the wavelet to the window of the original signal shown in Figure 3-6. This procedure is repeated through the whole signal, and the computation of the transform value is calculated for various scales at each location on the time domain. The WT uses the scaling value to have the daughter wavelets scaled to the frequency value known as the pseudo frequency [47].

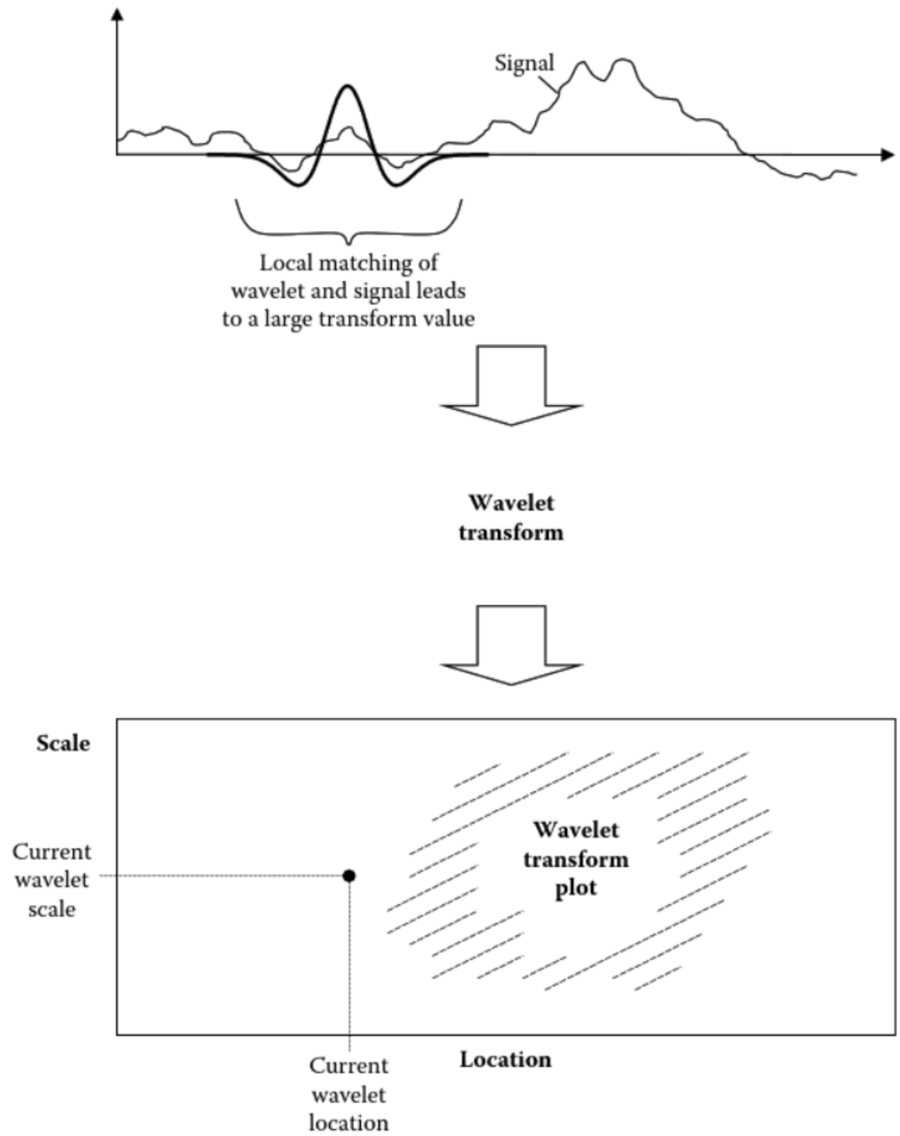

Figure 3-6: Wavelet matching with the original signal (top plot) to produce a wavelet transform plot called a Scalogram (bottom plot) [47].

Wavelet analysis is used for feature extraction and analysis of biosignals, as it can provide an almost perfect reconstruction of the signal from its transform coefficients without having the need to oversample the original signal. This means that wavelet transforms preserve time and frequency resolution. In contrast, the frequency resolution of STFT is dependent on the length of the window being used. The use of wavelet transform provides a time-scale analysis that uses varying scales providing a better time resolution in comparison to the STFT technique, which is limited to using a fixed resolution set by the window size throughout the signal [48].

The normalised mathematical expression of the daughter wavelets $\Psi_{a,\tau}$ produced from the mother wavelet by scaling and shifting of the mother wavelet $\Psi(t)$ can be demonstrated using the equation (3.5):

$$\Psi_{a,\tau}(t) = \frac{1}{\sqrt{a}}\Psi\left(\frac{t-\tau}{a}\right) \tag{3.4}$$

where a represents the scaling parameter and τ represents the shifting parameter.

When the value of a is changed, the scaling of the mother wavelet changes. The wavelet becomes dilated when the scaling factor increases, resulting in the daughter wavelet $\Psi_{a,\tau}$ becoming a stretched version of the mother wavelet Ψ. On the other hand, the wavelet becomes compressed when the scaling factor decreases, resulting in the daughter wavelet $\Psi_{a,\tau}$ becoming a compressed version of the mother wavelet Ψ. The value of the shifting parameter τ is used to move the daughter wavelets along the time domain that is required for the convolution of the wavelet function for identifying the matching regions of the original signal to the wavelet. The wavelet function produces the scalogram that is a representation of the signal regions that fulfil the matching criteria for the Wavelet Transform. The wavelet transform technique could be considered a bandpass filter, for the finite range of frequencies set by the scales and the mother wavelet. This implementation of the bandpass filter is based on the pseudo-frequency of the daughter wavelet that can change based on the value of the scale implemented, providing a wider or narrow frequency resolution. The time-scale representation of the signal using wavelets has an equivalent time-frequency expression using the value of the scale. Note that the use of $1/\sqrt{a}$ as the factor in the equation (3.4) of the daughter wavelets is for normalising the wavelet to preserve energy [47].

The normalised mathematical expression for the conversion of the scale of the wavelet to its equivalent pseudo-frequency f_a is given by equation (3.5):

$$f_a = \frac{f_0}{a} \tag{3.5}$$

where a represents the scaling parameter and f_0 is the centre frequency.

The mother wavelet is localised on a non-zero centre frequency f_0 at scale = 1. The inverse relation between the scale and the frequency of the wavelet is denoted by the expression. The pseudo frequencies of the daughter wavelets can be changed to the frequency of the signal for spectral analysis using the sampling frequency f_s.

$$f_a = \frac{f_s \times f_0}{a} \tag{3.6}$$

The selection of a mother wavelet is vital to the wavelet transform when assessing the scale and hence the pseudo frequency values. The different types of wavelet families that are commonly used in practice include Gaussian (first-order Gaussian derivative), Mexican Hat (second-order Gaussian derivative), Morlet (or Gabor), Haar, Coiflet, and Daubechies. The type of mother wavelet affects the wavelet selection procedure with its compatibility and shape of the wavelet required for signal processing. The shape of these wavelet families depends on the localisation of the wave features and the structure of the wave. Some of the wavelet families such as Coiflet and Daubechies have wavelet subclasses that are mother wavelets, which differ from the other wavelets within the same family based on the number of coefficients and the level of iteration [49].

The decomposition of a signal using WT produces coefficients known as wavelet coefficients that are used for reconstruction purposes as well as generation of the scalogram. The values of the wavelet coefficients are produced based on the matching of the wavelet with the original signal. The abrupt changes within the signal and the low-frequency components of the signal can be identified using the wavelet coefficients. The wavelet transform technique provides a better time resolution at high frequency and a better frequency resolution at low frequency. The signal can be reconstructed as a linear combination of the wavelet function based on its wavelet coefficients. The number of wavelet coefficients determines the level of detail during the reconstruction of the signal. The level of reconstruction of the signal is better or in more detail with the higher number of coefficients. In order to reconstruct the signal, enough coefficients are required to provide sufficient information for the reconstruction.

The two types of wavelet transform used are (a) continuous wavelet transform and (b) discrete wavelet transform. This research focuses only on the continuous wavelet transform, which is discussed in the following section.

3.3.1 Continuous Wavelet Transform (CWT)

The Continuous Wavelet Transform (CWT) is the computation of the signal by continually shifting the wavelet function over the entire time domain of the analysed signal. The CWT can operate at any scale and position within the time domain that is determined during the signal analysis. The CWT is not computed at arbitrary dilations nor at an isolated location, but rather over a continuous range defined between two points.

The CWT function for a signal can be defined as an integral function in the equation (3.7):

$$\mathrm{CWT_x}(a, \tau) = \int_{-\infty}^{\infty} x(t)\Psi^*_{a,\tau}(t)dt \tag{3.7}$$

The scaling parameter is represented by a, τ defines the translation parameter by which the wavelet is shifted in the time domain of the signal. The wavelet function $\Psi^*_{a,\tau}$ is obtained from the conjugate of the function obtained from the mother wavelet manipulated using the scaling parameter a and translation diameter τ. The conjugate of the wavelet function is used for all continuous wavelet transforms, apart from the Mexican Hat wavelet that is made of real functions and is not a complex function. Since the wavelet function $\Psi_{a,\tau}$ is defined in the equation (3.4), the equation (3.7) for CWT can be modified as:

$$\mathrm{CWT_x}(a, \tau) = \frac{1}{\sqrt{a}} \int_{-\infty}^{\infty} x(t)\Psi^*\left(\frac{t-\tau}{a}\right) dt \tag{3.8}$$

The scalogram plot of the CWT analysis provides the time-scale view of the signal. It shows information similar to the STFT spectrogram of the magnitude of the signal, but in the case of the spectrogram, the magnitude is analysed in relation to frequency. However, for the scalogram, the magnitude is assessed in relation to the scale for an instant within the time domain of the signal. The scalogram coefficients hold the information regarding the presence of the signal features and their scales, that can be assessed using pseudo-frequency values within the time domain of the signal. This helps in identifying the dominant frequencies within the signal and also the time localisations, detecting when they occur in the time domain.

The scalogram can be represented as the power by the squaring the magnitude of the coefficients obtained from the CWT [47].

$$|CWT_x(a,\tau)|^2 = \left| \left| \frac{1}{\sqrt{a}} \right| \int_{-\infty}^{\infty} x(t)\Psi^* \left(\frac{t-\tau}{a} \right) dt \right|^2 \tag{3.9}$$

Figure 3-7 shows the analysis of the sEMG signal. The sEMG signal in Figure 3-7 (a) is the same as that in Figure 3-4, which is obtained from the activity of the lower erector spinae muscle group at 50% MVIC. Figure 3-7 (b) shows the reconstruction of a wavelet signal that has been obtained from the coefficients of the transform, using Morlet Wavelet scales from 1 to 1500. Figure 3-7 (c) shows the scalogram of the signal based on the coefficients generated from the CWT. Figure 3-7 (d) shows the equivalent power spectrum obtained on a time-frequency plot, with the pseudo-frequency values obtained using the scales.

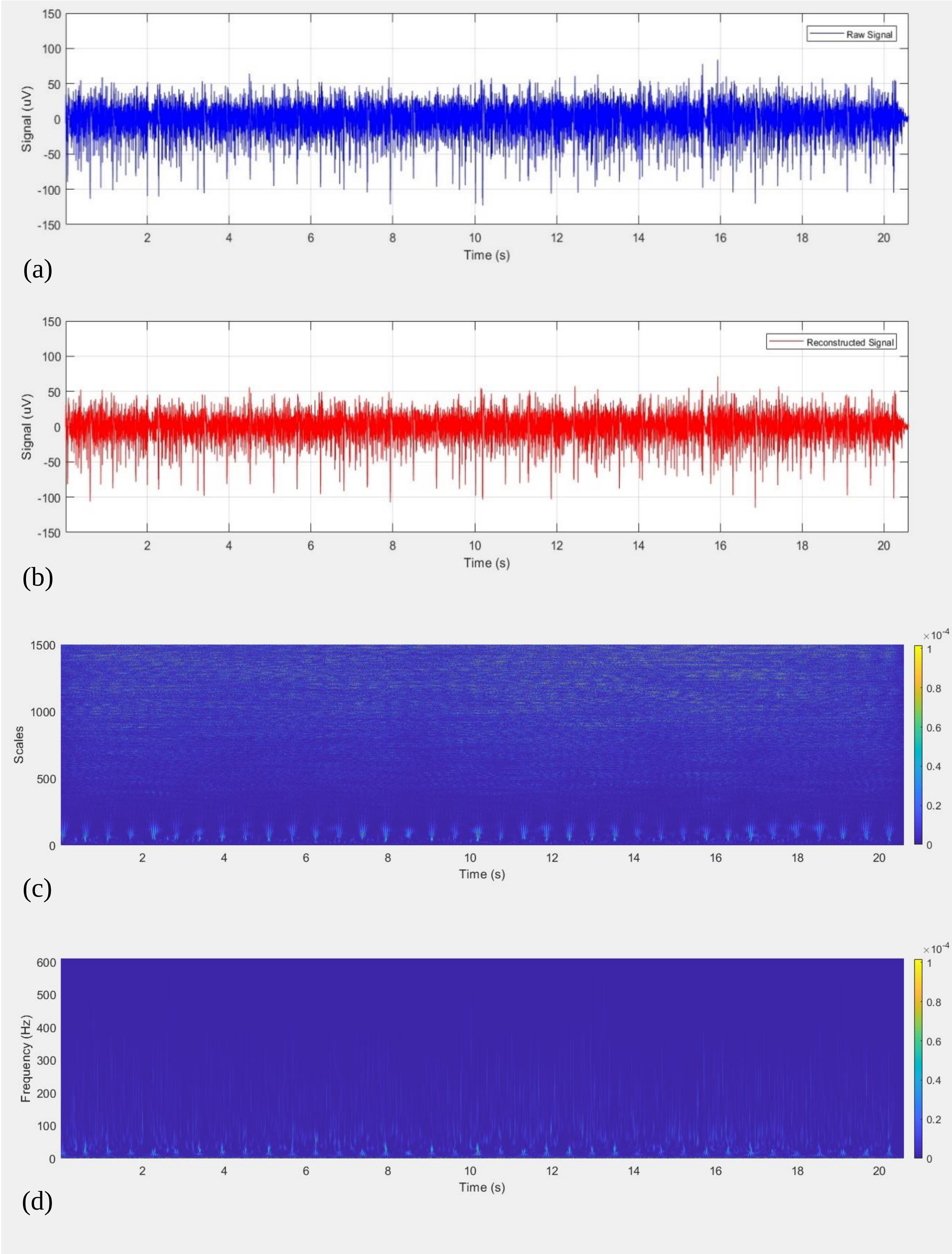

Figure 3-7: (a) sEMG signal from the lower erector spinae muscles at 50% MVIC.
(b) CWT reconstruction of the sEMG signal using the Morlet Wavelet, scales from 1 to 1500.
(c) Scalogram of the sEMG signal shown in (a).
(d) Distribution of power plotted using the CWT coefficients against the pseudo frequency values calculated using the scale.

3.4 Thresholding

Thresholding is the manipulation of the values based on a limit or threshold that is determined during the analysis process. The estimation of the threshold value is based on the threshold function selection and the data. The thresholding process is used in processing statistical data when the data itself is either removed or manipulated based on the threshold parameter. In signal processing, the thresholding function is directly implemented on the signal itself for noise mitigation or elimination of features within the signal that are not required during processing [50, 51].

Research has been done using thresholding functions to implement it on variables that are used to develop the functions [38, 50-52]. The use of threshold functions on signal processing provides an approximation of the original signal that has been distorted by the noise signal. In this research, the thresholding procedure was used on the wavelet coefficients generated from the CWT prior to its reconstruction.

The thresholding process involves the estimation of the threshold value and the implementation of the thresholding process.

3.4.1 Threshold Value Estimation

The threshold value estimation is vital for the development of the thresholding process. Donoho [53] proposed the Length Modified Universal Thresholding that uses a threshold value λ calculated using the equation (3.10).

$$\lambda = \frac{\sigma\sqrt{2\log(N)}}{\sqrt{N}} \tag{3.10}$$

where σ represents the noise level, and N is the length of the analysed signal. This threshold value estimation was adopted because of the stochastic nature of the EMG signal, like noise.

The noise level σ is calculated using the equation (3.11).

$$\sigma = \mathrm{MAD}/0.6745 \tag{3.11}$$

where MAD is the median absolute deviation estimated using the median of the coefficients generated by the wavelet transform, the mathematical expression for MAD is given by equation (3.12).

$$\mathrm{MAD} = \mathrm{median}(|\omega - \mathrm{median}(\omega)|) \tag{3.12}$$

where ω denotes the data points.

The threshold value is calculated for a set of coefficients for the CWT of each sample of the signal. The thresholding method proposed by Johnstone and Silverman [54] uses a level-dependent threshold that uses the threshold obtained at each level of transform in the DWT implemented in their research.

For this research, the Length Modified Universal Thresholding method was adopted for the coefficients of the CWT at each sample of the signal. The value for each sample calculated based on this method provides a threshold for that particular sample within the sEMG signal.

3.4.2 Threshold Implementation

The thresholding function is implemented based on the threshold value estimated. For this research, the hard thresholding method was used for the elimination or truncation of the EMG signal components from the sEMG signals when isolating the ECG signal.

Hard Thresholding function uses a predetermined threshold value to manipulate the values, to mitigate or remove values below the threshold. The threshold value for the hard thresholding provides the cutoff for the signal such that all elements of the function below the threshold value are removed.

$$y = f(x) = \begin{cases} 0, & x \leq \lambda \\ x, & x > \lambda \end{cases} \tag{3.13}$$

This is applied to the coefficients of the CWT to remove the components of the lower scale values that are made of the higher-frequency components of the sEMG signal. Since the threshold value is calculated for each sample, it can preserve any abrupt changes within the signal that is detected using the wavelet. The lower frequency components obtained from the CWT that is primarily dominated by the ECG signal is preserved during the thresholding procedure. This thresholding method aids in the removal of the sEMG components within the ECG signal that is detected using the CWT.

3.5 Quantitative Measures in Feature Selection

In this research, the signal features before and after the removal of the ECG artefacts were observed using the median frequency values from the power spectrum. The median frequency was selected as it is done in most EMG researches using the Fourier transform method. The median frequency provides information on the spectral nature of the signal as well as the changes in the frequency spectrum within the time domain.

The power spectrum using STFT provides the individual frequency components within the window of the signal analysed. The power spectrum with linear scales is measured in volts square per hertz (V^2/Hz). The area of the graph under the power spectrum provides the total power within the signal window being analysed. The median frequency is the frequency where there is 50% of the total power is present on the frequency distribution. The median frequency is shown in equation (3.14) [55]:

$$\int_0^{\mathrm{MDF}} \mathrm{P}(\omega)\mathrm{d}\omega = \int_{\mathrm{MDF}}^{\infty} \mathrm{P}(\omega)\mathrm{d}\omega \qquad (3.14)$$

Where MDF is the median frequency, and $\mathrm{P}(\omega)$ is the power spectrum of the signal window being analysed.

Chapter 4

Data Acquisition and SEMG Signal Processing

4.1 Introduction

This chapter gives an overview and discusses the procedures for the data acquisition, and digital signal analysis for the extraction of the Electrocardiography (ECG) features from the signals collected from the sEMG signals used in this research. This includes the description of the procedures associated along with the equipment used for the collection of data involving the experimental setup and the physical preparation of the individuals for the collection process. Also covered is the development of the signal processing program using MATLAB along with the results from the processing of the signals from one participant are presented in this chapter. These results are discussed in terms of the detection of the ECG signal, removal of the signal and the power spectrum analysis of the signals before and after the removal of the ECG signals from the sEMG signals using Continuous Wavelet Transform (CWT) analysis.

This research will develop a technique for extracting the ECG and EMG components the surface Electromyography (EMG) signals from the erector spinae muscles of healthy participants. This was carried out for varying levels of activity of Maximum Voluntary Isometric Contraction (MVIC) for the lower erector spinae muscles to provide an appreciation of how much the ECG artefact influences the power of the EMG signal during different levels of muscle effort. The development of the algorithm and program code are done using sEMG signals obtained from the study for this research.

To fulfil the aims and objectives of this research, it was structured using the following four stages:

Stage 1. Software Development Stage
Stage 2. Data Collection and Acquisition
Stage 3. Signal Pre-processing
Stage 4. Feature Extraction and Signal Analysis

All the four stages of the research are summarised in the block diagram shown in Figure 4-1.

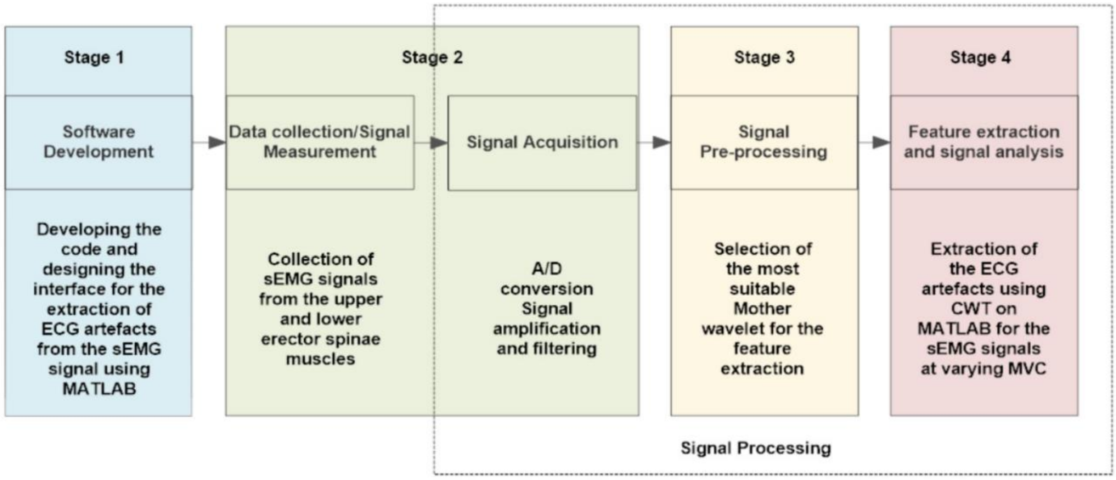

Figure 4-1: Block Diagram outlining the Stages of the Research

4.2 Software Development

This stage of the research involved the process of developing the program code using MATLAB for FT and CWT along with Thresholding. The CWT program developed used all the MATLAB supported wavelet families for CWT, to identify the wavelet most suitable for the extraction of the ECG from the sEMG signals. For this stage, EMG signals from the left UES and LES muscle groups of a single healthy subject were collected at a sample rate of 1500 Hz during muscle contractions between 10 and 30 percent of MVIC. These levels of muscle contraction were chosen because ECG artefact could be visually detected within the EMG signal, and this range of muscle contraction is typically observed during a number of activities of daily living. The 3-lead ECG data were collected simultaneously, using the same software and sampling rate (1500 Hz) for cross-validation purposes. Details of EMG and ECG set-up and collection are detailed in a later chapter (4.3 Data Collection and Signal Acquisition).

When comparing the various wavelets, all the parameters of extraction must be similar. Each wavelet family and its subclasses have different centre frequency values that determine the scales-frequency relation. Since the transform for the CWT is represented by time-scale domain and not in the time-frequency domain, there is a need to convert all the scale values to frequency to provide a nominal value of the frequency range along which the CWT is performed.

The scalogram provided in the CWT on MATLAB does not provide the time-frequency plot of the signal and hence does not provide the frequency equivalent value at which the dominant power spectrum features from the CWT are present. Due to the variation of the centre frequency between the mother wavelets of different families, the frequency parameter is used for setting the parameters of the CWT. The mathematical expression is given by the equation (3.7) in chapter 3 was used for the conversion of scale values to the pseudo frequency values. To obtain a better resolution of the frequency spectrum, power values of the frequencies were obtained by squaring the coefficients from equation (3.10) given in chapter 3 and plotting these on the time-frequency domain using the pseudo frequency values as a reference in for the corresponding scales. This makes it possible to identify the dominant frequency components in the signal and its time localisation using the CWT.

The validation of this step was done using sample sEMG signal obtained from a participant collected at 20% from the lower erector spinae muscle. This signal was analysed using CWT using MATLAB for each of the mother wavelets available to obtain complete reconstructions of the signal. This involved setting the scale values from 1 to the equivalent scale value or the closest value for the frequency of 1 Hz. The time-frequency plot generated from the CWT coefficients were used to observe the frequency range along which the QRS equivalent ECG artefact within the sEMG signal would be present. This information was observed across all the mother wavelets, and a nominal frequency range was selected for the signal. This frequency range was converted into the corresponding scale values for each of the mother wavelets, and the CWT of the signal was obtained, and a comparison made.

This analysis showed using the CWT with the Morlet mother wavelet produced satisfactory results. So, the Morlet mother wavelet was used for the later stages of signal processing when analysing sEMG signals from the lower erector spinae muscles at different levels of MVIC. The concept of thresholding was then introduced in order to reduce the EMG artefacts that were extracted along with the ECG artefacts from the sEMG signals during the implementation of the CWT.

4.2.1. Software Development Concept

The primary purpose of this section was to develop code on MATLAB for the extraction of the ECG artefacts from the sEMG signals. The associated signal processing techniques and the output of the results are shown in Figure 4-2.

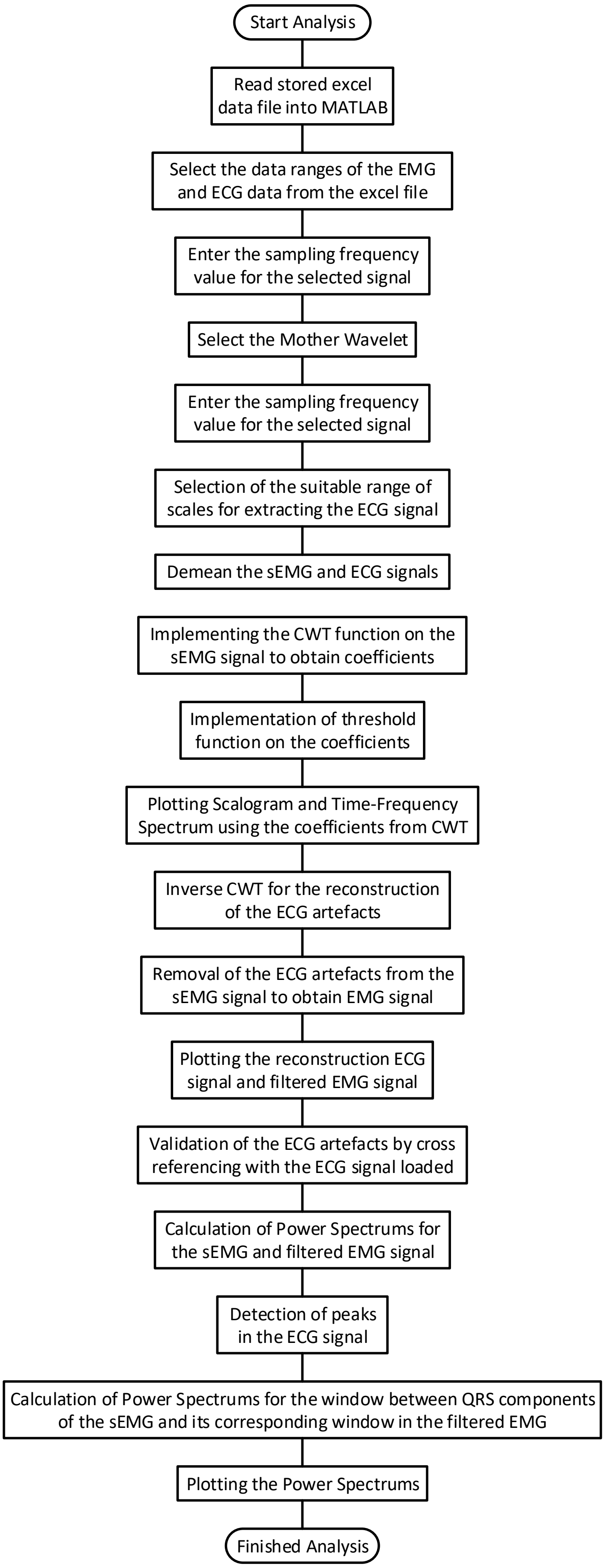

Figure 4-2: MATLAB program flow chart for the extraction of ECG from sEMG and the display of the results using CWT

The 3 lead ECG and sEMG signal were collected simultaneously to ensure that there is an equal number of data points to cross-reference the ECG artefact reconstructed from the CWT of the sEMG signal and the ECG data collected during the activity. The conversion of the scales to pseudo frequency was done using the centre frequency value obtained using the information on the wavelet available within MATLAB using the 'centfrq' function. Both the ECG and EMG signals were demeaned to remove the DC offset or bias that may be present.

The 'cwt' function in MATLAB was used to apply the CWT on the sEMG signal and obtain the wavelet coefficients. The threshold function was implemented with the threshold value being calculated using the equation (3.11) given in chapter 3. The coefficients from the CWT after thresholding were used to plot the scalogram and the time-frequency spectrum. The coefficients were then used to reconstruct the signal using the 'icwtlin' function that provides the inverse continuous wavelet transform.

The signal obtained from the reconstruction of the CWT coefficients was compared with the actual 3-lead ECG signal initially loaded into the program. Then validation of the signal was done through visual inspection. The reconstructed ECG signal was then removed from the original sEMG signal (EMG and ECG artefact), and it was plotted to observe the remaining EMG signal. The R-peaks of the 3-lead ECG signal that was initially loaded into the program were identified using the 'findpeaks' function in MATLAB. These R-peaks were aligned with the ECG artefacts present on the reconstructed signal and were used as reference points to identify the windows between the consecutive QRS complexes present in the signal. The power spectrum of the whole sEMG signal and the signal obtained after the removal of the ECG signal were calculated and plotted. This was done using the 'fft' function in MATLAB, followed by squaring all the values of the coefficients generated. The same procedure was repeated for each window present in the signal to observe the difference in the power across the signal.

The 'cwt' function and the 'icwtlin' functions are built-in functions of the MATLAB Signal Processing Toolbox that process and analyse signals based on the analysis scheme appointed for the function. The 'cwt' function in MATLAB can perform the CWT using other mother wavelets than the ones listed during the pre-processing stage. However, the reconstruction of the signal using the 'icwt' function that computes the Inverse Continuous Wavelet transform using the coefficients does not support the manipulation of its scale parameters. It uses a scale determining function based on the coefficients being provided to automatically assign scale values that do not prove to be successful when the coefficients are obtained using the ‘cwt’ function with the scales being set manually. On the other hand, the ‘icwtlin’ can provide the reconstruction of the signals from the coefficients based on the scale parameters being manually assigned during the reconstruction process. However, the reconstruction of the signals using the ‘icwtlin’ function with coefficients of CWT, is only supported for certain wavelets. The selection of the mother wavelets was based on the available wavelets with the reconstruction function in MATLAB that is listed in the pre-processing stage.

4.3 Data Collection and Signal Acquisition

This section covers the description of the participants, equipment, procedures, and protocols used for the data collection of the sEMG signals for the different levels of Maximum Voluntary Isometric Contraction (MVIC), as well as the maximal strength test for identifying the MVIC.

Since the sEMG signals and the ECG signals were collected from human participants, the ethics approval was mandatory for the experimental part of this research. The application for ethical approval to proceed with the experimental procedure and collection of the data from the participants was submitted and approved by the Auckland University of Technology (AUT) Ethics Committee (AUT ethics number: 18/219).

4.3.1 Participants

Seven participants with no previous history of back injury or any other form of musculoskeletal ailments participated in this research. The participants were students from the Auckland University of Technology North Shore campus. The participants for the research were selected from individuals who responded to advertisement notices that requested the voluntary participation of individuals for this research. Male and female participants between the ages of 18 and 35 with no history of back injury within the last year participated in the study. Individuals were excluded from participating in this research if they had a back injury within the last year, had any previous back surgery or had any current cardiovascular, neurological, cognitive and musculoskeletal ailments. This research is designed to establish normative data in a healthy population.

The participants who had responded to the advertisement were screened for the inclusion and exclusion criteria to determine if they were suitable to participate in this study. They were provided with a written and verbal explanation of the details of this study. The information sheet provided included the procedure and practices involved in the data collection process, see Appendix C. The participants were provided with the opportunity to have any of their questions to be answered before obtaining the written consent for their participation in the study and were advised that they could withdraw from the study at any point.

4.3.2 Procedure

The preparation of the EMG signal collection, maximal strength test, and submaximal sustained voluntary isometric back extension test procedures and protocols of the participants are presented in this section.

4.3.2.1 EMG preparation

After obtaining the written consent of the participant to agree to participate in the study, the participant was prepared for the data collection procedure. The participants were shaved on the skin surface of the back superficial to left upper erector spinal (UES), 5 cm lateral to the T9 spinous process and left lower erector spinal (LES), 3 cm lateral to the L3 spinous process shown in Figure 4-3 (left). The region around the chest where the ECG electrodes (right arm (RA), left arm (LA) and left leg (LL) were placed was also shaved shown in Figure 4-3 (right). This step was necessary to ensure good skin-electrode contact, and the skin surface was then cleaned using 70% isopropyl alcohol swabs prior to the electrode is attached. The bipolar silver/silver chloride surface electrodes were then attached to the back muscles for the detection of the sEMG signals. Interelectrode impedance was then measured, and an impedance of less than 5 k ohms was considered acceptable [56].

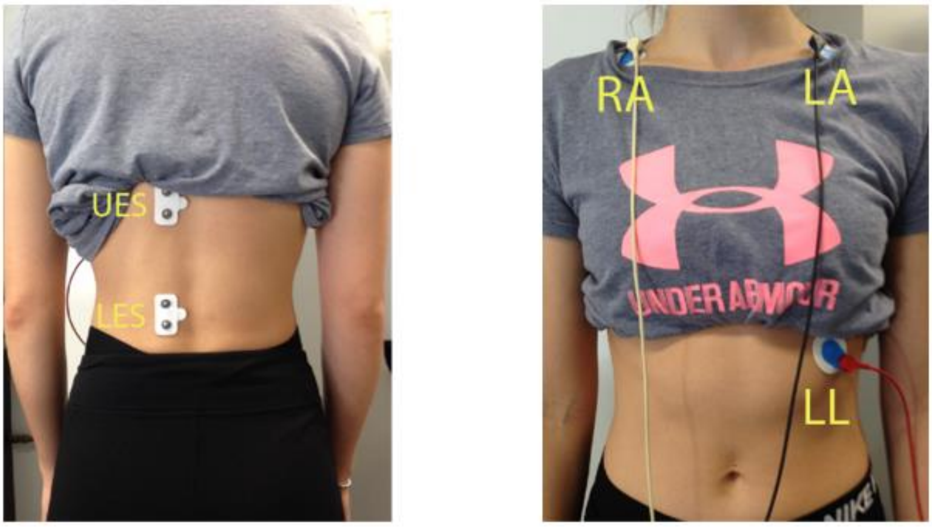

Figure 4-3: Placement of EMG electrodes (left) and ECG electrodes (right)

4.3.2.2 Maximal Strength Test

The participant performed a five-minute standardised warm-up exercise, which included riding an exercise bike that was self-paced to suit the participant. Following the exercise bike ride, the participants performed a warm-up that targeted the back muscles. This involved the participant lifting and lowering a 3 kg box from the floor to mid-thigh to the beat of a metronome (10-15 lifts per minute) for 1-2 minutes. The lifting technique was self-selected by the participant to ensure their comfort during the warmup exercise.

Upon completion of the warmup exercise, the participant was positioned in an upright standing posture on the Active Therapeutic Movement (ATM) back device with the pelvis fixated using quick-release harness shown in Figure 4-4. Fixation of the harness ensured that the participant is not moving or lifted from the ground during the data collection process. A quick-release chest harness was then attached to the participant around the mid-chest area at the T6 level. The chest harness was then attached to a force gauge located at the end of a pulley cable. This force gauge measured the voluntary contraction force exerted by the participant, and the sliding end of the pulley system was locked in place.

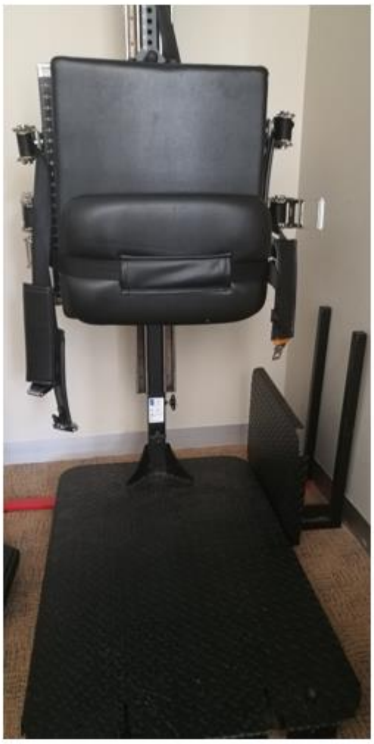

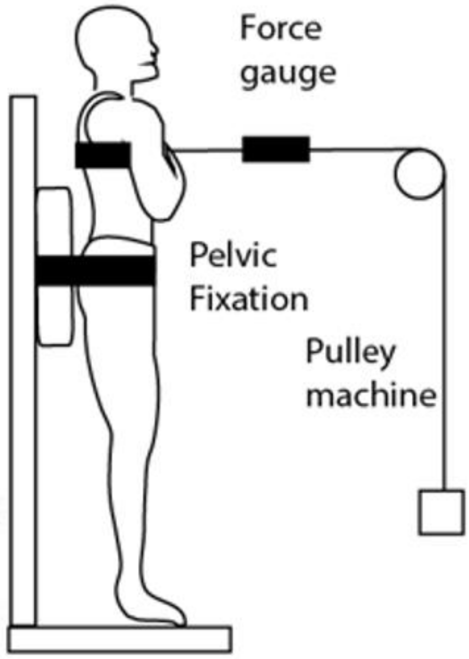

Figure 4-4: AMT back device (left) and experimental setup (right)

After the participant was positioned on the ATM device, they performed a series of 3 to 5 short five-second submaximal isometric back extensions to familiarise themselves with the procedure and also to ensure that the back muscles were successfully warmed up. Approximately three minutes after the warm-up, each participant performed three Maximal Voluntary Isometric Contraction (MVIC) back extensions. This required the participants to try and extend their trunk against the locked pulley system as hard as possible for a period of five seconds. A three-minute rest period was given between each MVIC back extension. The highest peak force recorded during the three MVIC back extensions recorded was selected as the participant's MVIC value.

4.3.2.3 Submaximal Sustained Voluntary Isometric Back Extension Test

After the participants completed the maximal strength test to identify the MVIC force, they were given a three-minute break before proceeding to the sustained submaximal Voluntary Isometric extension tests. The value was used to calculate the submaximal forces required for the participant at 5%, 10%, 15%, 20%, 25%, 30%, 35%, 40%, 45% and 50% of the MVIC.

These tests were conducted by unlocking the other end of the pulley system and attaching weights to until the appropriate submaximal force was recorded on the force gauge. The participant was instructed to maintain the same static upright posture and whilst resisting this force for a period of 15 seconds shown in Figure 4-5.

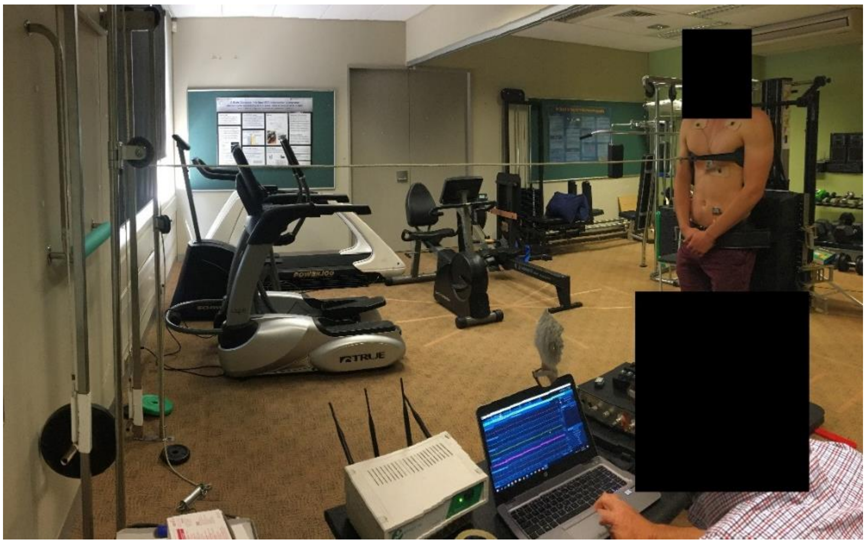

Figure 4-5: Participant performs the task for collection of EMG and ECG signals for different MVIC

The sEMG signals from the upper and lower erector spinae muscles along with the ECG signal from the participant were simultaneously recorded for each of submaximal force values. The participants were then given a 2-minute rest period between each recording of the submaximal force. The order of submaximal forces was randomly allocated to each participant to avoid muscle learning.

4.3.3 Equipment

The equipment used for the collection of the signals from the participants is detailed in Table 4-1, along with their purpose.

Table 4-1: List of equipment used for data collection of sEMG signals from the upper and lower erector spinae muscles and the ECG signals from the chest.

Equipment	Type	Source	Purpose
Noraxon Desk Receiver	Noraxon TeleMyo DTS	Noraxon	Signal Receiver with built-in amplifier, filter, and A/D converter to transmit signals to the computer
Noraxon EMG Transmitter	Noraxon EMG Transmitter	Noraxon	Wireless EMG signal transmitter to measure EMG signals and transmit to the signal receiver, shown in Figure 4-6.
Noraxon ECG Transmitter	Noraxon ECG Transmitter	Noraxon	Wireless ECG signal transmitter to measure ECG signals and transmit to the signal receiver, shown in Figure 4-6

Table 4.1 (continued)

Equipment	Type	Source	Purpose
Standing platform with back support with the attached resistance load suspension for the back-muscle resistance	Active Therapeutic Movement (ATM) back device	Courtesy of the Department of Physiotherapy within the School of Clinical Sciences, AUT North Shore campus	Special standing platform with harnesses to support the posture of the participants when performing the tests
Bipolar Surface electrodes EMG	Norotrode 20™ Bipolar Silver/Silver Chloride EMG electrodes	Myotronics-Noromed, Inc.	Sensors to detect the sEMG signal from the upper and lower erector spinae muscles during the tests
Surface electrodes ECG	Ambu BlueSensor SP ECG electrodes	Ambu	Sensors to detect the ECG signal from the chest during the tests
Laptop PC installed with Noraxon M3 Software	Noraxon M3 platform with myoMUSCLE™ module	Noraxon	To acquire the signal from the Noraxon Desk Receiver.
Exercycle	Monark Ergomedic 828E	Courtesy of the Department of Physiotherapy within the School of Clinical Sciences, AUT North Shore campus	For participants to do the initial warm-up before having to perform the activity
Disposable shavers	BIC	BIC	To shave the hair around the area of the muscle for electrode placement

Table 4.1 (continued)

Equipment	Type	Source	Purpose
Alcoholic swabs	Medi-Swab™ 70% v/v isopropyl alcohol	Smith+Nephew	To cleanse and prepare the skin of the shaved area for electrode placement

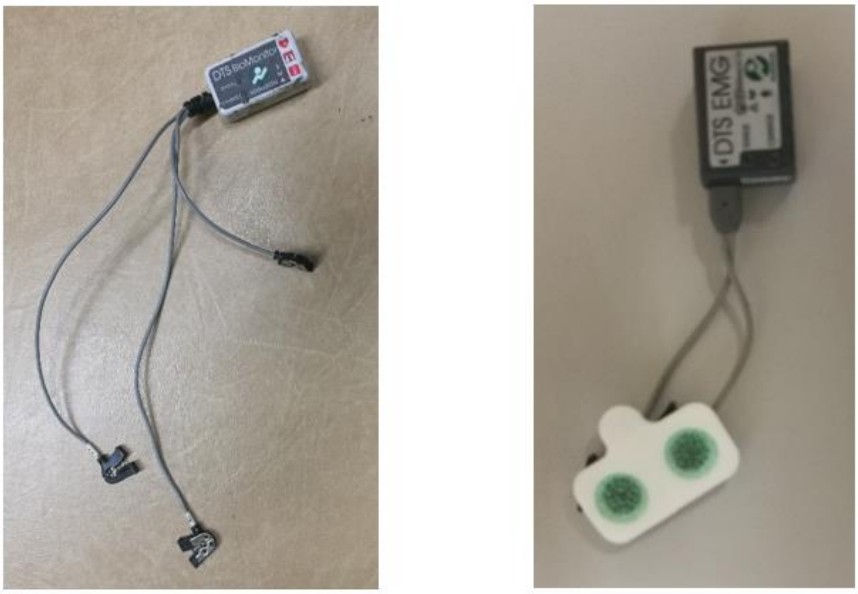

Figure 4-6 Noraxon ECG Transmitter (left) and Noraxon EMG Transmitter (right)

4.3.4 Signal Acquisition Settings

The signals were collected using the wireless Noraxon transmitters that were attached to the EMG and ECG electrodes. The data from the Noraxon transmitters were received using the Noraxon Desk Receiver that is equipped with built-in signal amplification and filter. The Noraxon Desk Receiver is also equipped with an Analogue to Digital (A/D) converter that has been pre-programmed to operate within the voltage output range of ±10 V from the amplifier. This information is transmitted to the computer using a USB cable, and the data is displayed and recorded using the Noraxon M3 Software. The Noraxon M3 Software provides the flexibility of setting certain data collection parameters such as the low pass filter cut-off.

The sEMG signal from the surface electrodes was amplified (x 500), filtered using a 10 Hz cut-off high pass filter that was prebuilt within the hardware of the Noraxon Desk

Receiver and further filtered with a low pass filter set at 1500 Hz cut-off set by the Noraxon M3 software. The signal was received by the computer and displayed on the channels of the Noraxon M3 software. The ECG signal collected from the three chest electrodes was not filtered to ensure better ECG signal detection. The ECG and sEMG signals acquired and recorded simultaneously by the Noraxon M3 system at a sampling frequency of 1500 Hz. As the equipment was electrically isolated, there was no risk of electric shock to either the data collector or the participant.

4.4 Signal Pre-processing

This section covers the pre-processing of the signals collected. One sample sEMG signal from the lower erector spinae muscle contracting at 50% was used in the CWT to determine the most suitable mother wavelets available in MATLAB. The mother wavelets used during the pre-processing stage were Morlet, Mexican Hat, Coiflets (1, 2, 3, 4, 5), Biorthogonal (2.2, 2.4, 2.6, 2.8, 4.4, 5.5, 6.8), Reverse Biorthogonal (2.2, 2.4, 2.6, 2.8, 4.4, 5.5, 6.8), Gaussian (2, 4, 6, 8) and Complex Gaussian (2, 4, 6, 8). This was done using the processes outlined in Figure 4-7 to determine a nominal frequency range for the CWT analysis.

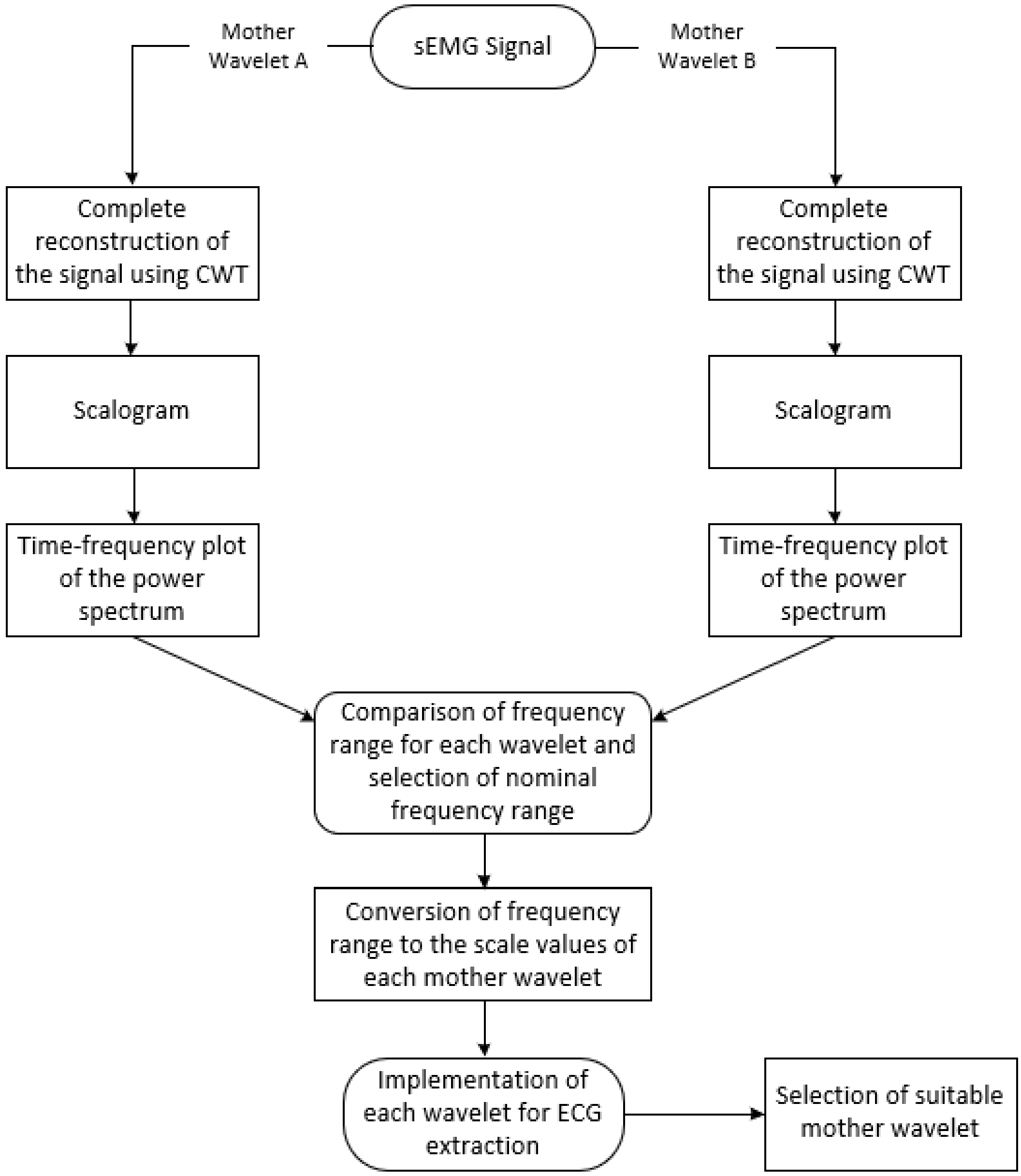

Figure 4-7: Mother Wavelet Selection Flowchart for the selection of the wavelet most suitable for the extraction of the ECG from the sEMG signal

The most satisfactory results were obtained from using the Morlet waveform when implementing the CWT function using the mother wavelets in the program developed in stage 1. The Morlet waveform was the most satisfactory wavelet for analysis as it was able to provide a better reconstruction of the ECG artefacts present within the sEMG signal. The scalogram for the CWT of the sEMG signal using the Morlet wavelet produced better intensity values for the scales at the time locations where the ECG components (QRS waveform) were detected. The Morlet wavelet was selected to provide the most satisfactory results as the reconstruction of the ECG artefacts had minimal effect in the area between the QRS waveforms in comparison to the other mother wavelets.

For further analysing the quality of extraction of the ECG artefacts of the sEMG signal, other functions that were implemented on the sEMG signals and the filtered EMG signals included the power spectrum analysis and total power calculations. The implementation of the window-based calculation of the power spectrum is discussed in section 4.5.

4.5 Feature Extraction and Signal Analysis

This stage of the research covers the signal processing and the analysis of data. The extraction of the ECG artefacts was done by implementing the CWT function using the Morlet wavelet.

The CWT analysis was performed on sEMG signals obtained from the lower erector spinae muscle group of each participant at different submaximal levels of MVIC. Although recorded, the data from the 100% was not included in the analysis as this level of muscle activation seldom occurs during activities of daily living. The 100% condition was mainly intended for the calculation of the force required to obtain the equivalent submaximal levels of MVIC for each participant.

The output of CWT analysis using the Morlet waveform produced the scalogram using the coefficients from the transform that provided the power intensities of each scale index over the time domain. This scalogram data was used to fine-tune the scales for the extraction of the ECG artefacts. The CWT function was implemented using an interface developed using the MATLAB code shown in Figure 4-8. The data files containing the sEMG and ECG signal data were stored in Microsoft Excel worksheets. These worksheets were then loaded into the MATLAB program to employ the CWT function and the signal analysis processes on the sEMG signals.

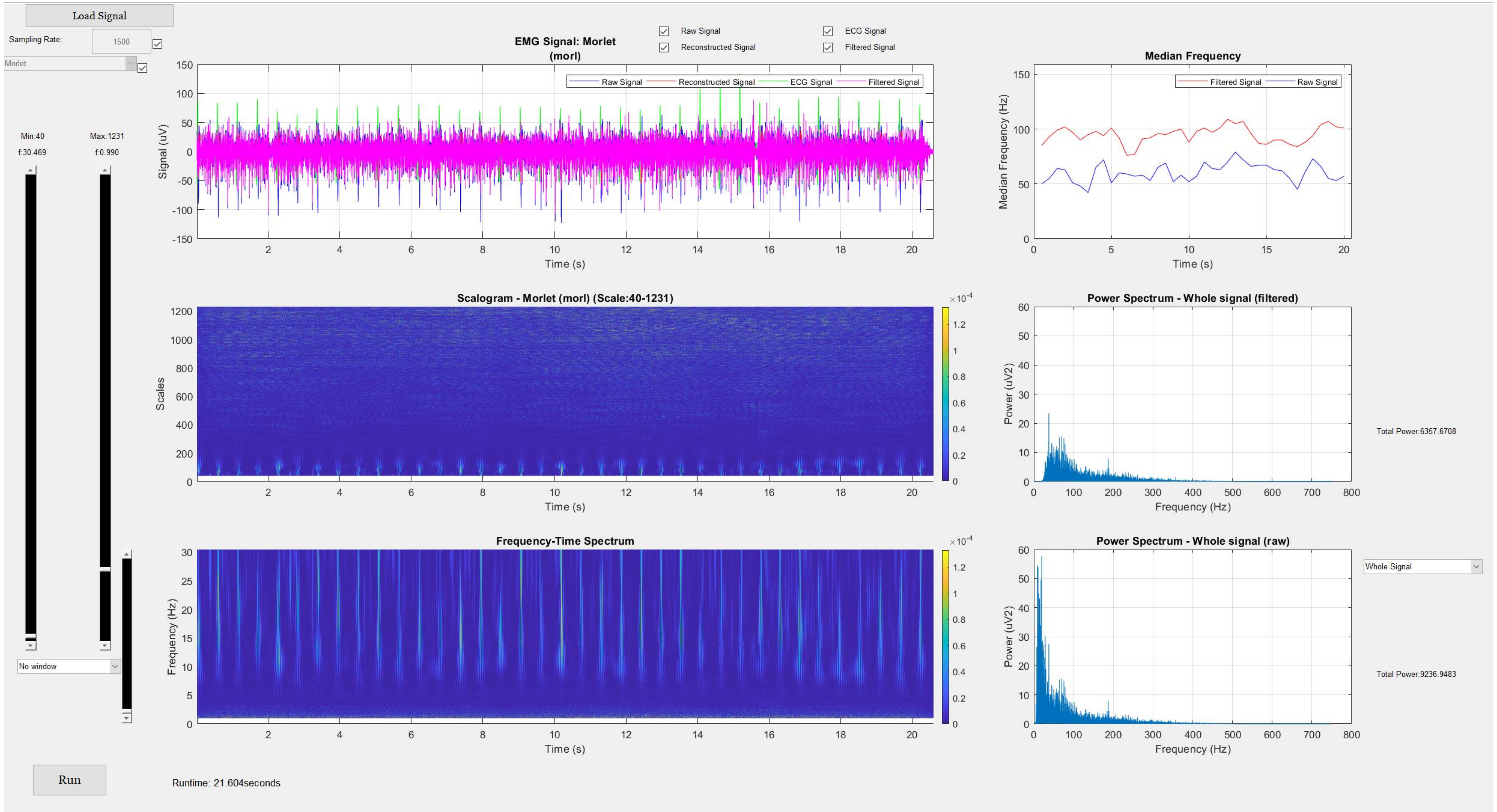

Figure 4-8: Interface developed in MATLAB for the implementation of the CWT on the signals, CWT implemented on sEMG signal from participant 2 at 50% MVIC

For the extraction of the ECG artefacts from the sEMG signals, the CWT function was implemented based on the scales analysed using the scalogram. The frequency spectrum that was generated using the pseudo frequency calculated using the centre frequency of the mother wavelet. The frequency spectrum plot provided information on the dominant frequencies of the extracted signal features and the time localisations of the extracted features.

The coefficients were then manipulated using the threshold function by removing the lower scale (high frequency) components based on the threshold that was calculated for that sample. This was done for the removal of the EMG components that were present in the extracted signal. The implementation of the threshold function on the coefficients of the CWT is illustrated in Figure 4-9.

Scales	Coefficients Sample 1	Coefficients Sample 2		Coefficients Sample N
1	c(1,1)	c(2,1)	....	c(N,1)
2	c(1,2)	c(2,2)	....	c(N,2)
3	c(1,3)	c(2,3)	....	c(N,3)
4	c(1,4)	c(2,4)	....	c(N,4)
5	c(1,5)	c(2,5)	....	c(N,5)
...	....	....	....	....
X	c(1,X)	c(2,X)	....	c(N,X)

Threshold value calculated using the coefficient values of the time sample

Threshold value = c(1,3)

Threshold value = c(2,4)

Threshold value = c(N,2)

Scales	Coefficients Sample 1	Coefficients Sample 2		Coefficients Sample N
1	0	0	....	0
2	0	0	....	c(N,2)
3	c(1,3)	0	....	c(N,3)
4	c(1,4)	c(2,4)	....	c(N,4)
5	c(1,5)	c(2,5)	....	c(N,5)
...	....	....	....	....
X	c(1,X)	c(2,X)	....	c(N,X)

Threshold function removes the coefficient values at low scale (high frequency) to eliminate EMG components

Figure 4-9: Implementation of the Threshold function on the CWT coefficients

The ECG artefacts were reconstructed using the coefficients obtained from the CWT of the sEMG signal. The reconstruction of the signal was set with the sampling frequency of 1500 Hz, the same frequency of the input signal. This was done to ensure that the time domain of the reconstructed signal was the same as the original sEMG signal that was collected from the participant. The ECG data were sampled at 1500 Hz simultaneously when collecting the sEMG data for analysis. The ECG artefacts extracted using the CWT functions were overlapped with the ECG signal to validate the observed ECG artefacts in the reconstructed signal.

The filtered EMG signal was obtained from subtracting the reconstructed ECG artefacts from the raw sEMG signal. The power spectrums of the collected sEMG signals and the filtered EMG signals were obtained using the FFT of the signals. The power spectrum for the window between consecutive QRS coefficient artefacts was observed for the raw sEMG and filtered EMG signal, as shown in Figure 4-10. This was done to observe the amount of power remaining in the signal after the removal of the reconstructed ECG artefacts. These windows were used to observe the amount of power that is removed from the signal when there is a lesser influence of the ECG artefacts as QRS being the dominant component of the ECG signal.

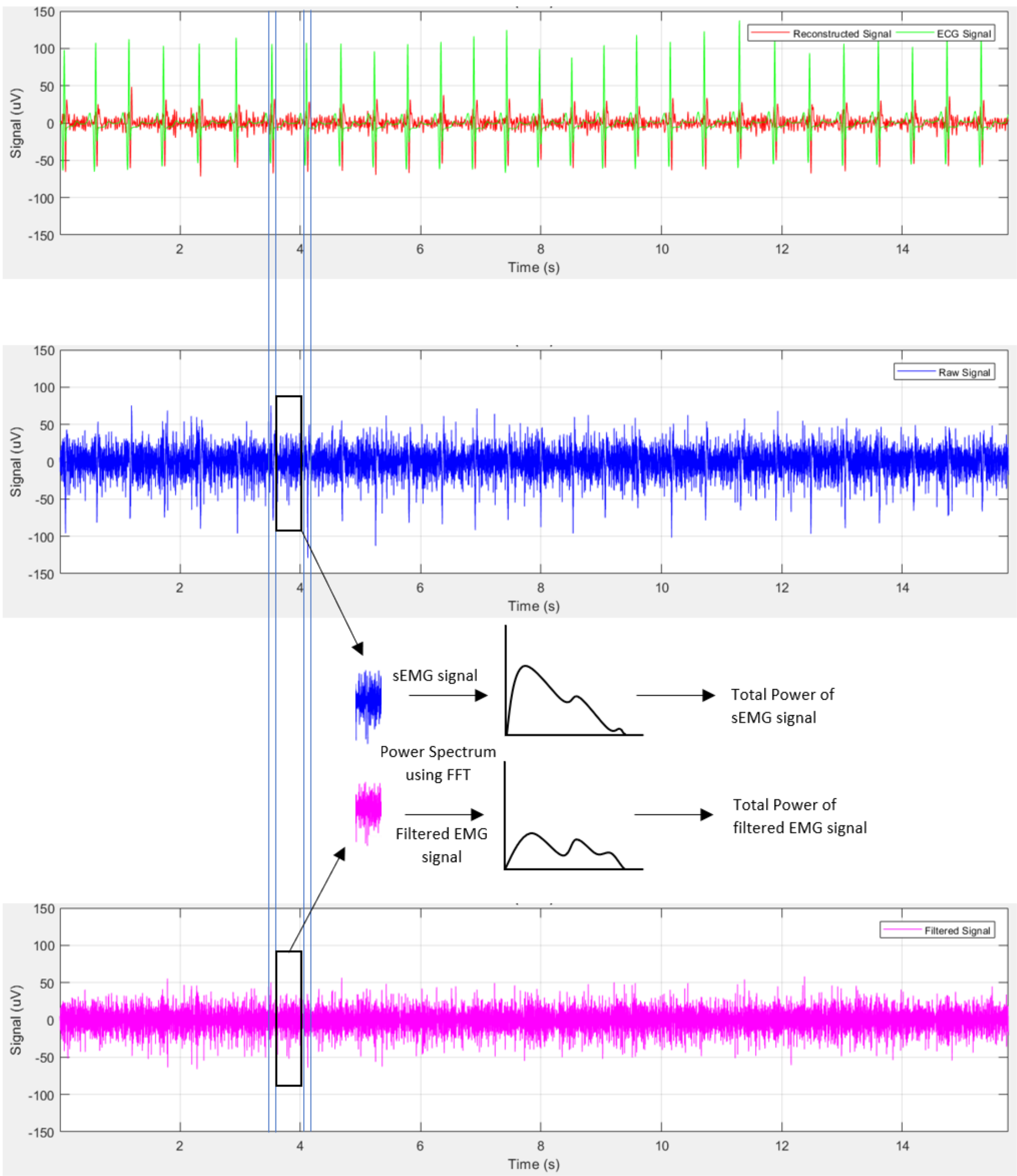

Figure 4-10: Power spectrum of the window between consecutive QRS components

The ECG artefact extraction and signal analysis process are summarized as follows:

1. The original sEMG signal from the lower erector spinae muscle group and the 3-lead ECG signal collected simultaneously for cross-referencing (comparison) from the participant.
2. Implementation of the CWT function on the sEMG signal.
3. The formation of the scalogram and the conversion of scales to pseudo frequencies for the formation of the frequency-time based spectrum plot.
4. The fine-tuning of the scale values based on the scalogram and frequency-time spectrum plot.
5. The reconstruction of the ECG artefacts from the sEMG signal.
6. Cross-referencing of extracted ECG artefacts with the 3-lead ECG signal collected from the participant.
7. The removal of the ECG artefacts from the sEMG signal to produce the filtered EMG signal.
8. Formation of the power spectrum and the calculation of the total power for the sEMG and filtered EMG signal.
9. The identification of QRS complex (estimated using the R peak)
10. The isolation of the equivalent windows between consecutive QRS complexes on the sEMG signal and filtered EMG signals.
11. Formation of the power spectrum and the calculation of the total power for the isolated windows of the sEMG and filtered EMG signal.
12. The median frequency with epochs of half of a second form the sEMG and filtered EMG signals were calculated and plotted.

The next section of the chapter details the results of the signal processing and the CWT analysis performed on the signals collected at various levels of submaximal MVIC from one of the participants.

4.6 Signal Analysis Results

This section presents the results for the analysis performed on one set of the data acquired from one of the seven participants. This includes the presentation of the following information:

1. The original sEMG signal collected from the lower erector spinae muscle.
2. The scalogram of the CWT implemented on the signal.

3. The frequency-time spectrum plot developed from the scale-frequency conversion using centre frequency.
4. The reconstruction of the ECG signal using the selected scales.
5. The cross-referencing of the ECG signal acquired from the participant and the ECG artefact signal from the reconstruction.
6. The filtered EMG signal produced from the removal of the ECG artefact signal from the sEMG signal.
7. The power spectrum of the sEMG signal and the filtered EMG signal.
8. The median frequency of the sEMG signal and the filtered EMG signal

The power spectrum of the filtered EMG signal and sEMG signal acquired from the participant is shown in Figure 4-11 to Figure 4-20. The total power of the windows between the QRS complexes are tabulated in Table 4-2 and plotted to compare the difference in power observed with the removal of the ECG artefacts from the signal. This was done to reinstate the influence of the ECG signal on the sEMG signal and the percentage of EMG signal left within the sEMG signal by observing the windows not influenced by the ECG artefacts. The graphs detailing the remaining power of the EMG in comparison to sEMG is shown in Figure 4-21.

Visual inspection of sEMG data shown in subplot (a) in Figure 4-11to Figure 4-20 from LES muscle contractions at between 5 and 20% MVIC clearly show a regular ECG artefact that corresponds to the QRS complexes detected by the 3-lead ECG shown in subplots (b) and (c) in Figure 4-11 to Figure 4-20. The presence of the ECG artefact in the original sEMG led to a power spectrum that was dominated by the low-frequency components (ECG artefact) of the signal shown in subplot (h) in Figure 4-11 to Figure 4-20. This resulted in median frequency values as low as 30Hz in some of the low-level contractions shown in subplot (g) in Figure 4-11 to Figure 4-20. When the ECG artefact was removed, and the SEMG signal was reconstructed shown in subplot (d) in Figure 4-11 to Figure 4-20 there was a decrease of between 54 and 64% of the total power from the signal. Most of this power was removed from the low-frequency portion of the power spectrum shown in subplot (i) in Figure 4-11 to Figure 4-20. This led to a 2-3-fold increase in the median frequency of the filtered signal when compared to the original signal shown in subplot (g) in Figure 4-11 to Figure 4-20.

ECG artefacts were difficult to be determined visually from the sEMG signals collected at contraction levels of the LES from 25% to 40% shown in subplot (a) in Figure 4-11 to

Figure 4-20. However, decomposition of the signal via wavelet analysis clearly identified ECG artefacts within the signal the corresponded to the 3-lead ECG complexes shown in subplots (b) and c in Figure 4-11 to Figure 4-20. The removal of these artefacts from the sEMG signal shown in subplot (d) in Figure 4-11 to Figure 4-20 substantially changed the power spectrum shown in subplots (h) and (i) in Figure 4-11 to Figure 4-20 and median frequency shown in subplot (g) in Figure 4-11 to Figure 4-20. Figure 4-11 shows the difference in the total power remaining in the signal after the removal of the ECG artefacts in the EMG signal shown subplot (d) in Figure 4 11 to Figure 4 20 in comparison to the original sEMG signal collected subplot (a) in Figure 4-11 to Figure 4-20.

Participant 2: 5% MVIC

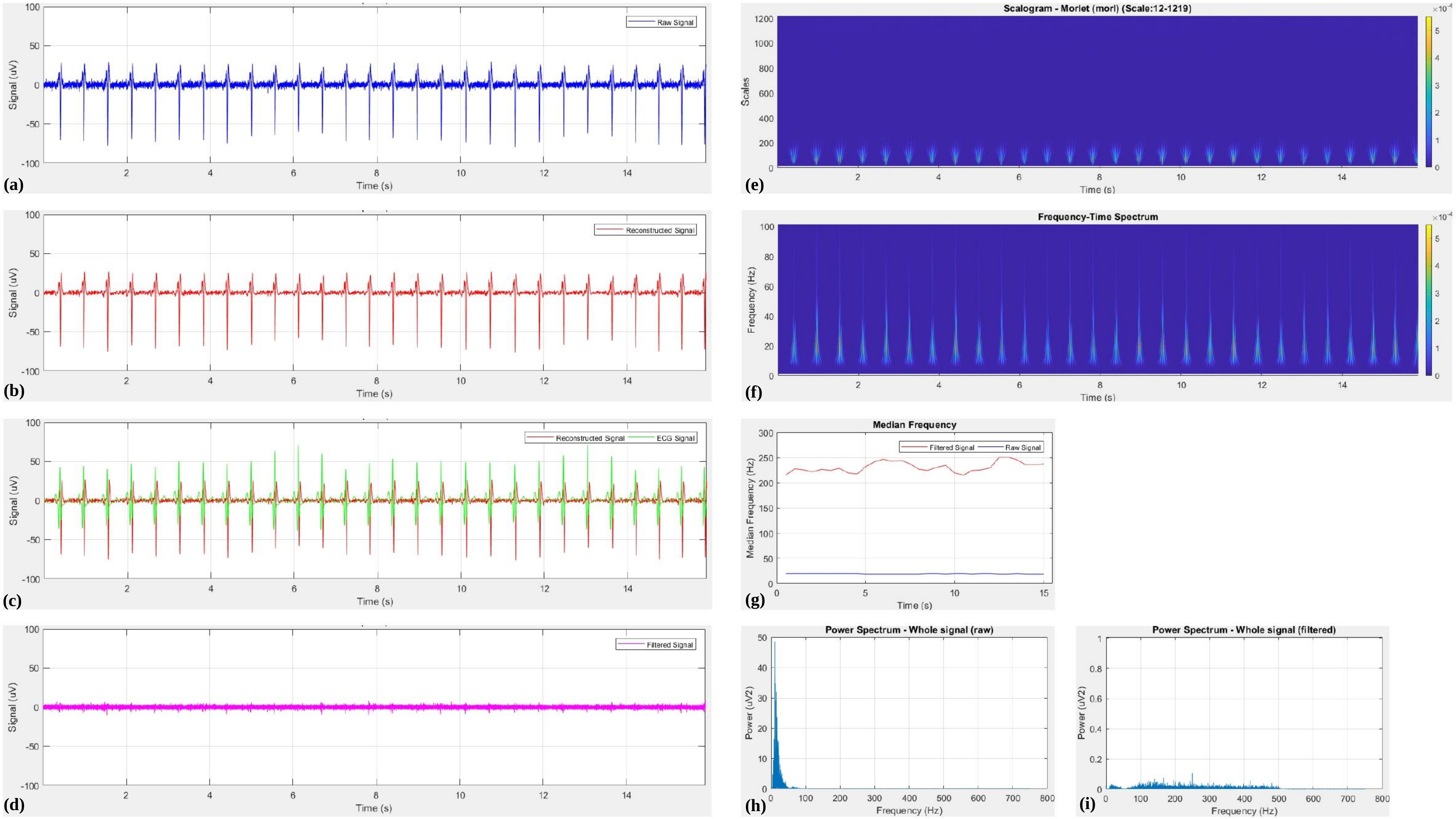

Figure 4-11: Signal output for 5% MVIC (a) Raw sEMG signal collected from participant, (b) Reconstructed ECG signal, (c) Reconstructed ECG signal cross-referenced with collected ECG signal, (d) Filtered EMG signal, (e) Scalogram of the CWT, (f) Frequency-time spectrum plot from the CWT, (g) Median Frequency of the sEMG signal before and after the removal of the ECG signal, (h) Power spectrum of the sEMG signal collected from participant and (i) Power spectrum of the filtered EMG signal.

Participant 2: 10% MVIC

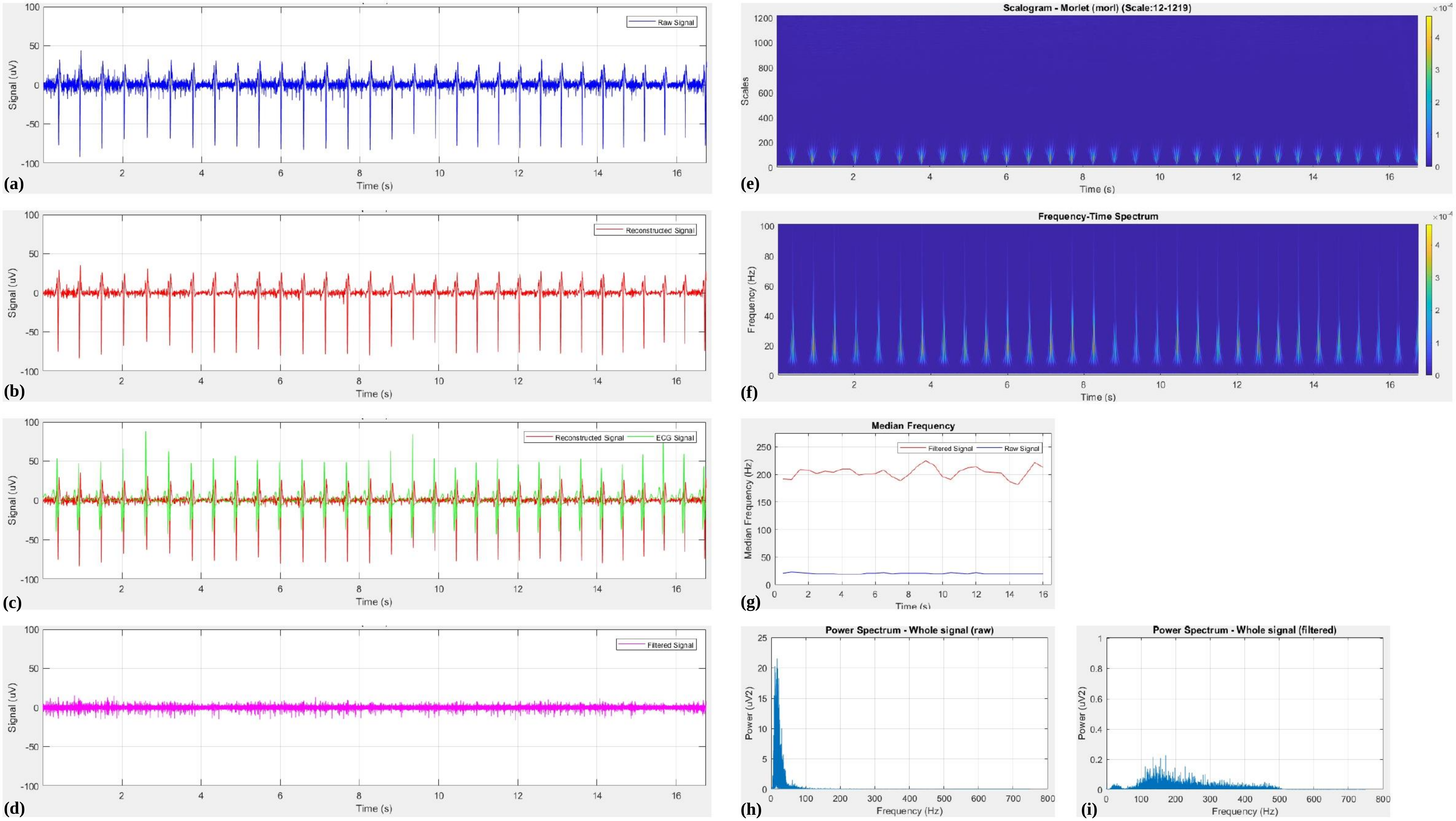

Figure 4-12: Signal output for 10% MVIC (a) Raw sEMG signal collected from participant, (b) Reconstructed ECG signal, (c) Reconstructed ECG signal cross-referenced with collected ECG signal, (d) Filtered EMG signal, (e) Scalogram of the CWT, (f) Frequency-time spectrum plot from the CWT, (g) Median Frequency of the sEMG signal before and after the removal of the ECG signal, (h) Power spectrum of the sEMG signal collected from participant and (i) Power spectrum of the filtered EMG signal.

Participant 2: 15% MVIC

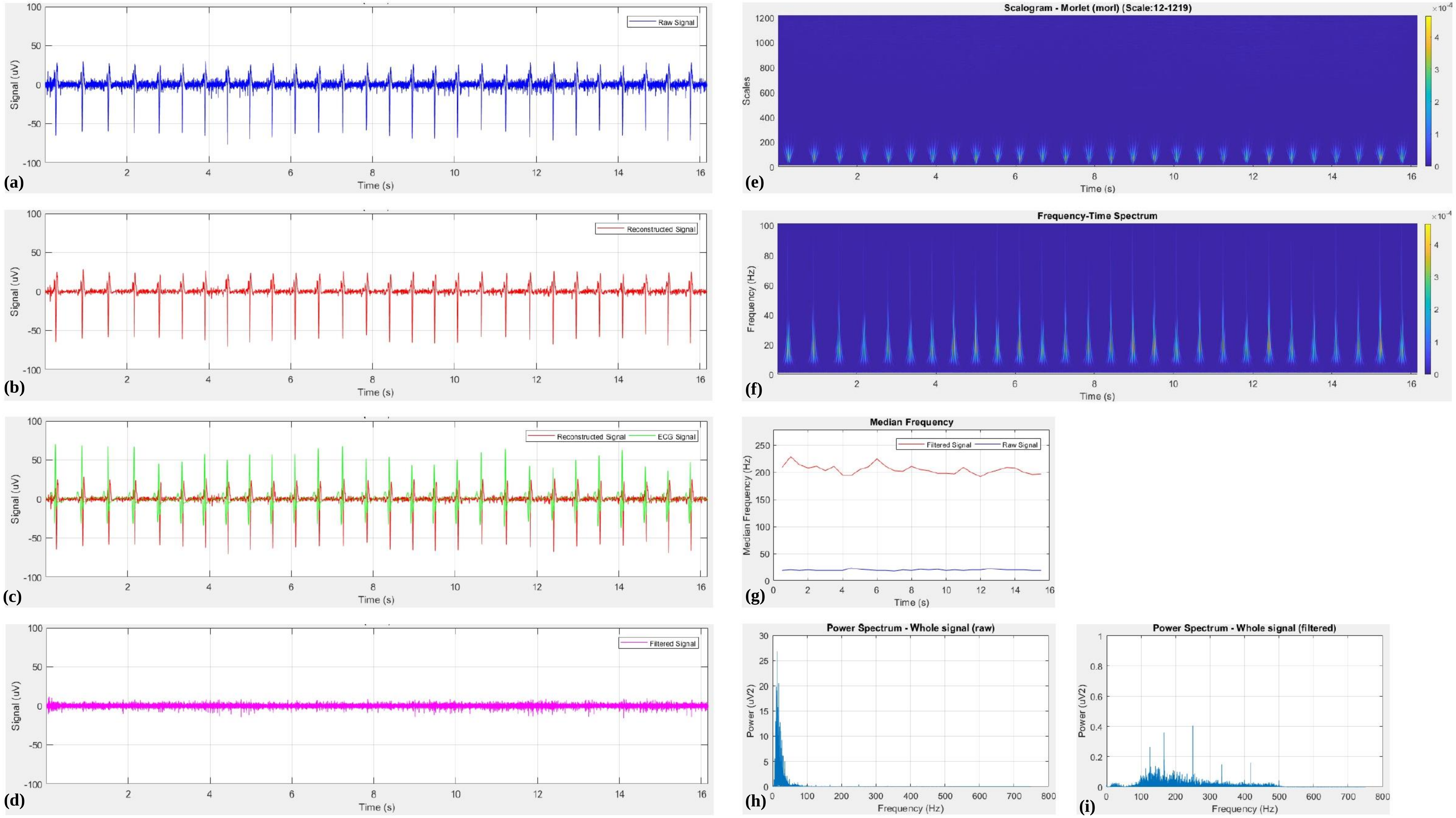

Figure 4-13: Signal output for 15% MVIC (a) Raw sEMG signal collected from participant, (b) Reconstructed ECG signal, (c) Reconstructed ECG signal cross-referenced with collected ECG signal, (d) Filtered EMG signal, (e) Scalogram of the CWT, (f) Frequency-time spectrum plot from the CWT, (g) Median Frequency of the sEMG signal before and after the removal of the ECG signal, (h) Power spectrum of the sEMG signal collected from participant and (i) Power spectrum of the filtered EMG signal

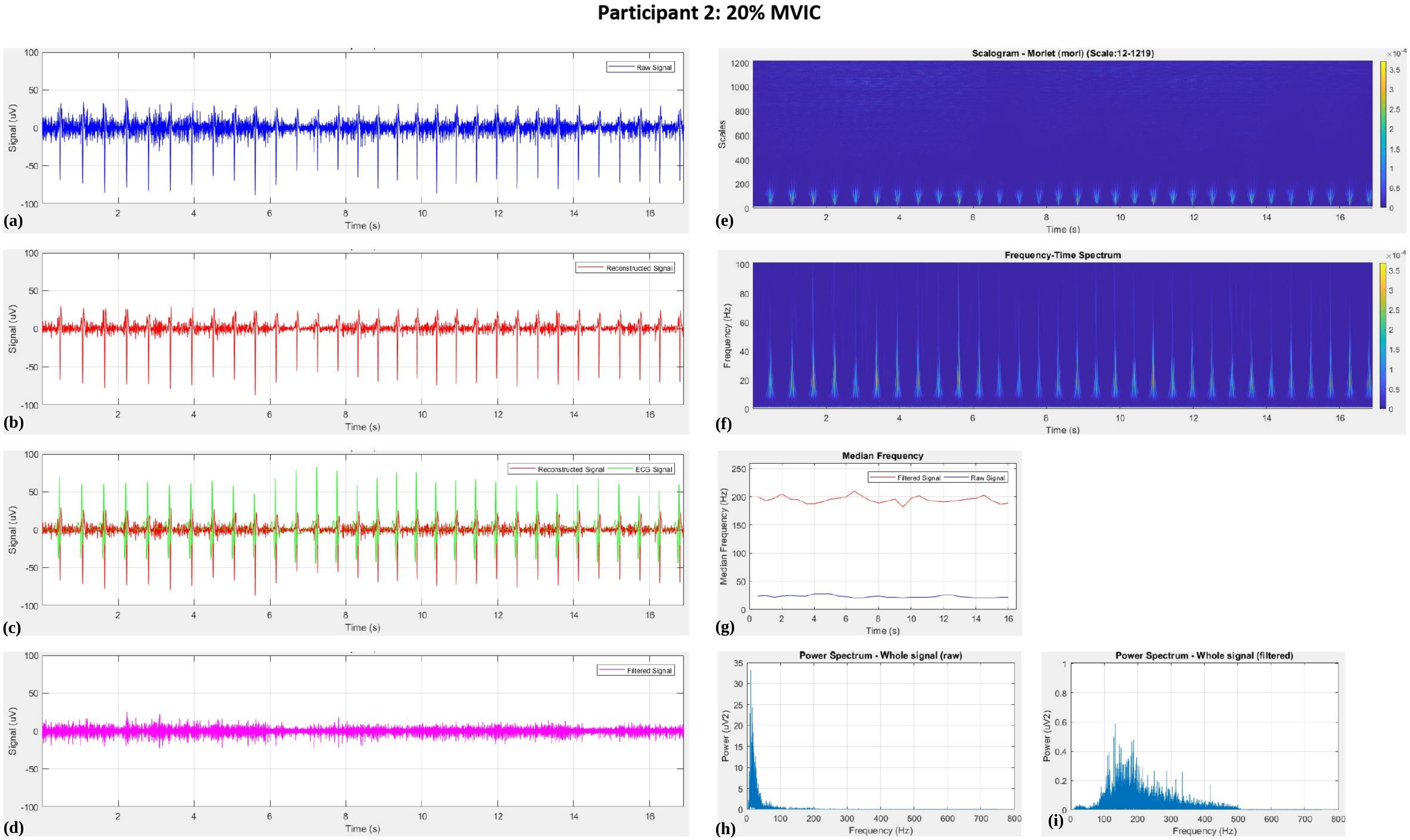

Figure 4-14: Signal output for 20% MVIC (a) Raw sEMG signal collected from participant, (b) Reconstructed ECG signal, (c) Reconstructed ECG signal cross-referenced with collected ECG signal, (d) Filtered EMG signal, (e) Scalogram of the CWT, (f) Frequency-time spectrum plot from the CWT, (g) Median Frequency of the sEMG signal before and after the removal of the ECG signal, (h) Power spectrum of the sEMG signal collected from participant and (i) Power spectrum of the filtered EMG signal.

Participant 2: 25% MVIC

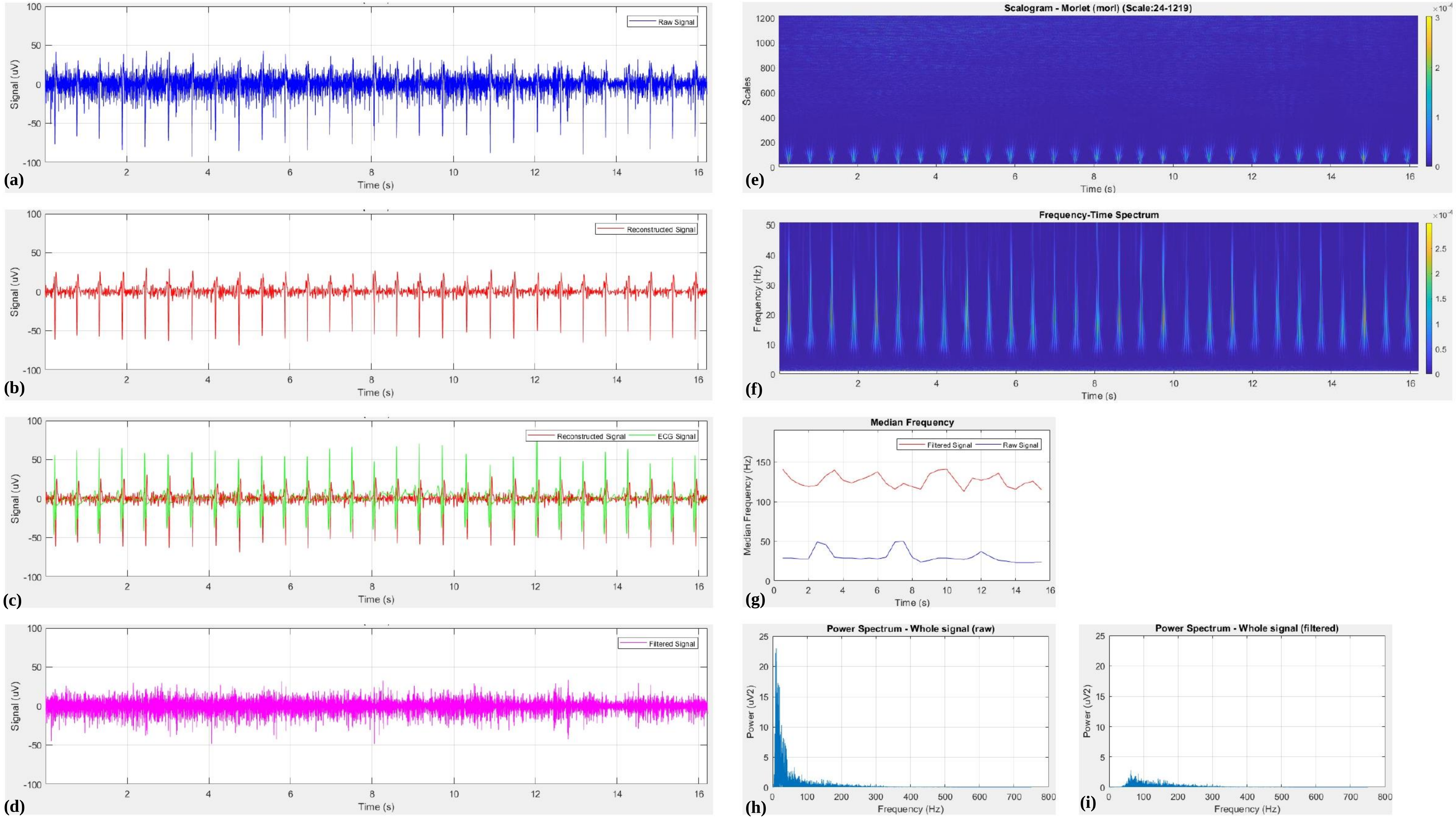

Figure 4-15: Signal output for 25% MVIC (a) Raw sEMG signal collected from participant, (b) Reconstructed ECG signal, (c) Reconstructed ECG signal cross-referenced with collected ECG signal, (d) Filtered EMG signal, (e) Scalogram of the CWT, (f) Frequency-time spectrum plot from the CWT, (g) Median Frequency of the sEMG signal before and after the removal of the ECG signal, (h) Power spectrum of the sEMG signal collected from participant and (i) Power spectrum of the filtered EMG signal.

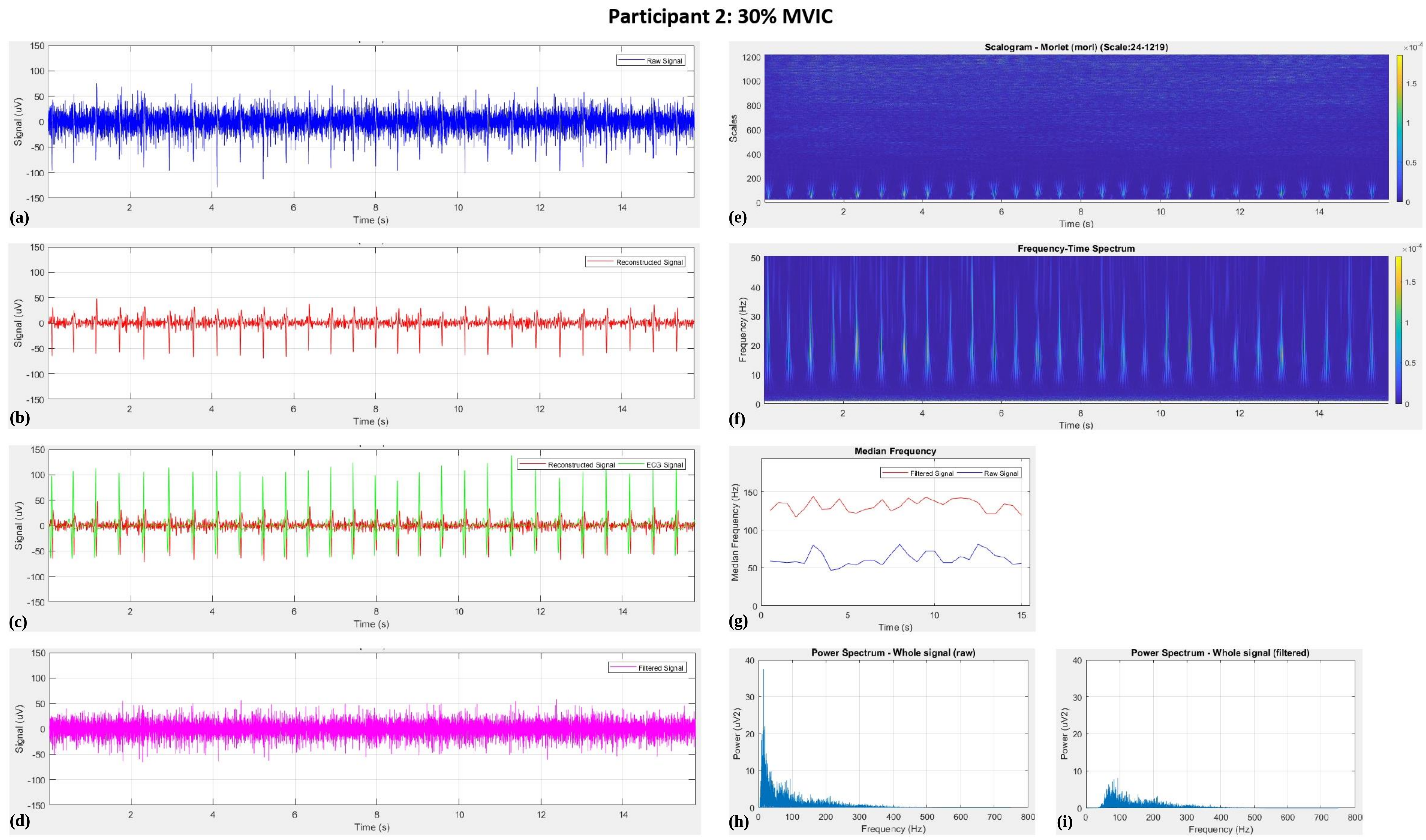

Figure 4-16: Signal output for 30% MVIC (a) Raw sEMG signal collected from participant, (b) Reconstructed ECG signal, (c) Reconstructed ECG signal cross-referenced with collected ECG signal, (d) Filtered EMG signal, (e) Scalogram of the CWT, (f) Frequency-time spectrum plot from the CWT, (g) Median Frequency of the sEMG signal before and after the removal of the ECG signal, (h) Power spectrum of the sEMG signal collected from participant and (i) Power spectrum of the filtered EMG signal.

Participant 2: 35% MVIC

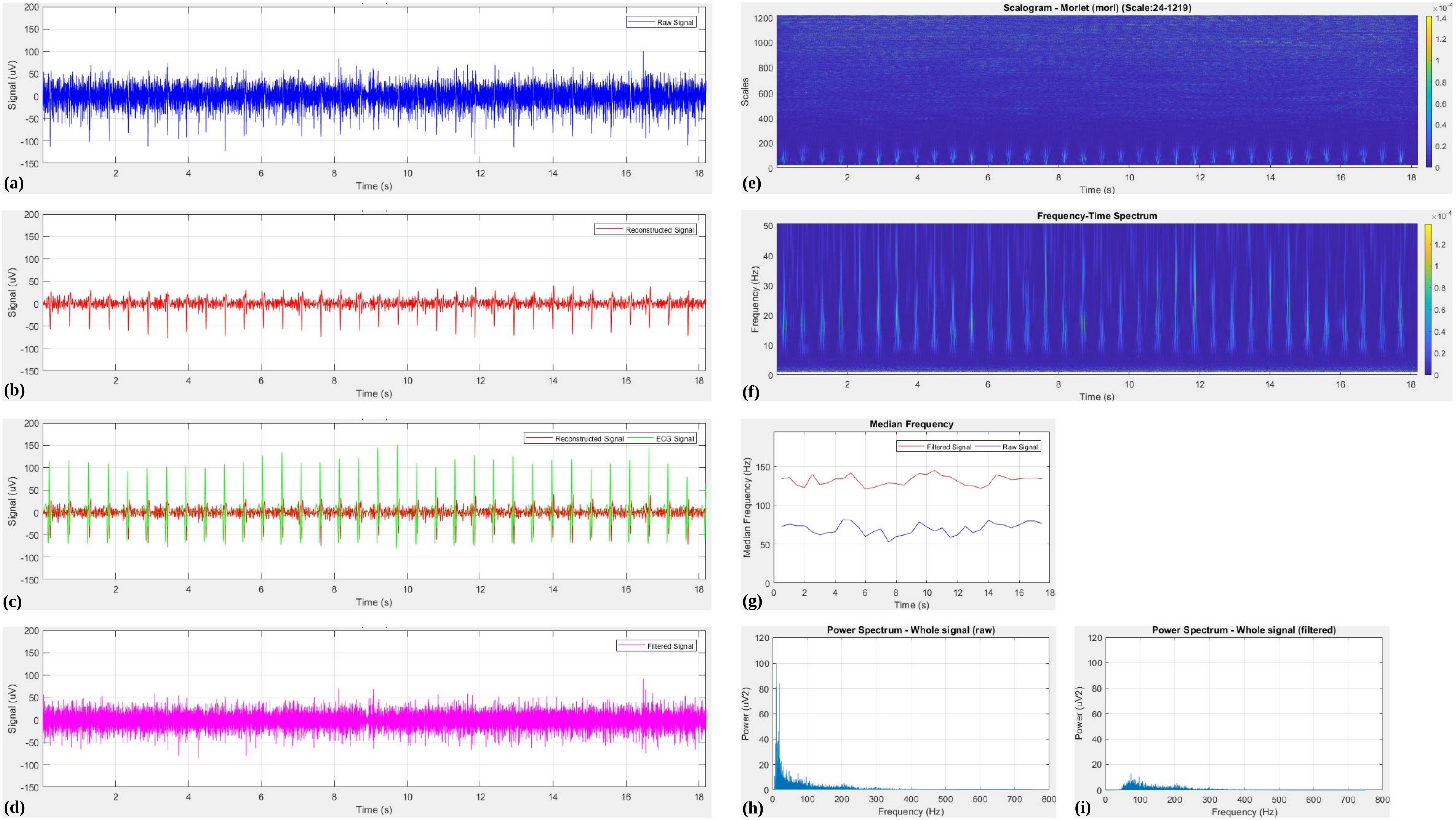

Figure 4-17: Signal output for 35% MVIC (a) Raw sEMG signal collected from participant, (b) Reconstructed ECG signal, (c) Reconstructed ECG signal cross-referenced with collected ECG signal, (d) Filtered EMG signal, (e) Scalogram of the CWT, (f) Frequency-time spectrum plot from the CWT, (g) Median Frequency of the sEMG signal before and after the removal of the ECG signal, (h) Power spectrum of the sEMG signal collected from participant and (i) Power spectrum of the filtered EMG signal.

Participant 2: 40% MVIC

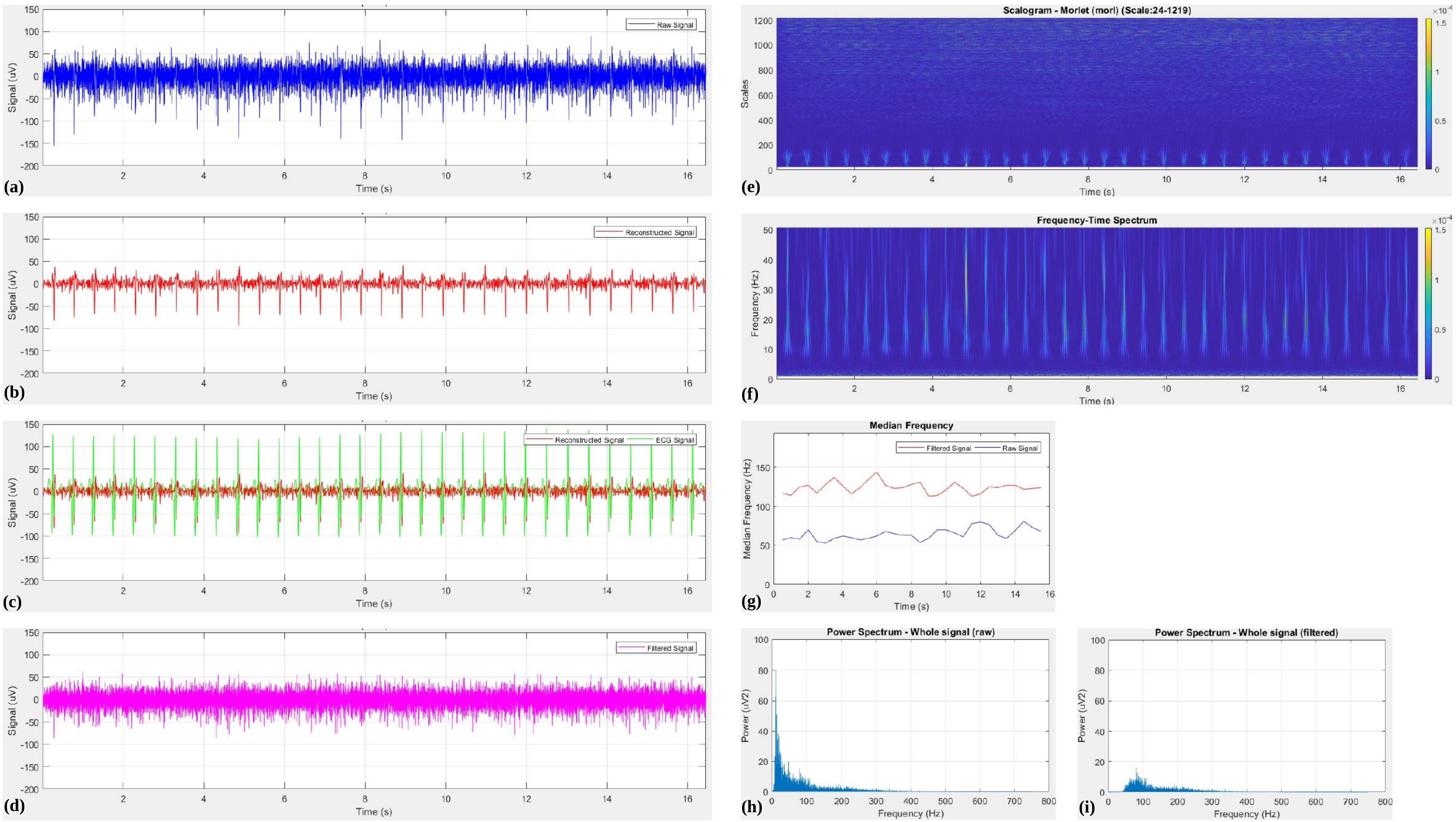

Figure 4-18: Signal output for 40% MVIC (a) Raw sEMG signal collected from participant, (b) Reconstructed ECG signal, (c) Reconstructed ECG signal cross-referenced with collected ECG signal, (d) Filtered EMG signal, (e) Scalogram of the CWT, (f) Frequency-time spectrum plot from the CWT, (g) Median Frequency of the sEMG signal before and after the removal of the ECG signal, (h) Power spectrum of the sEMG signal collected from participant and (i) Power spectrum of the filtered EMG signal.

Participant 2: 45% MVIC

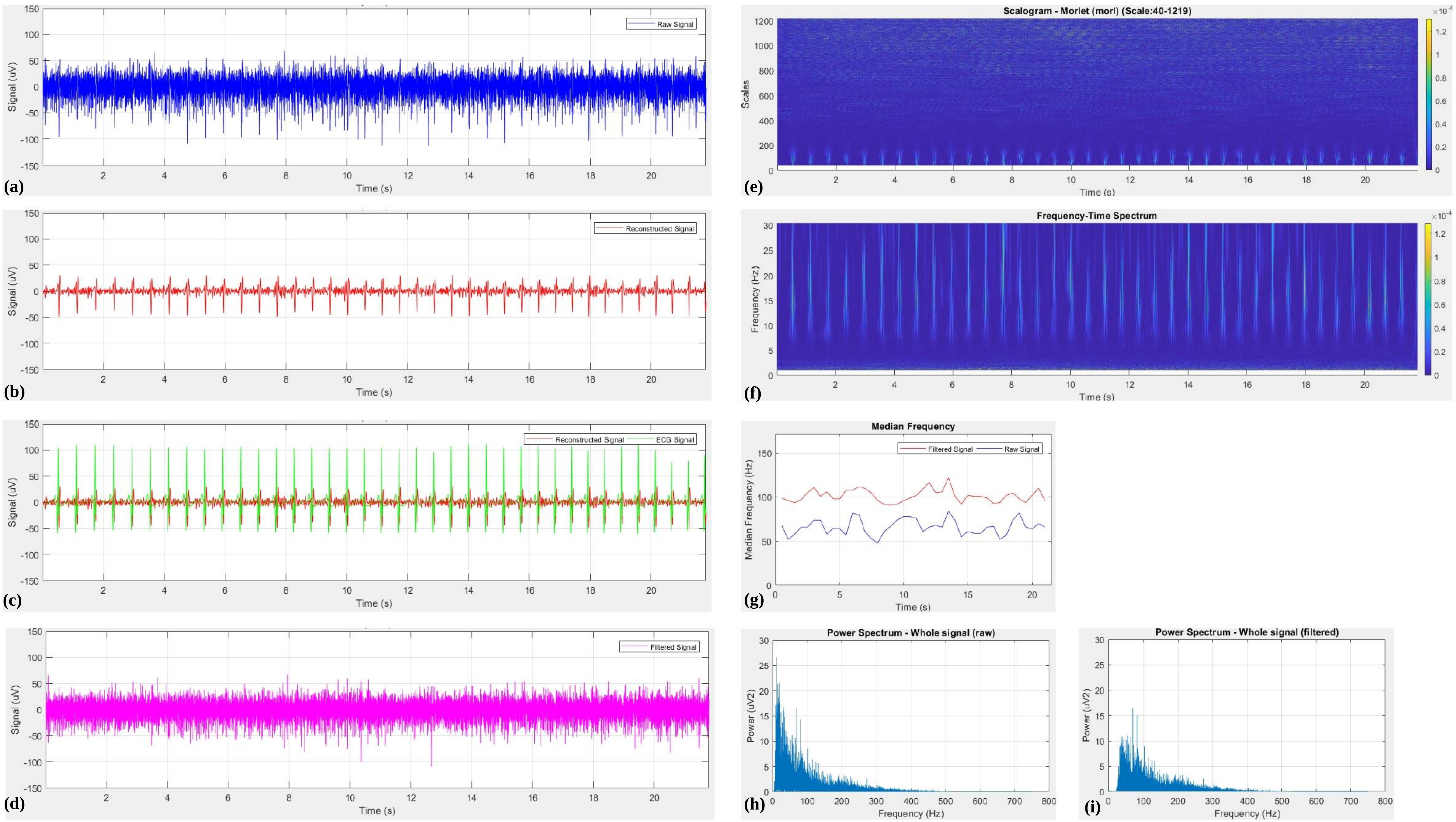

Figure 4-19: Signal output for 45% MVIC (a) Raw sEMG signal collected from participant, (b) Reconstructed ECG signal, (c) Reconstructed ECG signal cross-referenced with collected ECG signal, (d) Filtered EMG signal, (e) Scalogram of the CWT, (f) Frequency-time spectrum plot from the CWT, (g) Median Frequency of the sEMG signal before and after the removal of the ECG signal, (h) Power spectrum of the sEMG signal collected from participant and (i) Power spectrum of the filtered EMG signal.

Participant 2: 50% MVIC

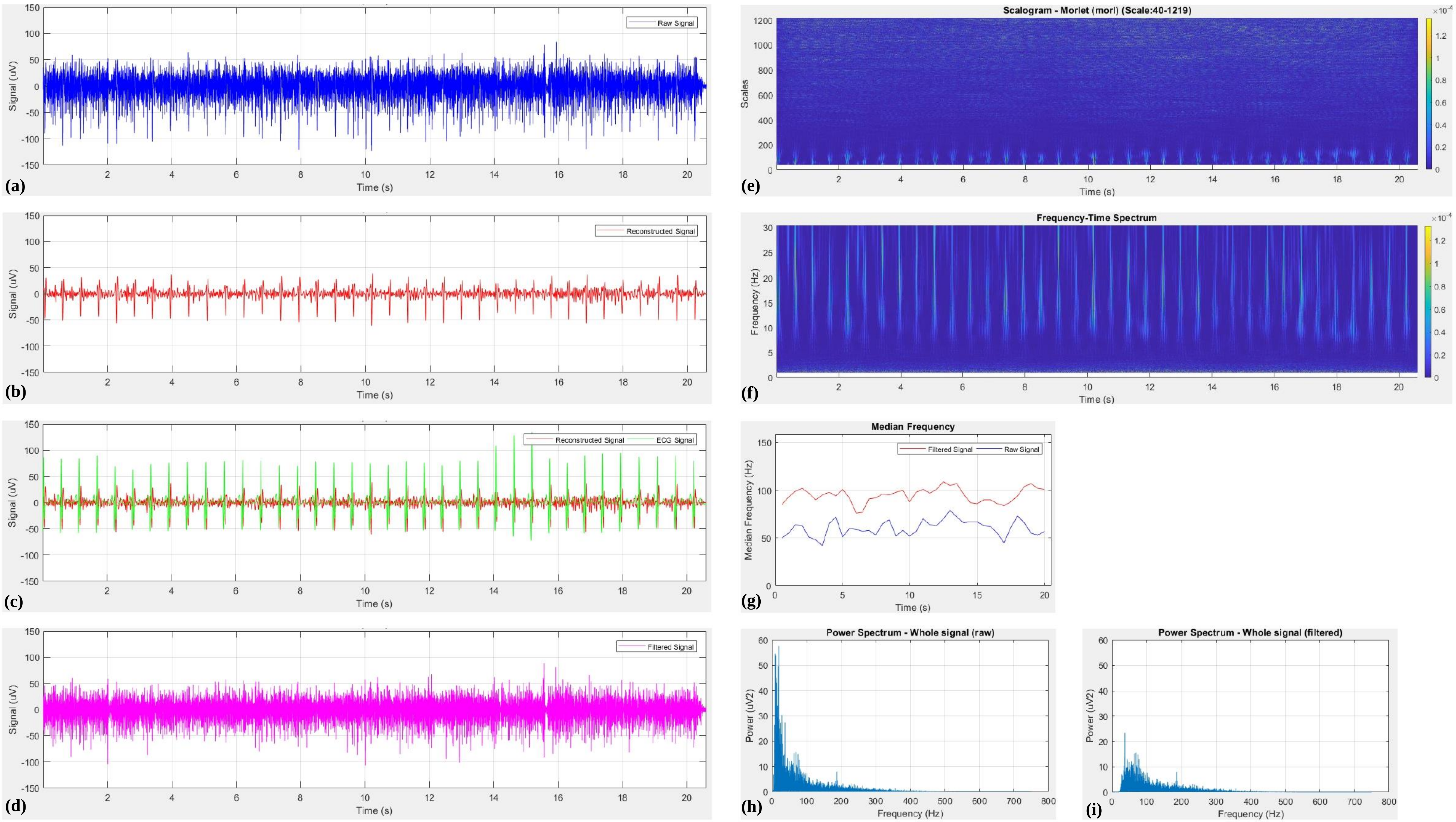

Figure 4-20: Signal output for 50% MVIC (a) Raw sEMG signal collected from participant, (b) Reconstructed ECG signal, (c) Reconstructed ECG signal cross-referenced with collected ECG signal, (d) Filtered EMG signal, (e) Scalogram of the CWT, (f) Frequency-time spectrum plot from the CWT, (g) Median Frequency of the sEMG signal before and after the removal of the ECG signal, (h) Power spectrum of the sEMG signal collected from participant and (i) Power spectrum of the filtered EMG signal.

Table 4-2: Percentage of power remaining in the EMG signal after the removal of the ECG artefacts (window-wise tabulation)

Window	Percentage of power left in EMG signal after removal of the ECG artefacts									
	5%	10%	15%	20%	25%	30%	35%	40%	45%	50%
1	33.27%	37.47%	46.56%	49.92%	70.17%	81.86%	70.74%	78.35%	88.17%	86.30%
2	37.28%	43.29%	43.56%	45.21%	78.36%	80.50%	81.91%	77.01%	86.85%	87.90%
3	38.03%	45.36%	50.61%	42.87%	78.08%	84.70%	82.29%	72.77%	91.38%	89.43%
4	33.88%	48.13%	41.29%	46.73%	77.50%	75.47%	77.85%	79.91%	93.17%	92.23%
5	34.41%	43.68%	50.15%	46.96%	80.32%	80.58%	81.11%	73.49%	90.16%	78.89%
6	31.27%	41.25%	36.60%	49.40%	71.99%	75.02%	78.56%	70.27%	86.86%	86.70%
7	34.57%	33.99%	41.99%	46.73%	77.34%	77.87%	81.51%	76.00%	92.97%	83.94%
8	36.27%	39.20%	41.84%	45.11%	69.36%	77.02%	70.10%	76.34%	89.92%	86.79%
9	36.05%	44.13%	39.71%	46.13%	75.00%	76.32%	82.23%	80.66%	87.99%	80.96%
10	39.37%	35.96%	34.18%	52.25%	71.12%	81.77%	76.59%	78.18%	91.97%	86.64%
11	44.46%	34.16%	40.43%	44.09%	74.46%	88.20%	76.54%	78.09%	92.43%	86.95%
12	32.80%	39.31%	43.66%	41.28%	67.43%	85.83%	70.89%	78.02%	91.53%	89.52%
13	35.54%	31.06%	35.42%	58.39%	72.25%	75.83%	79.88%	74.45%	83.65%	88.64%
14	30.06%	40.60%	40.55%	38.42%	79.73%	78.40%	82.18%	78.66%	90.73%	86.08%
15	31.43%	40.34%	46.01%	39.30%	70.47%	81.65%	75.74%	76.85%	93.54%	88.13%
16	36.94%	40.60%	53.46%	41.26%	72.32%	72.25%	76.98%	79.35%	87.93%	87.12%
17	28.57%	51.36%	46.15%	43.65%	67.17%	82.36%	74.02%	72.55%	91.75%	85.46%
18	31.16%	34.49%	42.12%	40.44%	72.74%	82.44%	74.52%	84.84%	93.39%	89.39%
19	32.98%	38.59%	47.51%	36.59%	79.85%	85.00%	76.92%	81.98%	87.45%	88.61%
20	33.29%	40.03%	50.10%	47.53%	72.15%	82.79%	74.01%	76.35%	93.83%	92.04%
21	30.89%	37.94%	44.08%	42.53%	63.45%	73.74%	79.63%	85.32%	89.22%	90.43%
22	33.80%	41.29%	36.96%	45.92%	75.38%	80.99%	75.76%	73.51%	90.35%	94.19%
23	45.85%	41.75%	47.12%	38.55%	70.36%	81.85%	80.53%	80.89%	88.95%	93.32%
24	31.42%	35.09%	42.11%	40.38%	70.42%	84.14%	78.82%	82.29%	87.50%	89.91%
25	29.74%	38.32%	41.97%	49.22%	65.19%	87.34%	80.07%	75.09%	87.60%	87.76%
26	34.37%	39.68%	37.28%	38.65%	74.06%	78.40%	78.24%	71.01%	87.10%	84.53%
27	29.87%	44.74%	38.66%	45.59%	72.07%	78.70%	79.27%	73.39%	91.61%	89.32%
28		41.97%		39.59%	60.74%		84.40%	88.82%	88.49%	90.24%
29		32.43%		38.27%			84.68%	78.18%	88.90%	90.44%
30		43.96%		42.26%			73.87%	78.12%	95.23%	80.07%
31							81.70%	74.56%	83.62%	79.20%
32							84.13%		91.42%	82.98%
33							80.38%		92.49%	86.28%
34									90.52%	79.13%
35									93.54%	88.11%
36									96.73%	87.98%
37									92.80%	
Average	33.98%	39.98%	42.81%	44.39%	73.19%	80.20%	78.43%	77.59%	90.20%	87.18%
Signal	2.98%	5.03%	5.69%	11.29%	32.82%	54.78%	58.99%	56.24%	71.21%	68.82%

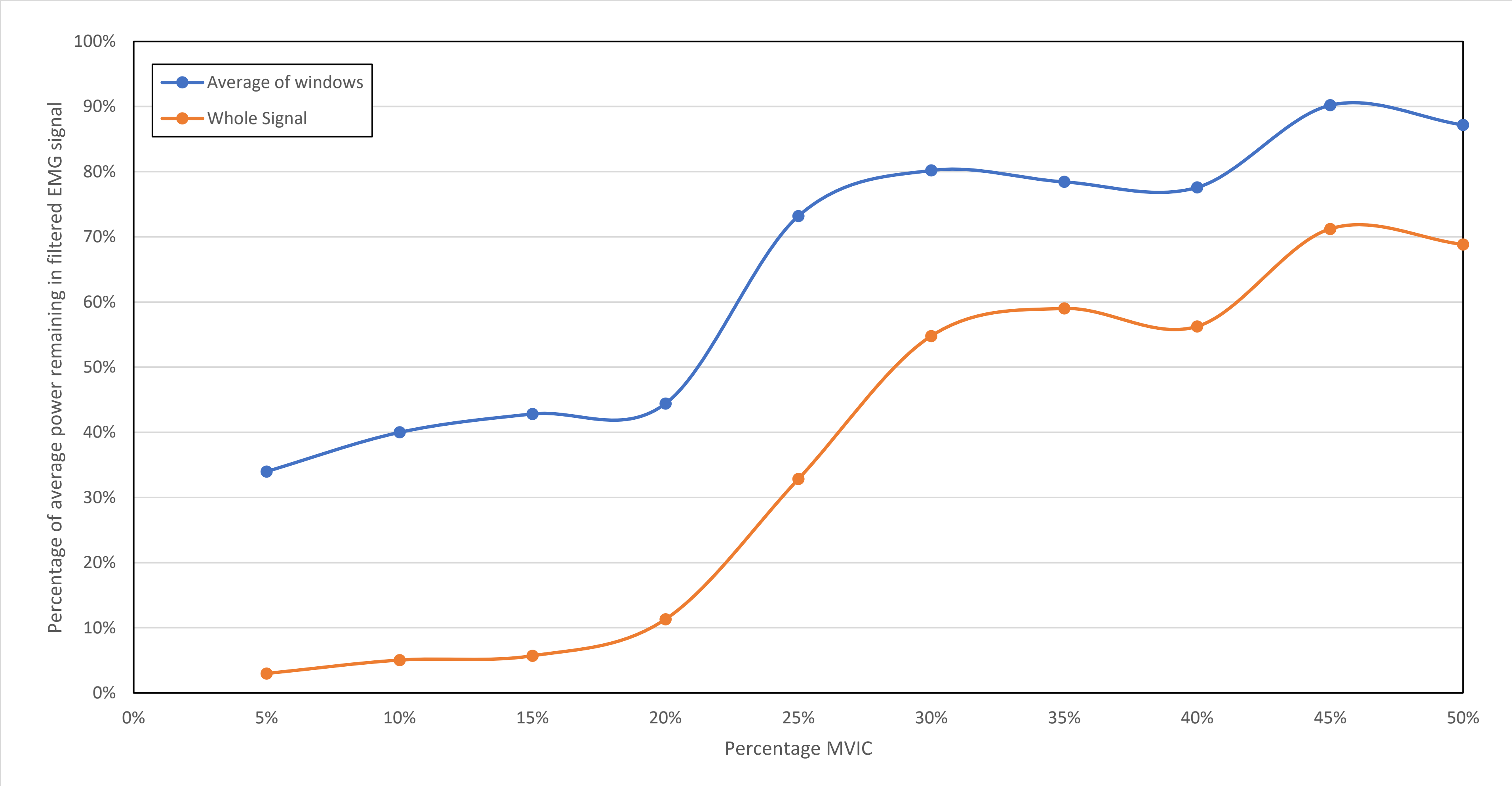

Figure 4-21: Plot showing the difference in power in power remaining in the EMG signal after the removal of ECG artefacts

Chapter 5
Discussion and Conclusions

5.1 Introduction

The aim of this research was to develop a graphical interface using MATLAB for the extraction of ECG artefacts from the EMG signal of the erector spinae (ES) muscles at varying levels of voluntary contractions. This chapter discusses findings from the different stages of this research, which consisted of different stages ranging from software development, signal acquisition, including data collection and conversion, signal pre-processing, and feature extraction. Each step of the research has been analysed and discussed further to observe the contributions and benefits of each stage as well as any possible flaws associated with each step that may have influenced this research in any manner.

The analysis presented in this thesis involved the use of continuous wavelets for feature extraction. The outcomes of the Continuous Wavelet Transform (CWT) procedure for feature extraction and the power spectrums generated from the Fourier Transform (FT) analysis of the signals are further analysed and discussed. The findings of the practical aspects during the signal acquisition stage are discussed. A brief discussion outlining the potential aspects of any future work that could be implemented for further research is also presented.

5.2 Software Development Phase

The software development stage involved the use of MATLAB that formed the core of the research for the development of the signal processing and analysis tools used in this research. The development of the generating windows of data was done using the signal feature identification tools available within MATLAB.

The software development stage used signals obtained from ES muscles during various MVIC as part of the pilot study for developing the program using MATLAB software. This was used to test the performance of the program code as it was being developed. The code was further refined alongside the data collection procedure to ensure improved performance during analysis. The graphical interface is presented in chapter 4.

A significant aspect of this research was the requirement of setting the parameters such as the CWT scale values for optimising the analysis of the signal. To achieve this, the program was required to be executed multiple times with having to manually update the parameters within the program code as needed. This problem was overcome by developing a graphical interface, which provided the flexibility of having to set the necessary settings by selection or entering the value, making it user-friendly.

5.3 Data Collection and Signal Acquisition Phase

The data collection of bio-signals was a significant part and was crucial to this research. EMG data were collected using standardised procedures from the erector spinae muscles of human subjects performing muscle efforts in a range that would be typically used in exercises and activities of daily living. The amplification, conditioning, analogue to digital conversion of the signals collected was done using the Noraxon equipment and data acquisition software. So, any interference in the signal such as movement artefacts were minimised by using these wireless EMG and ECG sensors. The signal acquisition and the data collection parameters like filtering (bandpass (10 Hz to 500 Hz)), amplification and sampling frequency were pre-set by the Noraxon hardware used. The signals were visually generated on the Noraxon collection software to inspect the signal before recording and storing them.

The signals acquired from the pilot study show there was a DC offset bias during the data collection this was removed using developed MATLAB code.

5.4 Signal Pre-processing Phase

The graphical interface developed using MATLAB for the implementation of CWT was limited to the available mother wavelets that included the Morlet, Mexican Hat, Coiflets (1, 2, 3, 4, 5), Biorthogonal (2.2, 2.4, 2.6, 2.8, 4.4, 5.5, 6.8), Reverse Biorthogonal (2.2, 2.4, 2.6, 2.8, 4.4, 5.5, 6.8), Gaussian (2, 4, 6, 8) and Complex Gaussian (2, 4, 6, 8) wavelets. Comparisons between the ECG extraction from the implementation of the CWT function using each of this mother wavelet and the 3-lead ECG signal obtained from a single the participant in the pilot study found that the Morlet wavelet produced the most satisfactory results for the extraction and reconstruction of the ECG signal that could be obtained from the original sEMG signal. This was due to QRS equivalent components within the sEMG signals were extracted in more detail using the Morlet wavelet.

The conversion of wavelet scales to the pseudo frequencies was an essential step in finding the most suitable mother wavelet. This was because the CWT does not provide a frequency-time spectrum that can be related to the signal in the time domain. Hence the need for conversion of the wavelet scales to the pseudo-frequencies. The pseudo-frequency-time spectrum power plot was observed for the selection of the nominal frequency range for extraction of the signal features using each of the mother wavelets. This frequency-time plot provided the details on the amount of power present at each frequency value in the time domain localisation using each mother wavelet.

The percentage of remaining power within each window shown in Figure 4-9 in chapter four was the other aspect for the selection of the suitable mother wavelet. The amount of power that was preserved in the windows post extraction of the ECG artefacts using CWT was the Morlet mother wavelet. Some of the other mother wavelets such as Coiflets, Gaussian and Complex Gaussian produced good reconstructions of the ECG artefacts with reasonable QRS detection. However, the power preservation within the windows of the EMG signal from the CWT using these wavelets was lower than the Morlet wavelet. As discussed in chapter 4, when using Morlet wavelet for CWT, the decrease in power within the window of the EMG signal between consecutive QRS was lower in comparison with the window containing the QRS artefact.

5.5 Feature Extraction and Signal Analysis Phase

The implementation of the CWT function using the Morlet mother wavelet was performed on the signals acquired from the various to extract the ECG artefacts if possible. The results for one of the participants obtained from the implementation of the CWT analysis using the code developed in MATLAB is presented in section 4.6 of chapter four. The results obtained for the seven participants shown in Appendix B are summarised in Table 5-1 with ‘Yes’ indicating successful extraction of ECG artefacts and ‘No’ indicating unsatisfactory results.

Table 5-1: ECG artefact extraction from sEMG signals for all participants from 5% MVIC to 50% MVIC

MVIC	Participant 1	Participant 2	Participant 3	Participant 4	Participant 5	Participant 6	Participant 7
5%	No	Yes	No	Yes	Yes	Yes	Yes
10%	No	Yes	No	Yes	Yes	No	Yes
15%	No	Yes	No	Yes	Yes	No	Yes
20%	No	Yes	No	Yes	Yes	No	Yes
25%	No	Yes	No	Yes	No	No	Yes
30%	No	Yes	No	Yes	No	No	No
35%	No	Yes	No	Yes	No	No	No
40%	No	Yes	No	Yes	No	No	No
45%	No	Yes	No	Yes	No	No	No
50%	No	Yes	No	No	No	No	No

The selection of the scaling parameters for the CWT was based on the scalogram generated for the signal. This was done for each of the signals collected since the power distribution for the signals acquired from each participant at different levels of MVIC were subject to variations such as the nature and activity of the muscle of the participant. The identification of the dominant frequency components using the scalogram and the frequency-time spectrum plot was vital to identify the required scale values. The implementation of the threshold function, as presented in chapter 3 was used to remove the lower scales (high frequency) EMG components that may be present in the CWT coefficients obtained prior to the ECG reconstruction. The reconstructed ECG artefacts were validated by visual comparison of the reconstructed ECG artefact cross-referenced by overlapping the signal on the ECG signal collected from the participant. The median frequency was observed to identify the changes in the frequency components of the signal before and after the removal of the ECG artefacts.

The level of muscle activation showed a direct relation to the EMG components within the sEMG signal. The level of EMG activity was found to be more significant at the higher MVIC which can also be seen in the EMG signal that is obtained after the removal of the ECG artefacts from the collected sEMG signal. The power preservation from the signals obtained from the participant showed that there is a significant difference between the power preservation of the whole signal (filtered EMG: sEMG with the ECG artefacts) and the power preservation from the average of the signal windows (the filtered EMG: sEMG without the ECG artefacts). This is shown in Figure 4-21; it indicates that the QRS equivalent component of the ECG artefacts in the sEMG signal has a significant influence in terms of the total signal power.

After the performing CWT on the sEMG and filtered EMG signals showed the power was preserved in the EMG signal after the removal of the ECG artefacts was higher at higher levels of MVIC, this can be seen in Figure 4-21 as reference for both the whole signal as well as the average of the signal windows. This was due to the increased EMG activity recorded when the ECG component collected with the sEMG signal did not have a significant variation. This showed that the implementation of the CWT with the thresholding gave results that were satisfactory in terms of feature extraction. However, future work to develop an extension programming code for the automated detection of the QRS equivalent components for the extracted ECG signal at different MVIC could be done to improve validation procedures.

The signal processing technique involving the implementation of the CWT and thresholding on the sEMG signals across all the participants were analysed. The results showed that for more than half of the participants, the EMG and ECG signals could be successfully extracted for levels of MVIC up to 20%. Considering the previous researches reviewed in the literature in Section 2.5, the analysis provided satisfactory outcomes. The investigations considered in the literature focused on studies involving signals with minimal muscle activity or consisted of a simulated element. The use of sEMG signals from the back muscle of participants at varying levels of MVIC provided the opportunity to assess the effectiveness of the proposed technique. The researches reviewed in Section 2.5 discusses the efficacy of various signal processing methods with low muscle activity that can be compared to that of the lower levels of MVIC. The findings of this research show that the proposed signal processing technique was successful in the separation of the ECG and EMG signals from sEMG signals collected at lower levels of MVIC.

5.6 Conclusions

This research has investigated the various aspects involved in the implementation of signal processing techniques of Wavelet and Fourier transforms. The extraction of ECG artefacts from the sEMG signal and analysing them was the focus of this research. The acquire signals from seven participants with healthy back muscles for analysis was a significant part of this research.

The summary of the research covered included:

- The development of the code using MATLAB was the CWT with thresholding to extract the ECG artefacts from the sEMG signal.
- Understanding the collection of the sEMG and ECG signals with the develop procedures and protocol.
- The selection of a mother wavelet to be used with CWT implementation for the extraction of the ECG artefacts from the acquired sEMG signals at various submaximal levels of MVIC.

This research produced results that demonstrated the developed technique is promising, and some future work may be done to improve the extraction quality and implementation of more validation methods.

References

[1] Y. Hu, L. He, J. Shi, and W. Wang, "A methodological approach to remove the ECG noise from the EMG signals," in IEEE 2011 10th International Conference on Electronic Measurement & Instruments, 2011, vol. 3, pp. 228-231.

[2] X. Cao and Z. Li, "Denoising of ECG Signal Based on a Comprehensive Framework," in 2010 International Conference on Multimedia Technology, 2010, pp. 1-4.

[3] F. R. Hashim, J. J. Soraghan, L. Petropoulakis, and N. G. N. Daud, "EMG cancellation from ECG signals using modified NLMS adaptive filters," in 2014 IEEE Conference on Biomedical Engineering and Sciences (IECBES), 2014, pp. 735-739.

[4] M. B. I. Raez, M. S. Hussain, and F. Mohd-Yasin, "Techniques of EMG signal analysis: detection, processing, classification and applications," Biological procedures online, vol. 8, pp. 11-35, 2006.

[5] R. Dozio and M. J. Burke, "Optimised design of the front-end analogue high-pass filter for a diagnostic quality ECG monitoring system," in 2009 Annual International Conference of the IEEE Engineering in Medicine and Biology Society, 2009, pp. 1770-1773.

[6] J. Sørensen, L. Johannesen, U. Grove, K. Lundhus, J. Couderc, and C. Graff, "A comparison of IIR and wavelet filtering for noise reduction of the ECG," in 2010 Computing in Cardiology, 2010, pp. 489-492.

[7] L. Smital, M. Vítek, J. Kozumplík, and I. Provazník, "Adaptive Wavelet Wiener Filtering of ECG Signals," IEEE Transactions on Biomedical Engineering, vol. 60, no. 2, pp. 437-445, 2013.

[8] A. Verma, Pratik, and G. Pradhan, "Electrocardiogram denoising using Wavelet decomposition and EMD domain filtering," in 2016 IEEE Region 10 Conference (TENCON), 2016, pp. 2185-2189.

[9] X. Zhou, X. Ma, and Y. Li, "An adaptive threshold algorithm based on wavelet in QRS detection," in 2014 International Conference on Audio, Language and Image Processing, 2014, pp. 858-862.

[10] R. H. Chowdhury, M. B. I. Reaz, and M. A. M. Ali, "Determination of Muscle Fatigue in SEMG Signal Using Empirical Mode Decomposition," in 2014 IEEE Conference on Biomedical Engineering and Sciences (IECBES), 2014, pp. 932-937.

[11] F. Nougarou, D. Massicotte, and M. Descarreaux, "Efficient combination of DWT and ICA to localize and remove ECG from surface electromyography measurement," in 2013 18th International Conference on Digital Signal Processing (DSP), 2013, pp. 1-6.

[12] S. Abbaspour, A. Fallah, M. Linden, and H. Gholamhosseini, "A novel approach for removing ECG interferences from surface EMG signals using a combined ANFIS and wavelet," vol. 26, ed, 2016, pp. 52-59.

[13] M. B. Raez, M. S. Hussain, and F. Mohd-Yasin, "Techniques of EMG signal analysis: detection, processing, classification and applications," Biological Procedures Online, vol. 8, pp. 11-35, 2006.

[14] G. Finkelstein, "Mechanical neuroscience: Emil du Bois-Reymond's innovations in theory and practice," Frontiers in Systems Neuroscience, vol. 9, no. 133, p. 133, September 2015.

[15] B. Lüderitz, "Etienne Jules Marey (1830–1904)," Journal of Interventional Cardiac Electrophysiology, vol. 12, no. 1, pp. 91-92, January 2005.

[16] M. Kazamel and P. P. Warren, "History of electromyography and nerve conduction studies: A tribute to the founding fathers," Journal of Clinical Neuroscience, vol. 43, pp. 54-60, September 2017.

[17] S. S. Barold, "Willem Einthoven and the Birth of Clinical Electrocardiography a Hundred Years Ago," Cardiac Electrophysiology Review, vol. 7, no. 1, pp. 99-104, January 2003.

[18] F. H. Netter, J. P. Iannotti, R. D. Parker, C. A. G. Machado, and J. A. Craig, The Netter Collection of Medical Illustrations: Musculoskeletal System, Volume 6, Part III - Biology and Systemic Diseases, 2nd ed. Philadelphia, PA: Saunders, 2013.

[19] Y. Gao, Biology of Vascular Smooth Muscle: Vasoconstriction and Dilatation. Singapore: Springer, 2017.

[20] R. Merletti and P. Parker, Electromyography: Physiology, Engineering, and Noninvasive Applications. Hoboken, NJ: IEEE/John Wiley & Sons, 2004.

[21] R. H. Chowdhury, M. B. Reaz, M. A. Ali, A. A. Bakar, K. Chellappan, and T. G. Chang, "Surface Electromyography Signal Processing and Classification Techniques," Sensors, vol. 13, no. 9, pp. 12431-66, September 2013.

[22] B. M. Idrees and O. Farooq, "Estimation of muscle fatigue using wavelet decomposition," in 2015 Fifth International Conference on Digital Information Processing and Communications (ICDIPC), 2015, pp. 267-271.

[23] S. Kalwa and H. T. Patil, "Neuromuscular disease classification based on discrete wavelet transform of dominant motor unit action potential of EMG signal," in 2015 International Conference on Information Processing (ICIP), 2015, pp. 708-713.

[24] A. Belkhou, A. Jbari, and L. Belarbi, "A continuous wavelet based technique for the analysis of electromyography signals," in 2017 International Conference on Electrical and Information Technologies (ICEIT), 2017, pp. 1-5.

[25] T. Kamali, R. Boostani, and H. Parsaei, "A Multi-Classifier Approach to MUAP Classification for Diagnosis of Neuromuscular Disorders," IEEE Transactions on Neural Systems and Rehabilitation Engineering, vol. 22, no. 1, pp. 191-200, 2014.

[26] M. Rezki, I. Griche, and M. Ayad, "Study of muscle fatigue across typical physical exercise by using different techniques of analysis," in 2017 5th

International Conference on Electrical Engineering - Boumerdes (ICEE-B), 2017, pp. 1-5.

[27] M. Arvetti, G. Gini, and M. Folgheraiter, "Classification of EMG signals through wavelet analysis and neural networks for controlling an active hand prosthesis," in 2007 IEEE 10th International Conference on Rehabilitation Robotics, 2007, pp. 531-536.

[28] N. S. Rekhi, H. Singh, A. S. Arora, and A. K. Rekhi, "Analysis of EMG signal using wavelet coefficients for upper limb function," in 2009 2nd IEEE International Conference on Computer Science and Information Technology, 2009, pp. 357-361.

[29] G. A. Stouffer, M. S. Runge, C. Patterson, J. S. Rossi, and F. H. Netter, Netter's cardiology. Philadelphia, PA : Elsevier, 3rd edition., 2019.

[30] R. Stroobandt, S. S. Barold, and A. F. Sinnaeve, ECG from Basics to Essentials: Step by Step. Wiley Blackwell, 2016.

[31] K. P. Moses, Atlas of clinical gross anatomy. Philadelphia, PA : Elsevier/Saunders, Second edition., 2013.

[32] J. T. Hansen, F. H. Netter, and C. A. G. Machado, Netter's Clinical Anatomy (Netter Basic Science). Philadelphia, PA: Elsevier, 2019.

[33] R. L. Drake, W. Vogl, A. W. M. Mitchell, R. Tibbitts, P. Richardson, and A. Horn, Gray's Basic Anatomy. Philadelphia, PA: Elsevier, 2018.

[34] J. Cholewicki and S. M. McGill, "Mechanical stability of the in vivo lumbar spine: Implications for injury and chronic low back pain," (in English), Clinical Biomechanics, Article vol. 11, no. 1, pp. 1-15, 01 / 01 / 1996.

[35] J. Taelman, S. V. Huffel, and A. Spaepen, "Wavelet-Independent Component Analysis to remove Electrocardiography Contamination in surface Electromyography," in 2007 29th Annual International Conference of the IEEE Engineering in Medicine and Biology Society, 2007, pp. 682-685.

[36] H. Satoshi et al., "Independent Component Analysis using wavelet transform and its application to biological signals," in 2008 International Conference on Wavelet Analysis and Pattern Recognition, 2008, vol. 1, pp. 436-441.

[37] L. Smital, M. Vitek, J. Kozumplik, and I. Provaznik, "Adaptive wavelet Wiener filtering of ECG signals," IEEE Trans Biomed Eng, vol. 60, no. 2, pp. 437-45, Feb 2013.

[38] C. Mahipal Singh, K. Rajiv Kumar, and S. Akshay Kumar, "Comparison between different wavelet transforms and thresholding techniques for ECG denoising," in 2014 International Conference on Advances in Engineering & Technology Research (ICAETR - 2014), 2014, pp. 1-6.

[39] S. Gang, R. Liang, and G. Yuhan, "Research on the method of ECG denoising based on improved wavelet packet," in 2015 IEEE International Conference on Cyber Technology in Automation, Control, and Intelligent Systems (CYBER), 2015, pp. 1425-1428.

[40] S. Cerutti and C. Marchesi, Advanced Methods of Biomedical Signal Processing (IEEE Press Series on Biomedical Engineering). Hoboken, N.J: John Wiley & Sons, 2011.

[41] A. Cohen, Biomedical Signal Processing. CRC Press, 1986.

[42] J. Kilby, K. Prasad, and G. Mawston, "Development of a New Multi-Channel Electrode and Signal Processing for Surface Electromyography Signals Feature Extraction," Theses, Auckland University of Technology New Zealand, 2017.

[43] H. Liang, J. D. Bronzino, and D. R. Peterson, Biosignal processing : principles and practices. Boca Raton : Taylor & Francis, 2013.

[44] G. De Luca, "Fundamental concepts in EMG signal acquisition," Copyright Delsys Inc, 2003.

[45] A. K. Das, D. Biswas, and S. Halder, "Analysis of de-noising techniques of non-stationary ECG signal based on wavelet and PSO optimized parameters for Savitzky golay filter," in 2017 Third International Conference on Research in Computational Intelligence and Communication Networks (ICRCICN), 2017, pp. 39-44.

[46] B. Arvinti, A. Isar, and M. Costache, "An adaptive compression algorithm for ECG signals," in 2011 IEEE 12th International Symposium on Computational Intelligence and Informatics (CINTI), 2011, pp. 91-95.

[47] P. S. Addison, The Illustrated Wavelet Transform Handbook : Introductory Theory and Applications in Science, Engineering, Medicine and Finance, Second ed. Boca Raton, FL: Taylor & Francis Group, 2016.

[48] P. J. Sparto, M. Parnianpour, E. A. Barria, and J. M. Jagadeesh, "Wavelet and short-time Fourier transform analysis of electromyography for detection of back muscle fatigue," IEEE Transactions on Rehabilitation Engineering, Rehabilitation Engineering, IEEE Transactions on, IEEE Trans. Rehab. Eng., Periodical no. 3, p. 433, 2000.

[49] Y. Chompusri, K. Dejhan, and S. Yimman, "Mother wavelet selecting method for selective mapping technique ECG compression," in 2012 9th International Conference on Electrical Engineering/Electronics, Computer, Telecommunications and Information Technology, 2012, pp. 1-4.

[50] S. Li and J. Lin, "The Optimal De-noising Algorithm for ECG Using Stationary Wavelet Transform," in 2009 WRI World Congress on Computer Science and Information Engineering, 2009, vol. 6, pp. 469-473.

[51] N. Nikvand, H. B. Rafsanjani, and M. A. Khalilzadeh, "ECG signal denoising using noise invalidation," in 2010 17th Iranian Conference of Biomedical Engineering (ICBME), 2010, pp. 1-4.

[52] H. Lin, L. Sz-Ying, Y. Ho, Y. Lin, and H. Ma, "Discrete-wavelet-transform-based noise reduction and R wave detection for ECG signals," in 2013 IEEE 15th International Conference on e-Health Networking, Applications and Services (Healthcom 2013), 2013, pp. 355-360.

[53] D. L. Donoho, "De-noising by Soft-Thresholding," IEEE Transactions on Information Theory, vol. 41, no. 3, pp. 613-627, 1995.

[54] I. M. Johnstone and B. W. Silverman, "Wavelet Threshold Estimators for Data with Correlated Noise," Journal of the Royal Statistical Society: Series B (Statistical Methodology), vol. 59, no. 2, p. 319, 06/1997.

[55] C. J. De Luca, A. Adam, R. Wotiz, L. D. Gilmore, and S. H. Nawab, "Decomposition of surface EMG signals," vol. 96, ed, 2006, pp. 1646-1657.

[56] H. J. Hermens, B. Freriks, C. Disselhorst-Klug, and G. Rau, "Development of recommendations for SEMG sensors and sensor placement procedures," Journal of Electromyography and Kinesiology, vol. 10, no. 5, pp. 361-374, 10/01/2000.

Appendix A

Figure A.1 (repeated from Figure 2.7) shows the erector spinae muscles of the back and Table A.1 gives the origin and insertion of each muscle [33].

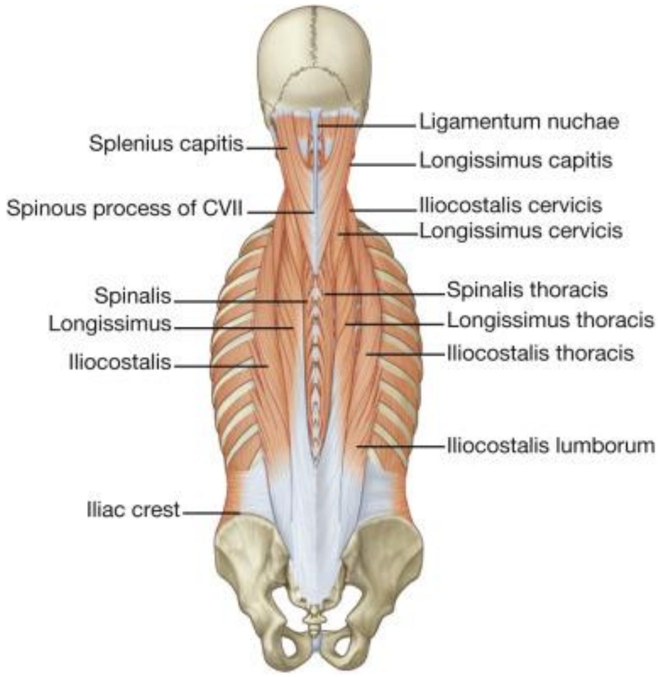

Figure A-1: Erector Spinae Muscles

Table A-1: Erector spinae group of muscles

Muscle	Origin	Insertion
Iliocostalis lumborum	Sacrum, spinous processes of lumbar and lower two thoracic vertebrae and their supraspinous ligaments, and the iliac crest	Angles of the lower six or seven ribs
Iliocostalis thoracis	Angles of the lower six ribs	Angles of the upper six ribs and the transverse process of CVII
Iliocostalis cervicis	Angles of ribs III to VI	Transverse processes of CIV to CVI
Longissimus thoracis	Blends with iliocostalis in lumbar region and is attached to transverse processes of lumbar vertebrae	Transverse processes of all thoracic vertebrae and just lateral to the tubercles of the lower nine or ten ribs
Longissimus cervicis	Transverse processes of upper four or five thoracic vertebrae	Transverse processes of CII to CVI
Longissimus capitis	Transverse processes of upper four or five thoracic vertebrae and articular processes of lower three or four cervical vertebrae	Posterior margin of the mastoid process
Spinalis thoracis	Spinous processes of TX or TXI to LII	Spinous processes of TI to TVIII (varies)
Spinalis cervicis	Lower part of ligamentum nuchae and spinous process of CVII (sometimes TI to TII)	Spinous process of CII (axis)
Spinalis capitis	Usually blends with semispinalis capitis	With semispinalis capitis

Appendix B

Participant 2: 5% MVIC

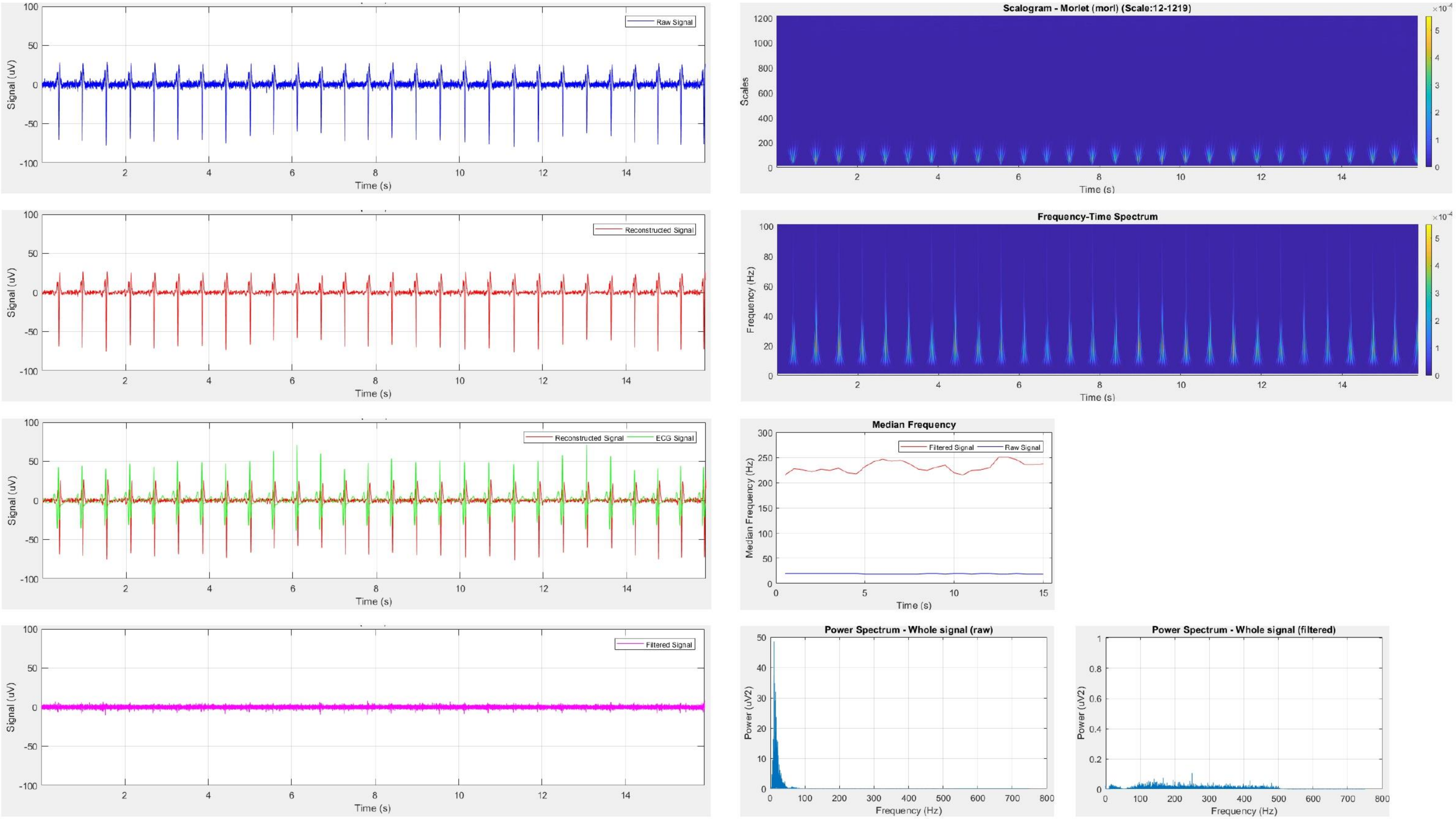

Figure B-1: Participant 2 results 5% MVIC

Participant 2: 10% MVIC

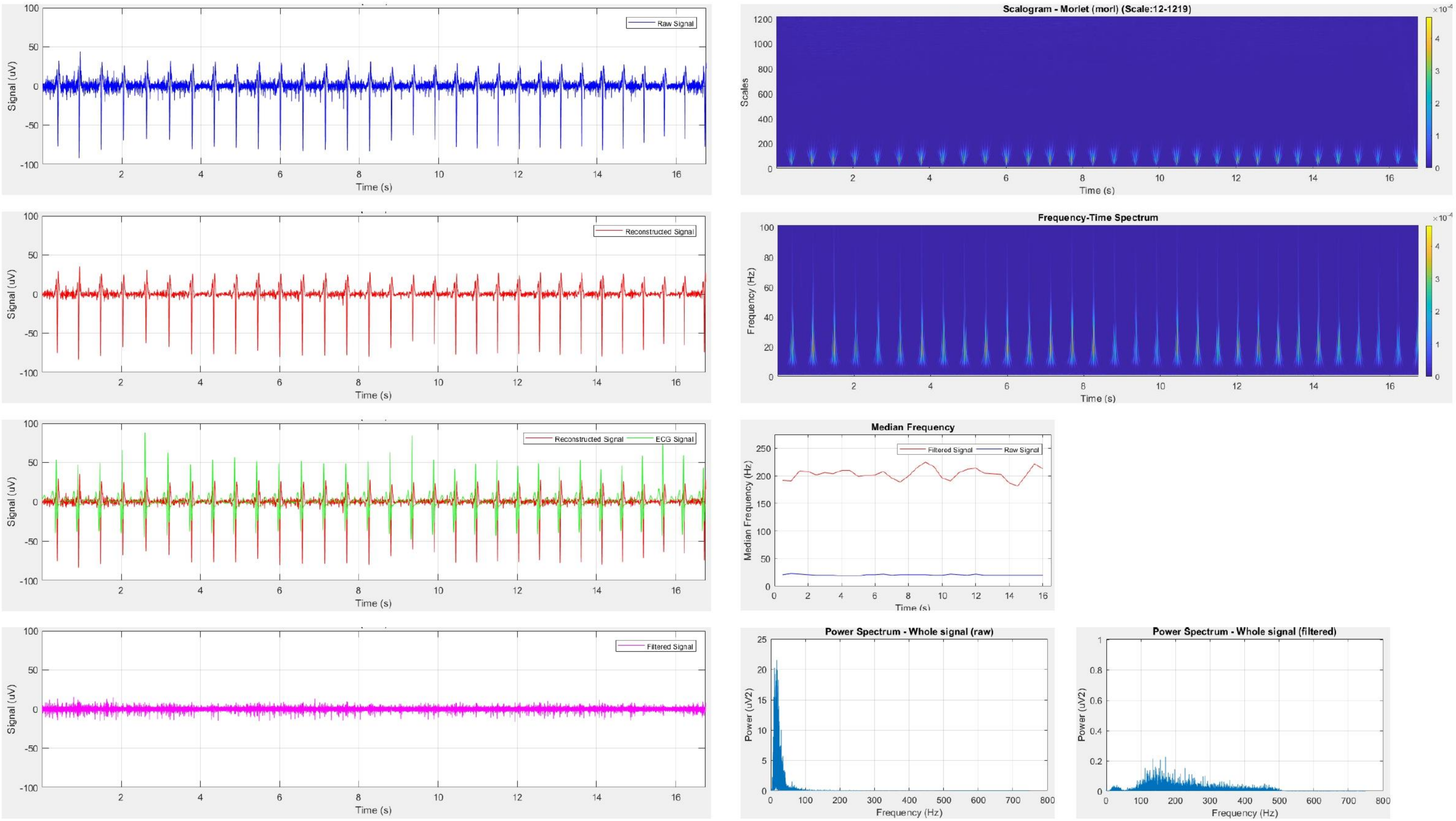

Figure B-2: Participant 2 results 5% MVIC

Participant 2: 15% MVIC

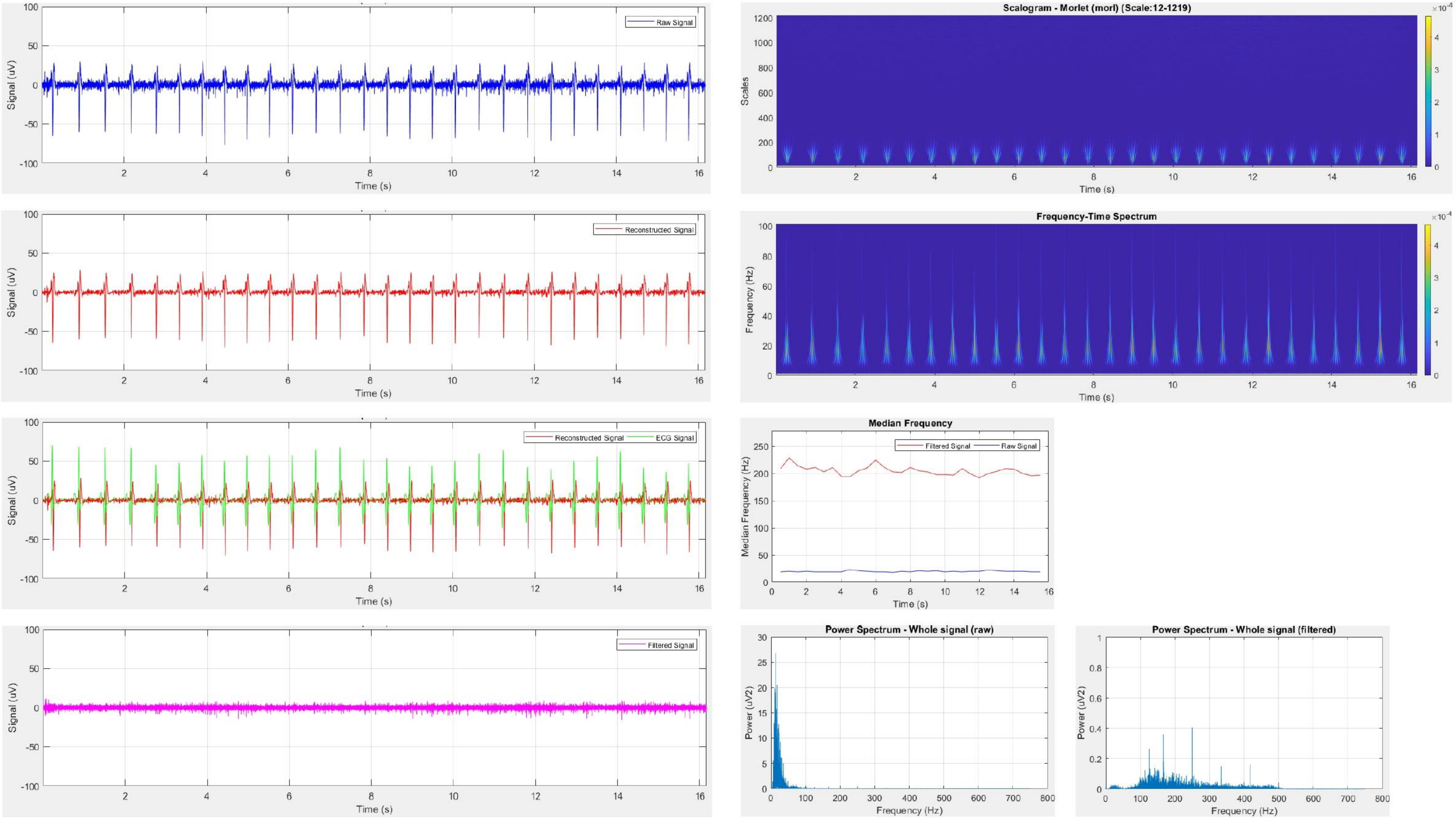

Figure B-3: Participant 2 results 15% MVIC

Participant 2: 20% MVIC

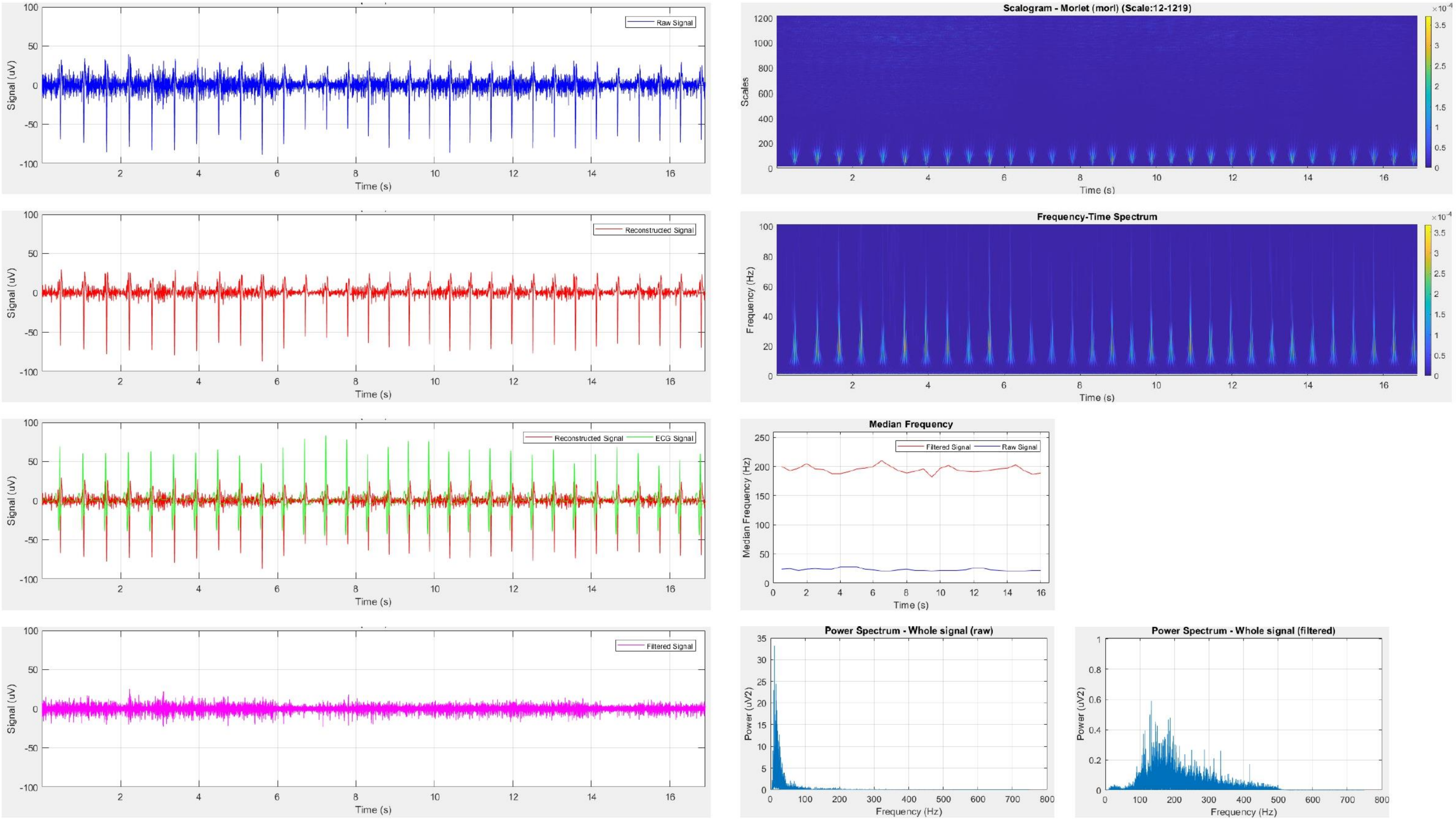

Figure B-4: Participant 2 results 20% MVIC

Participant 2: 25% MVIC

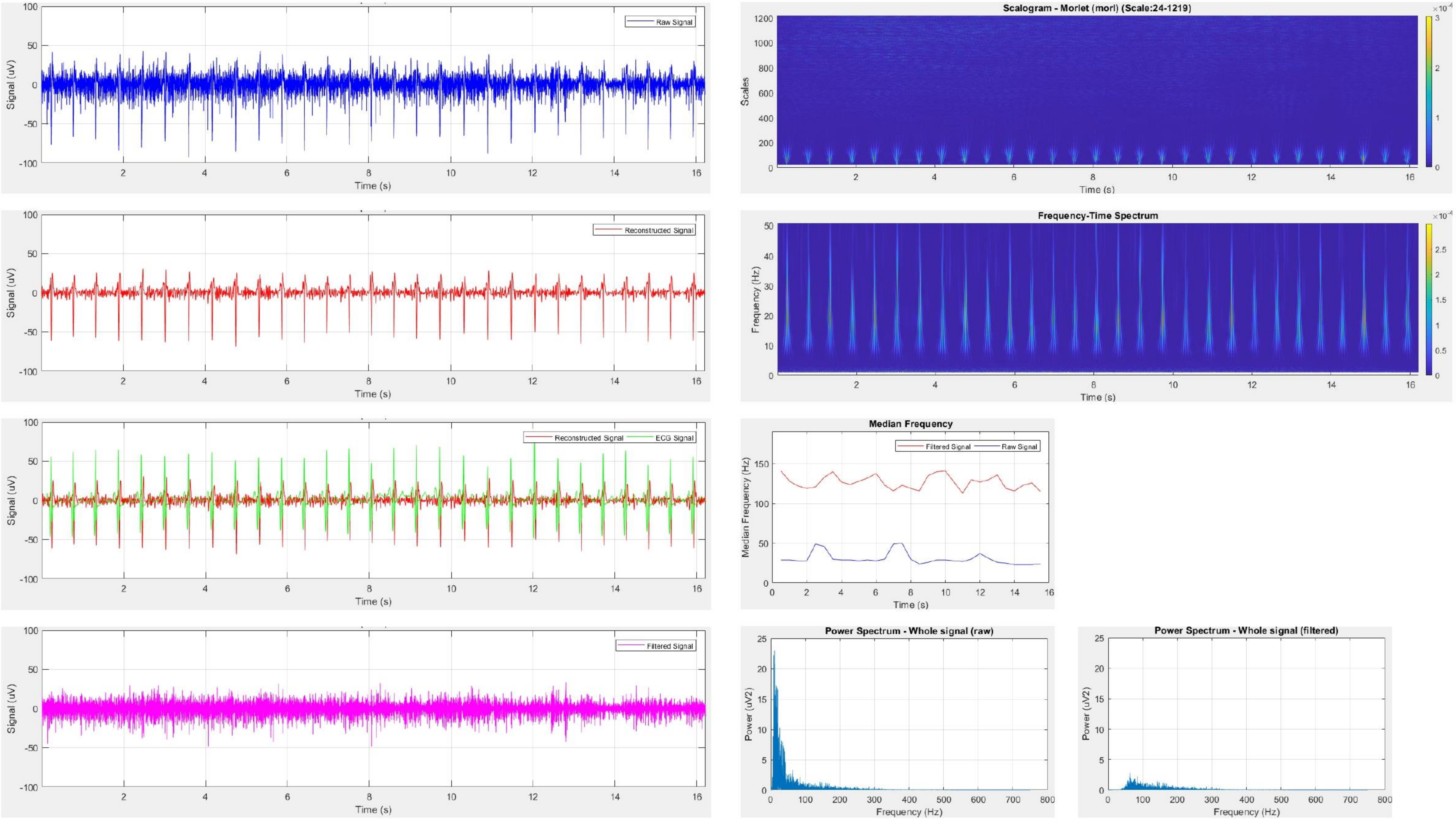

Figure B-5:   Participant 2 results 25% MVIC

Participant 2: 30% MVIC

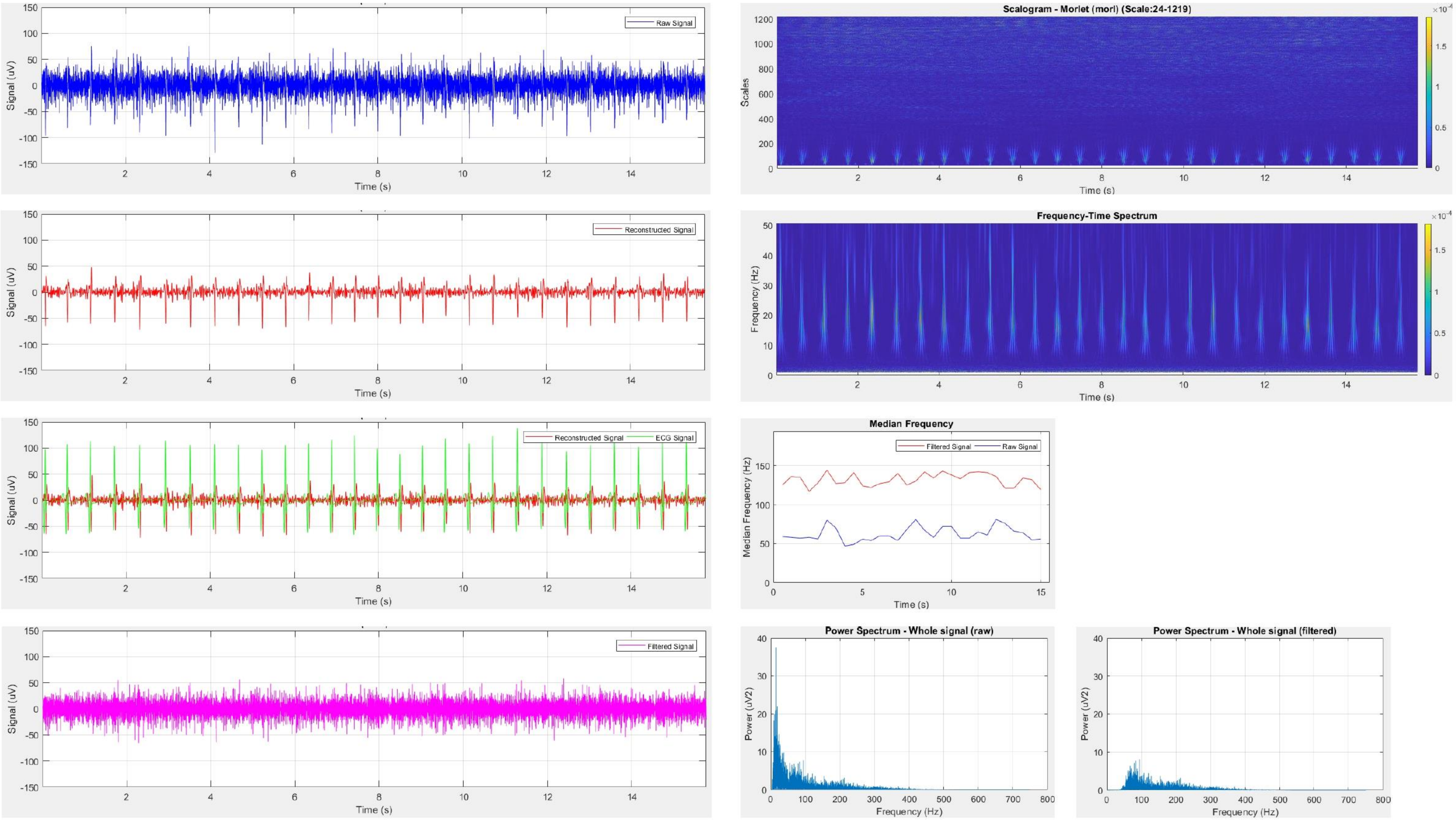

Figure B-6: Participant 2 results 30% MVIC

Participant 2: 35% MVIC

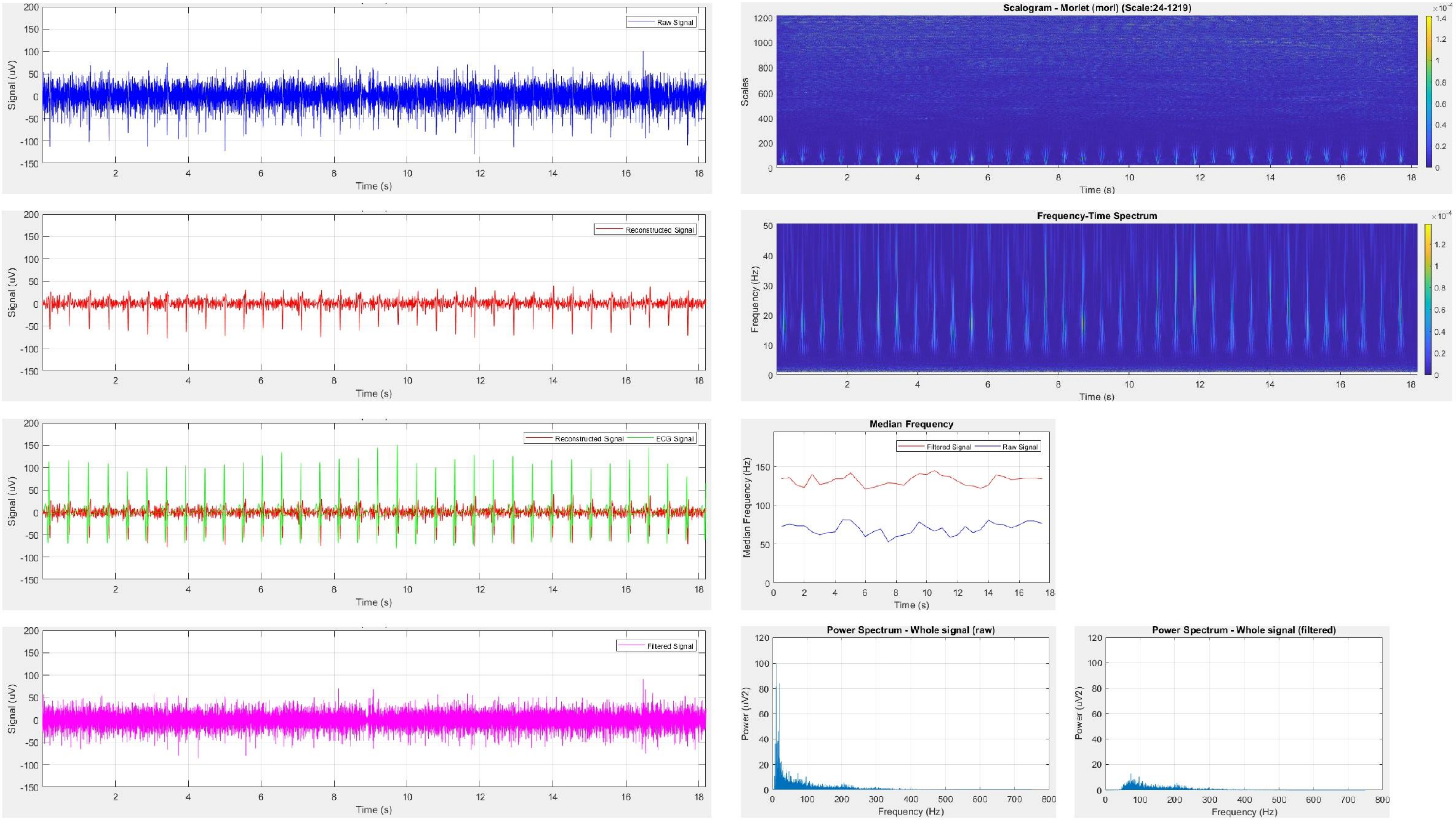

Figure 0-7: Participant 2 results 35% MVIC

Participant 2: 40% MVIC

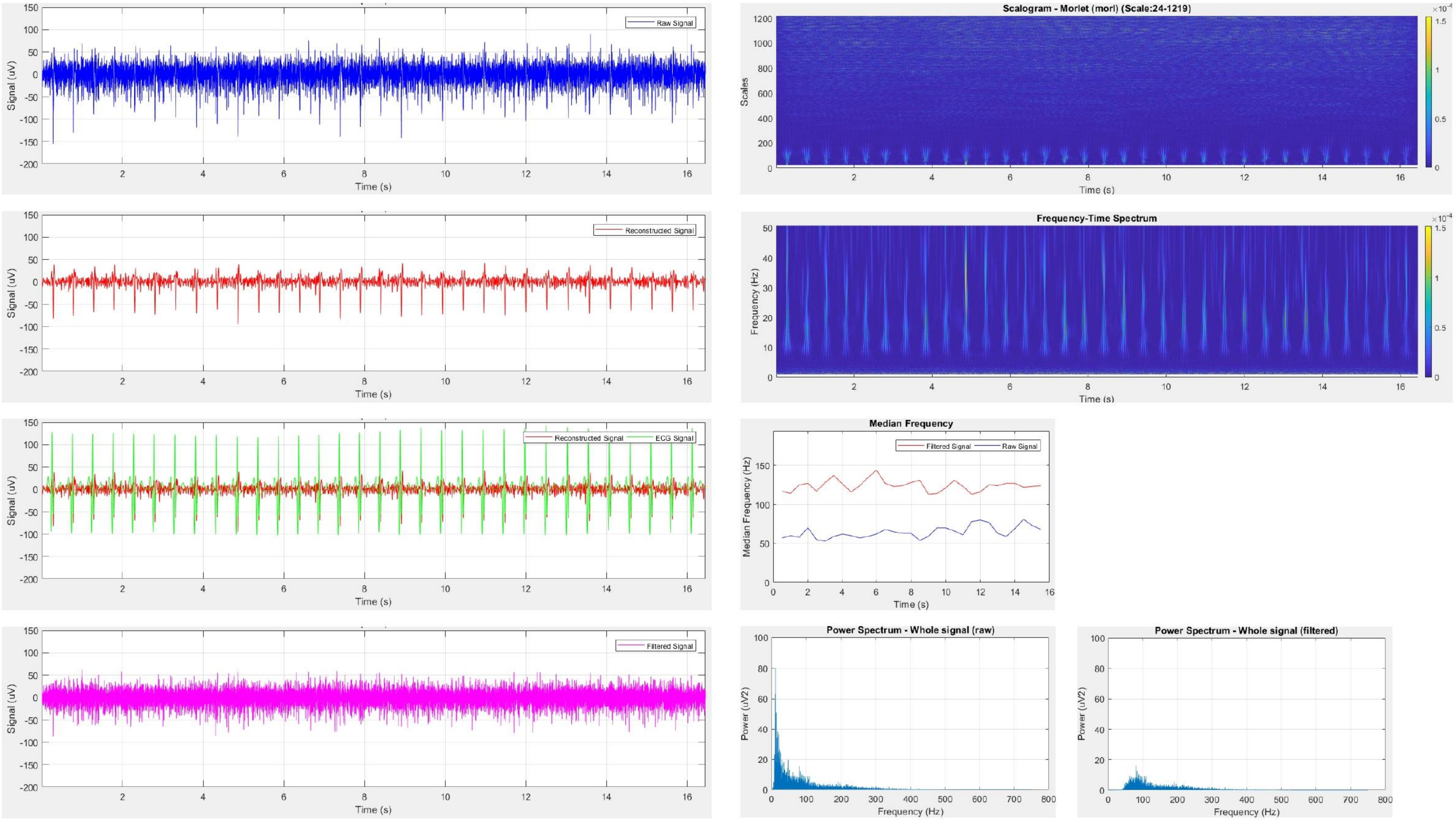

Figure B-8: Participant 2 results 40% MVIC

Participant 2: 45% MVIC

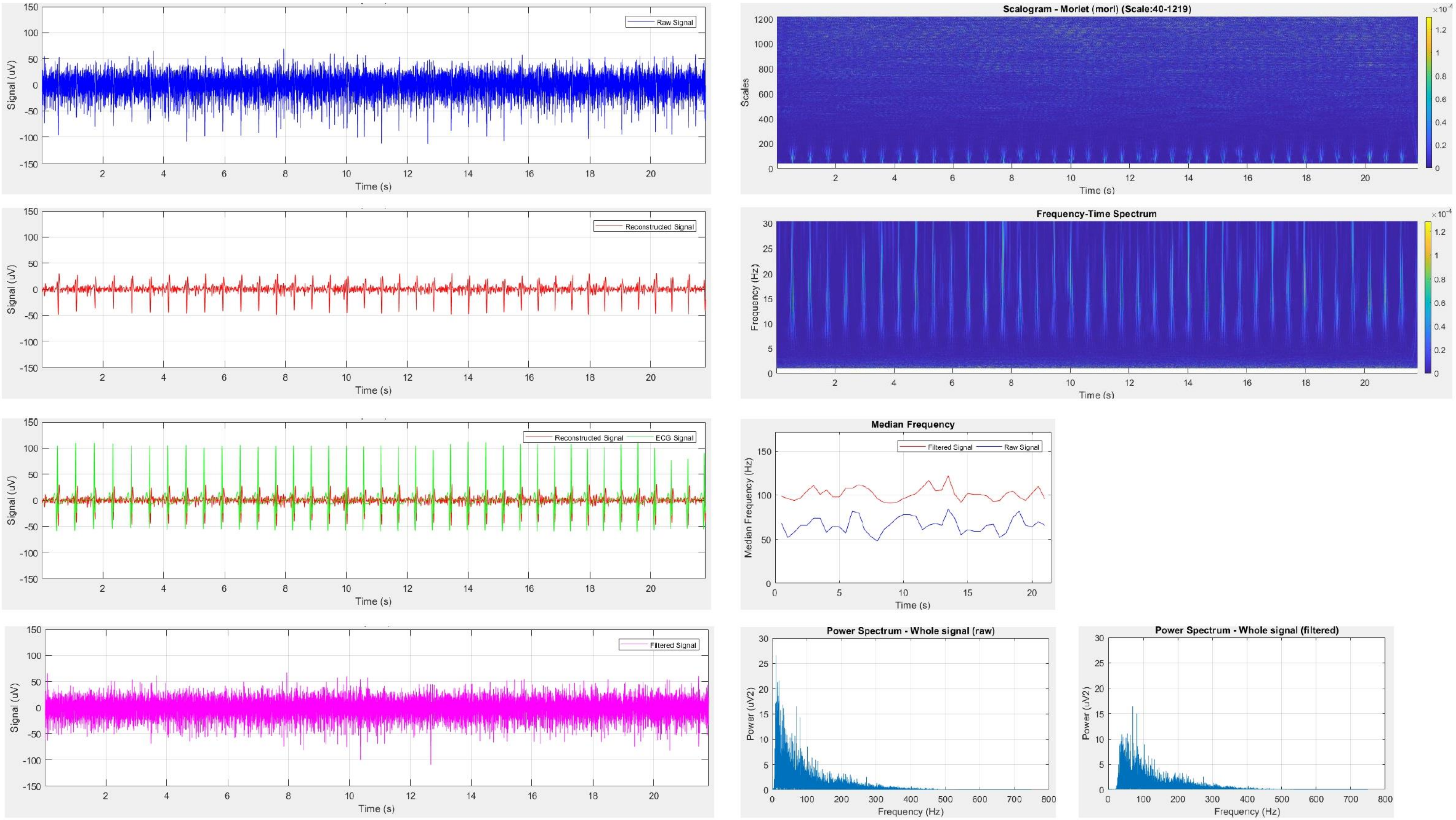

Figure B-9: Participant 2 results 45% MVIC

Participant 2: 50% MVIC

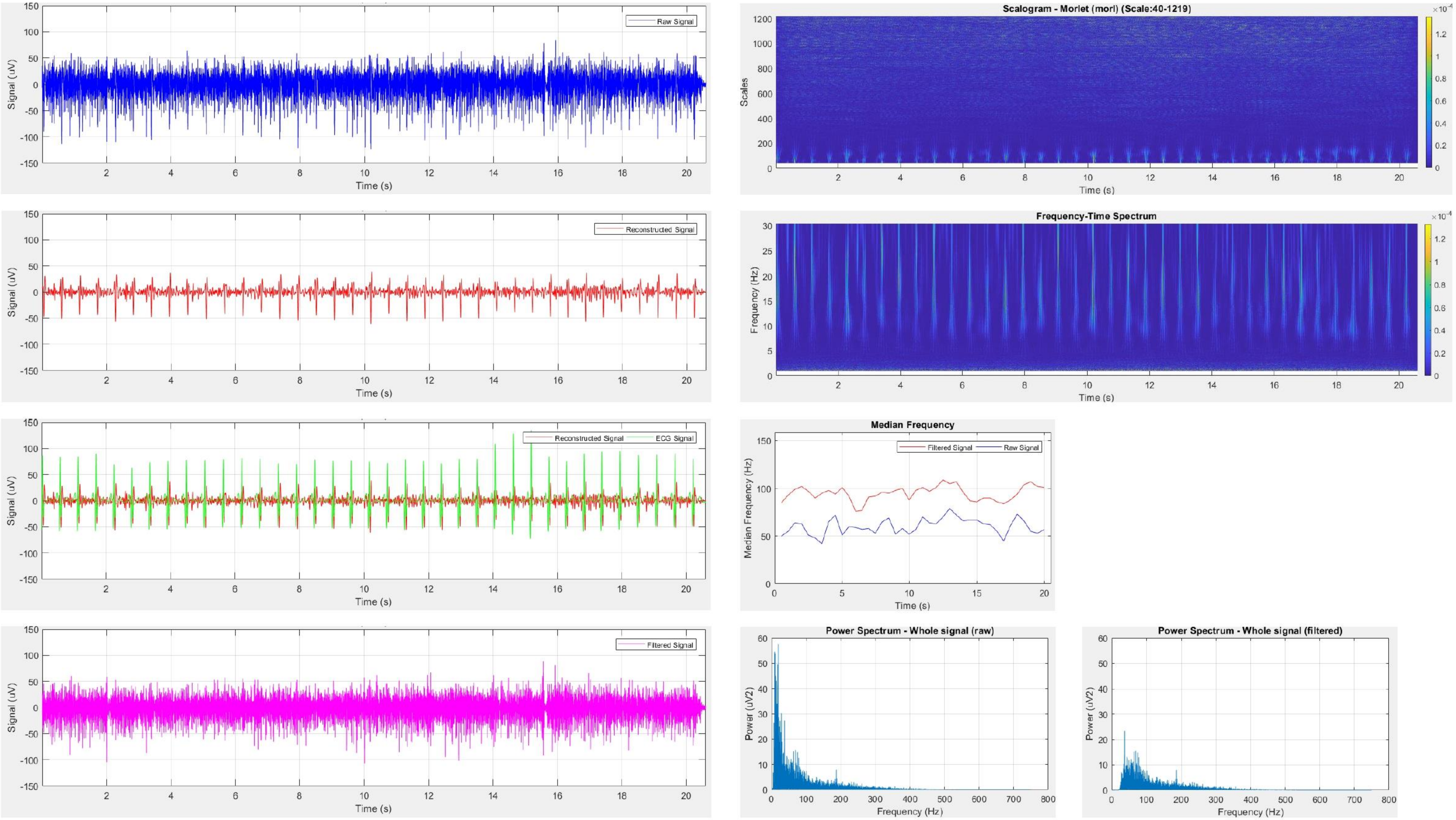

Figure B-10: Participant 2 results 50% MVIC

PARTICIPANT 4: 5% MVIC

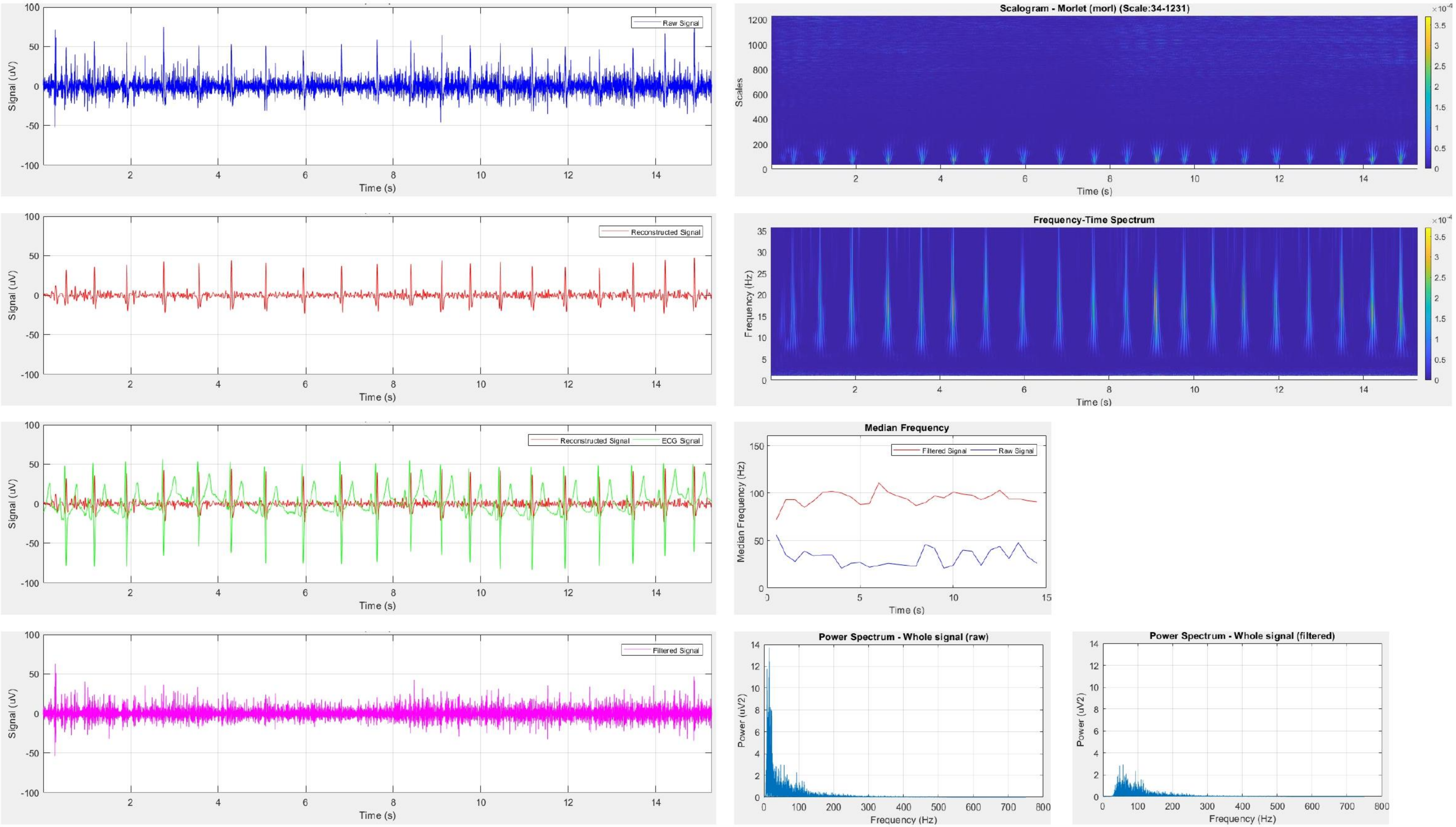

Figure B-11: Participant 4 results 5% MVIC

PARTICIPANT 4: 10% MVIC

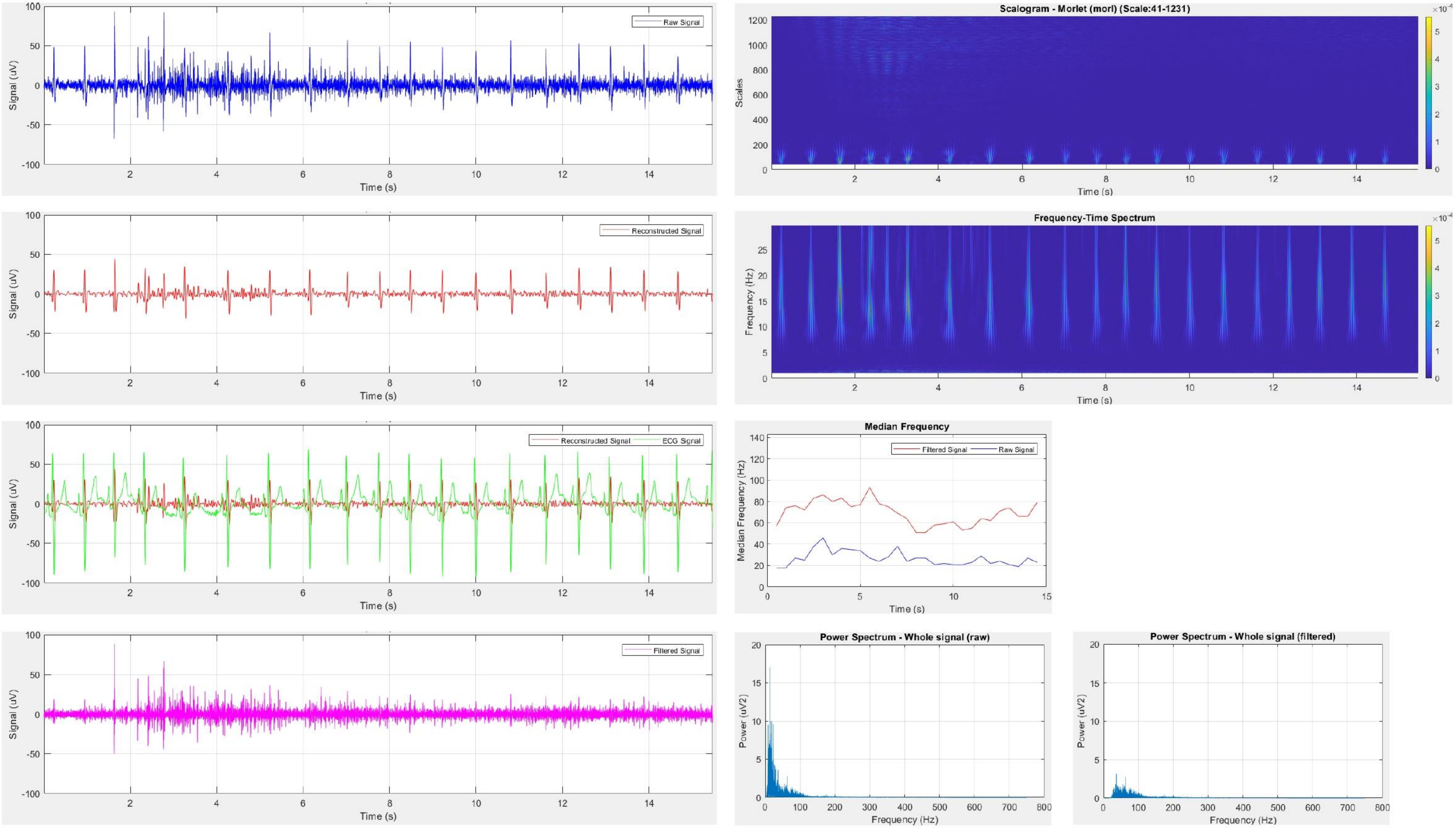

Figure B-12: Participant 4 results 10% MVIC

PARTICIPANT 4: 15% MVIC

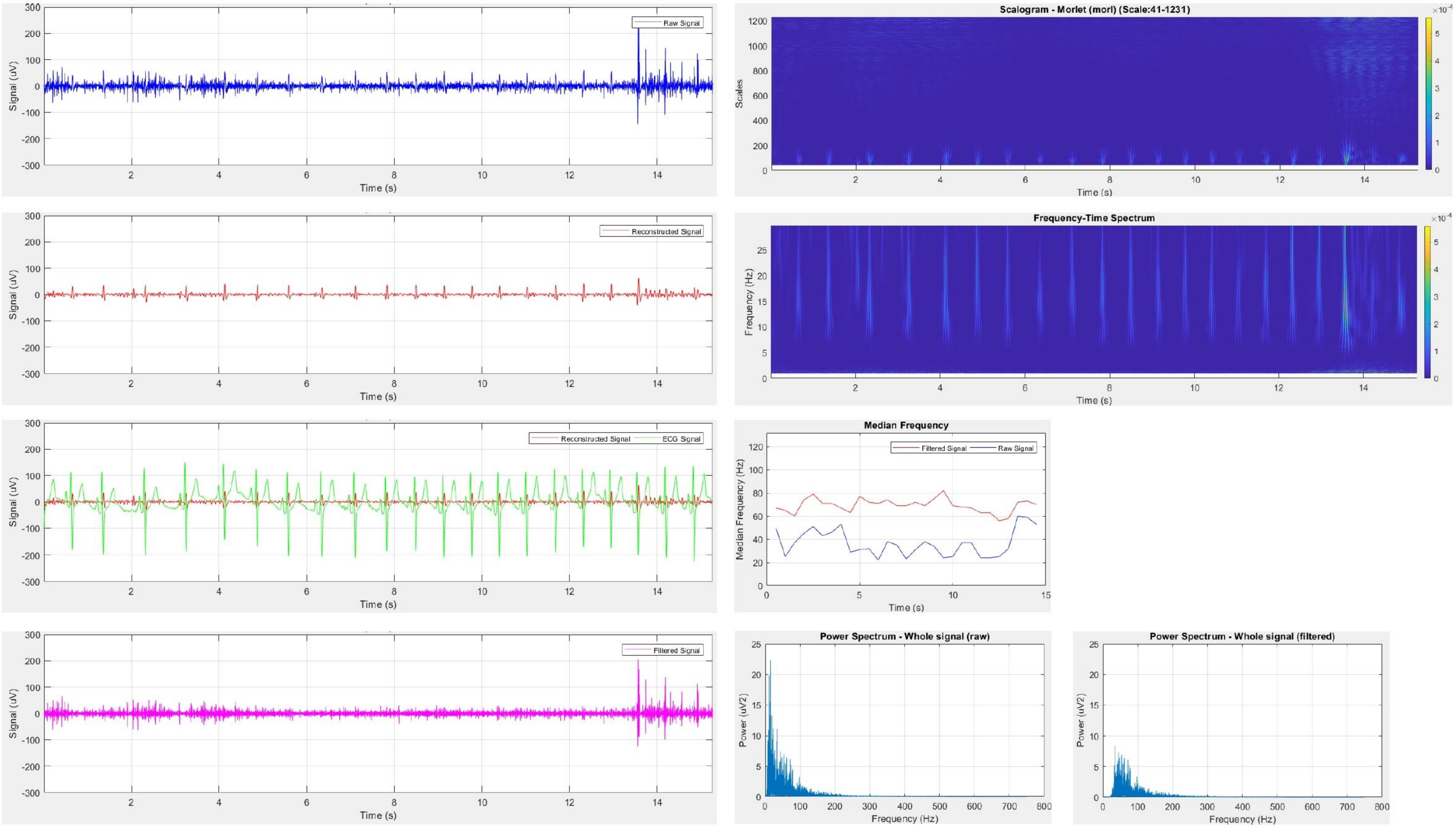

Figure B-13: Participant 4 results 15% MVIC

PARTICIPANT 4: 20% MVIC

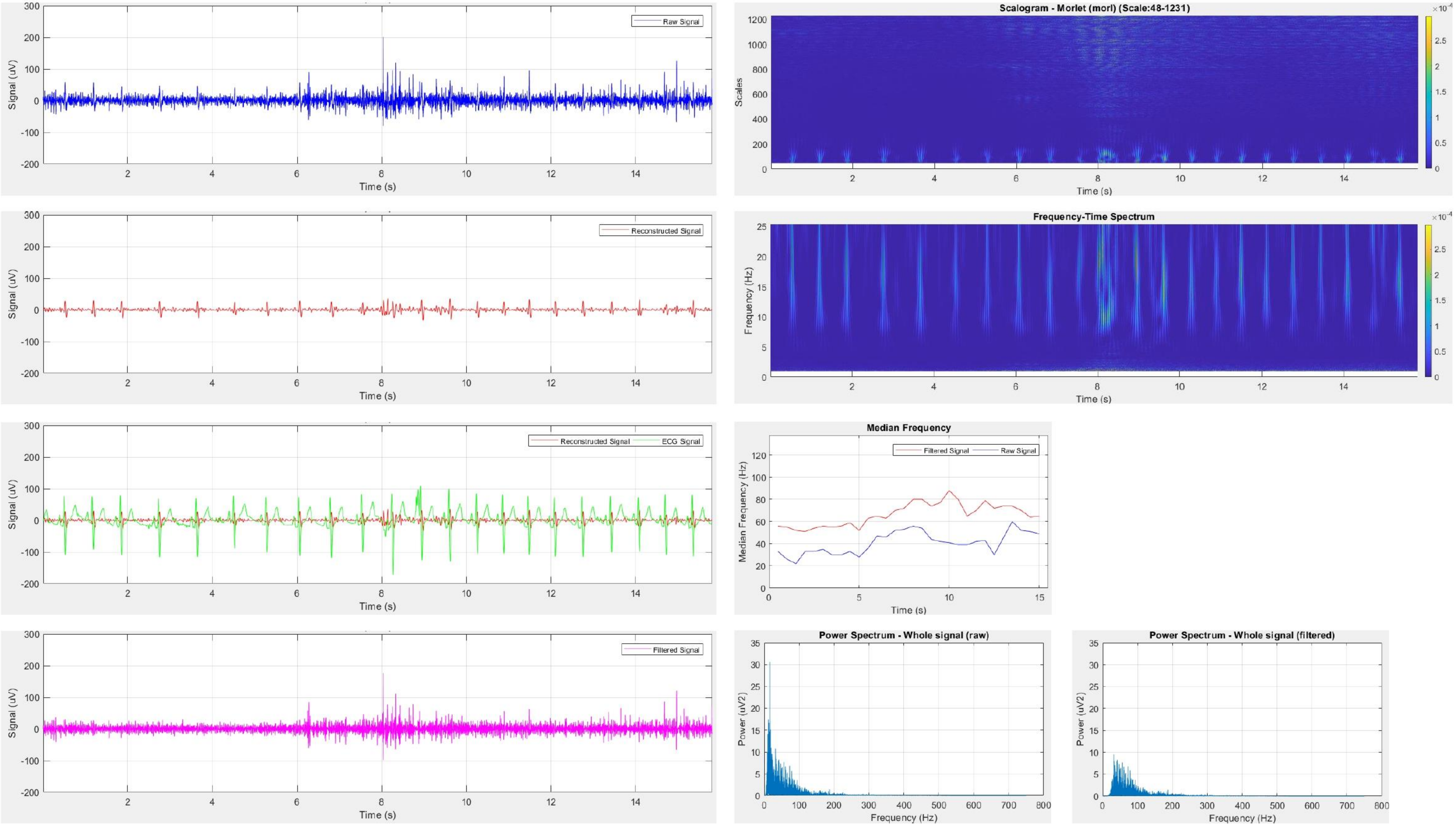

Figure B-14: Participant 4 results 20% MVIC

PARTICIPANT 4: 25% MVIC

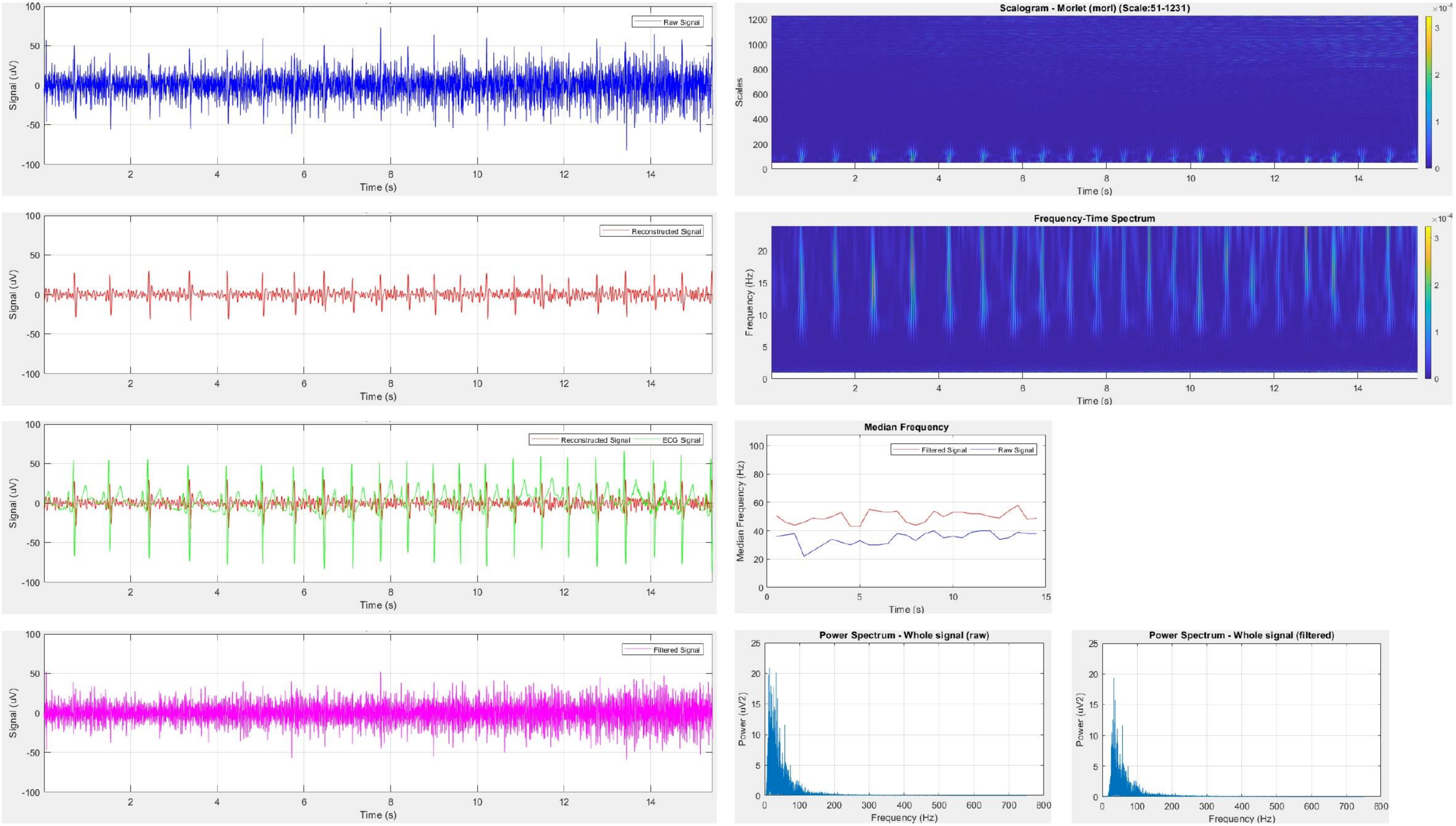

Figure B-15: Participant 4 results 25% MVIC

PARTICIPANT 4: 30% MVIC

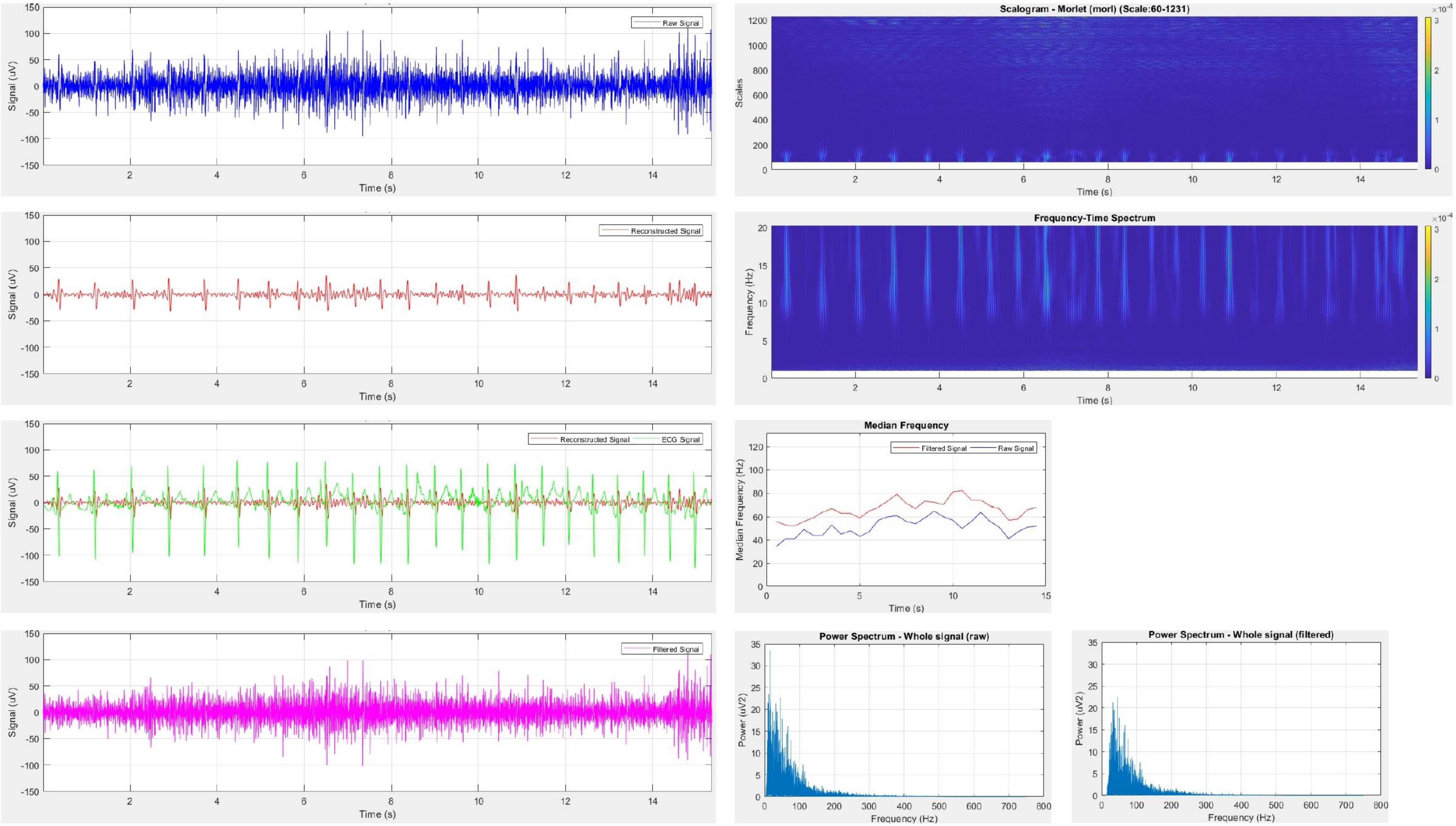

Figure B-16: Participant 4 results 30% MVIC

PARTICIPANT 4: 35% MVIC

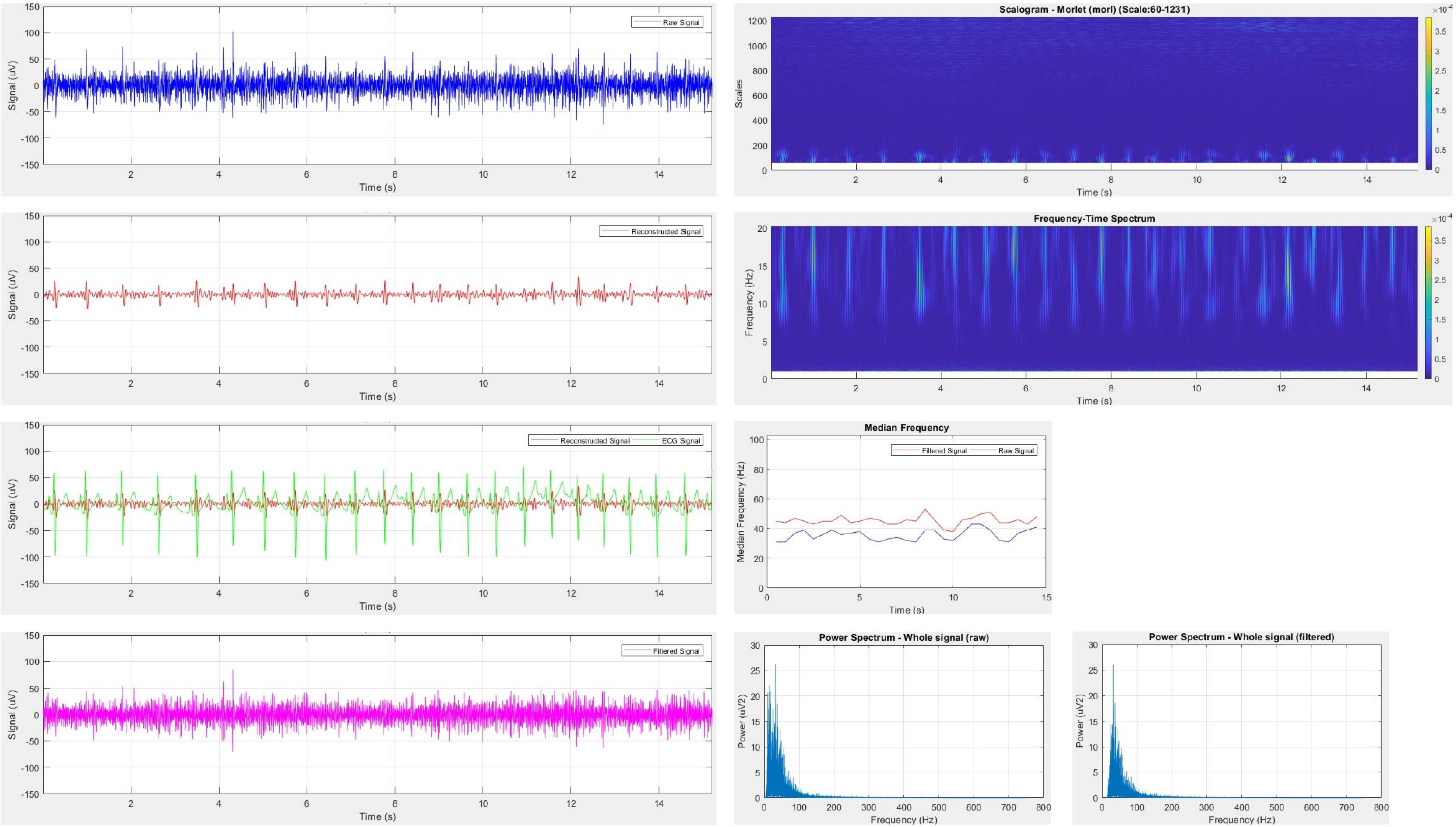

Figure B-17: Participant 4 results 35% MVIC

PARTICIPANT 4: 40% MVIC

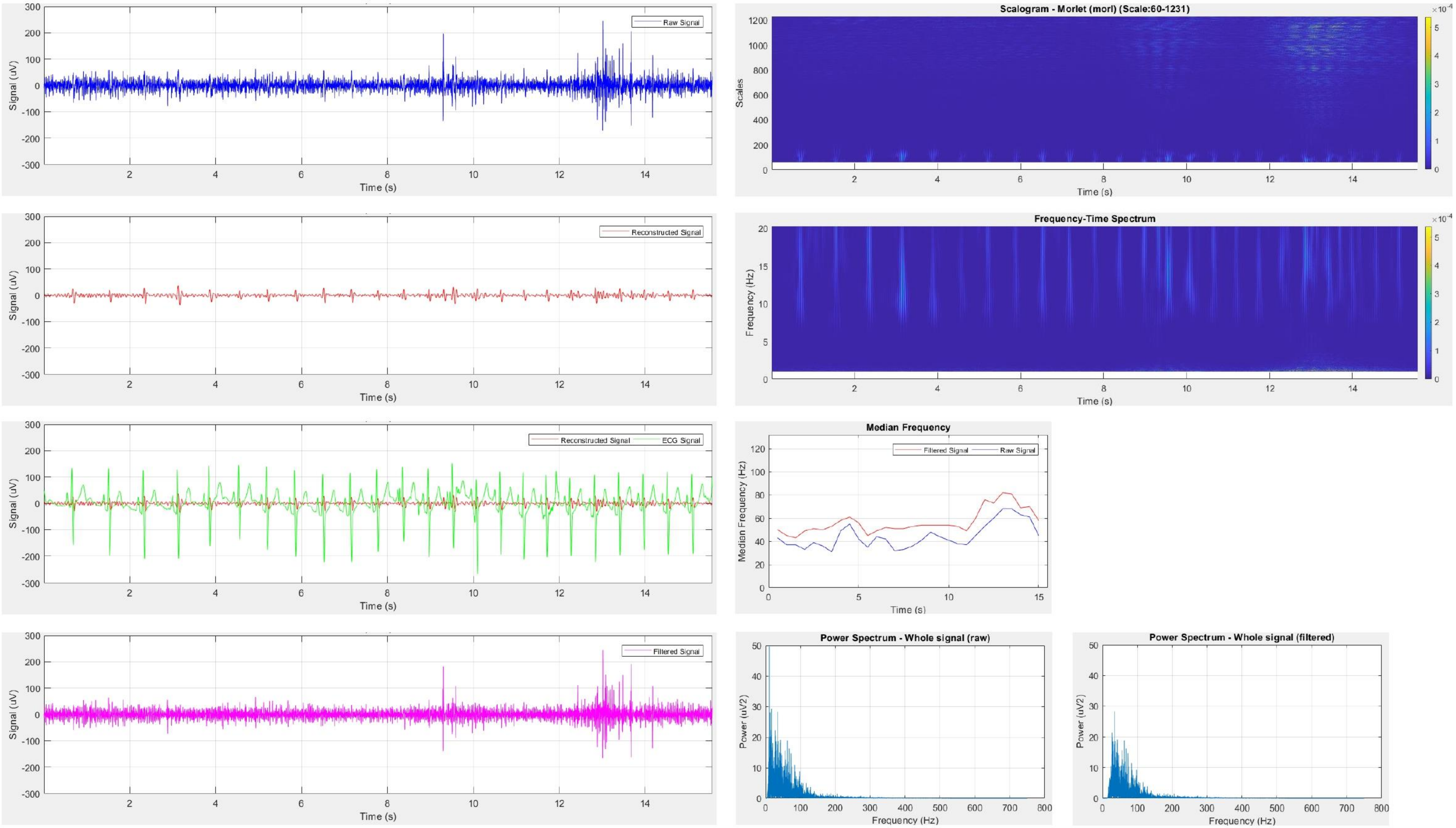

Figure B-18: Participant 4 results 40% MVIC

PARTICIPANT 4: 45% MVIC

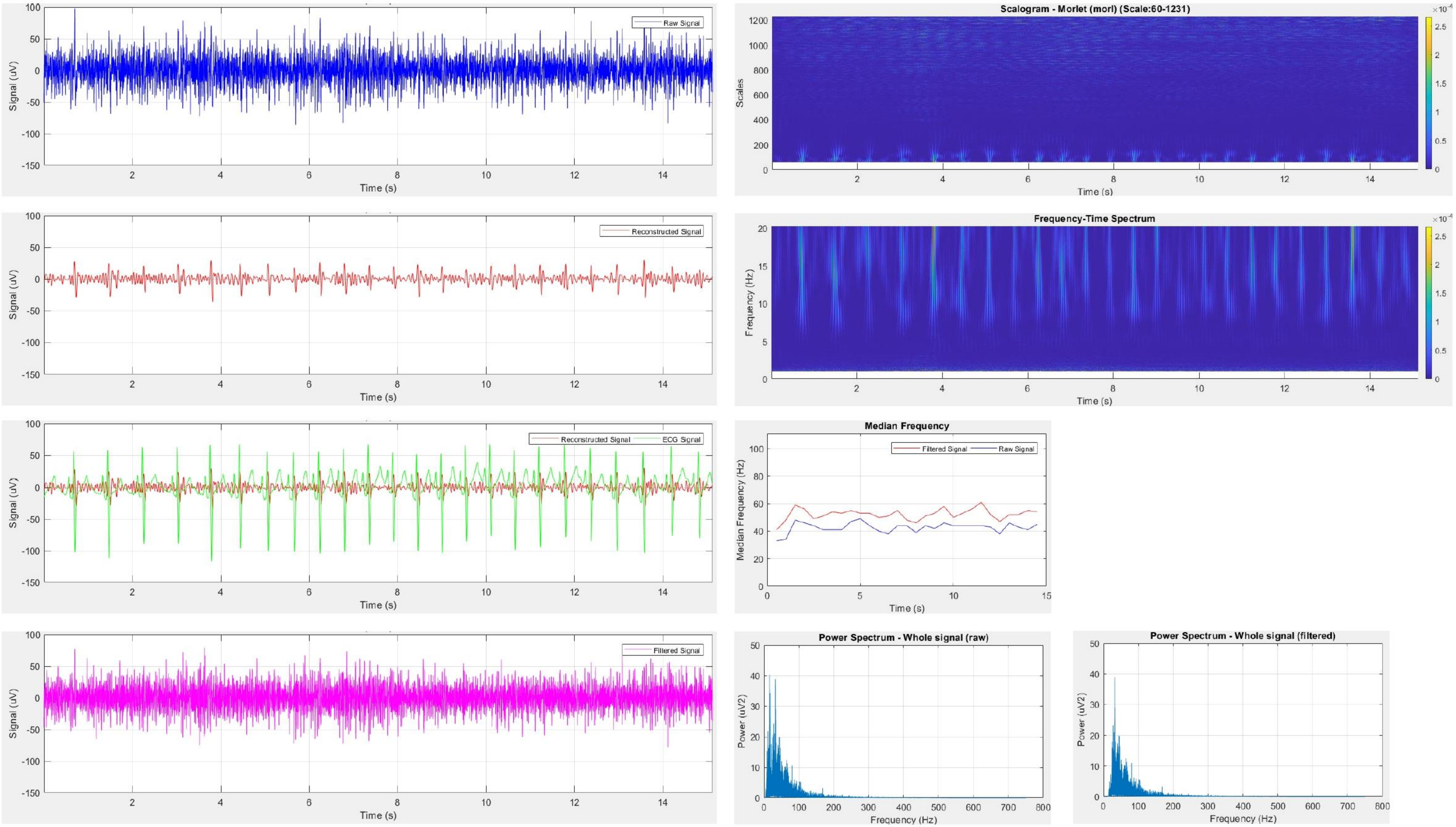

Figure B-19: Participant 4 results 45% MVIC

PARTICIPANT 5: 5% MVIC

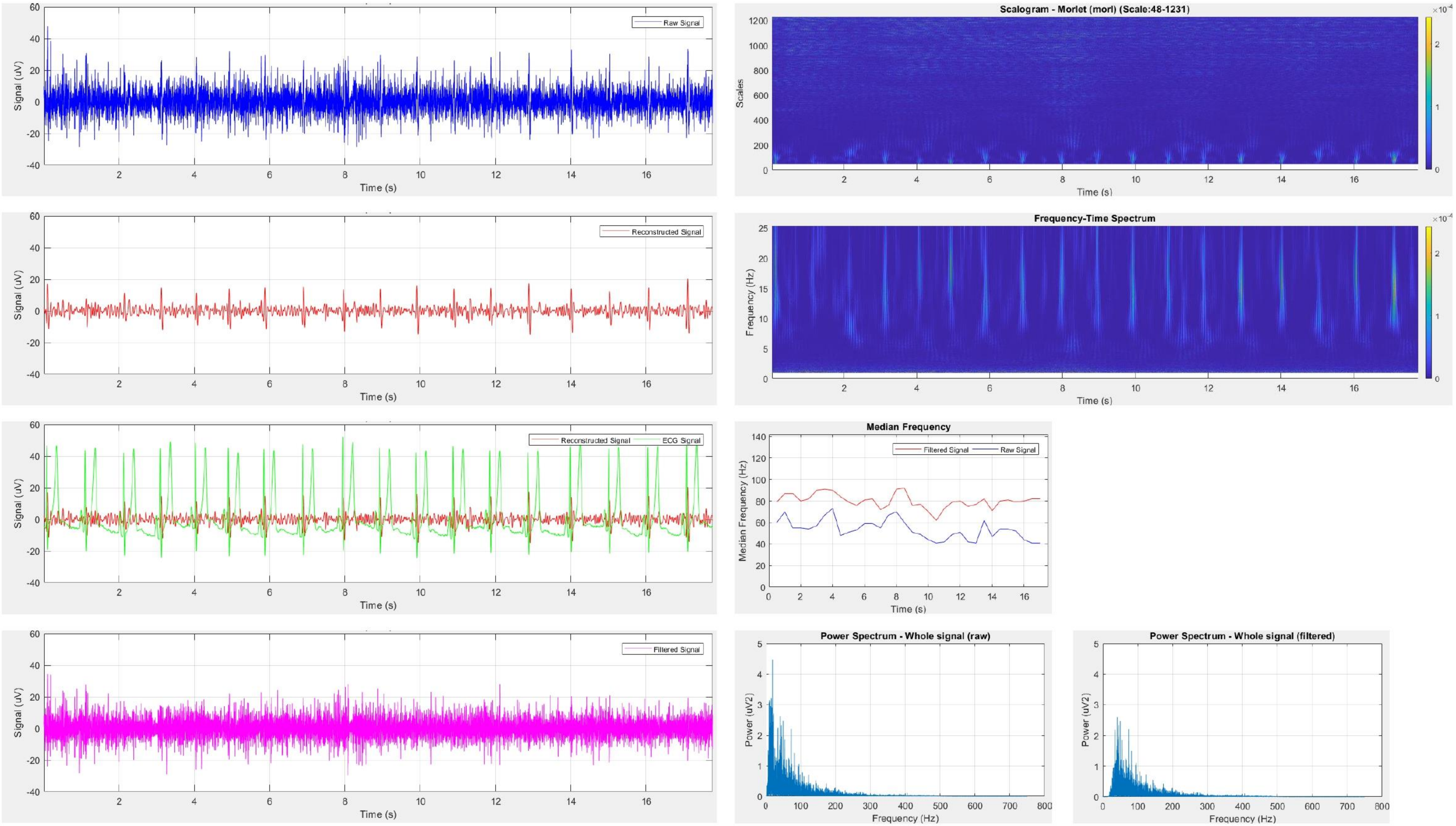

Figure B-20: Participant 5 results 5% MVIC

PARTICIPANT 5: 10% MVIC

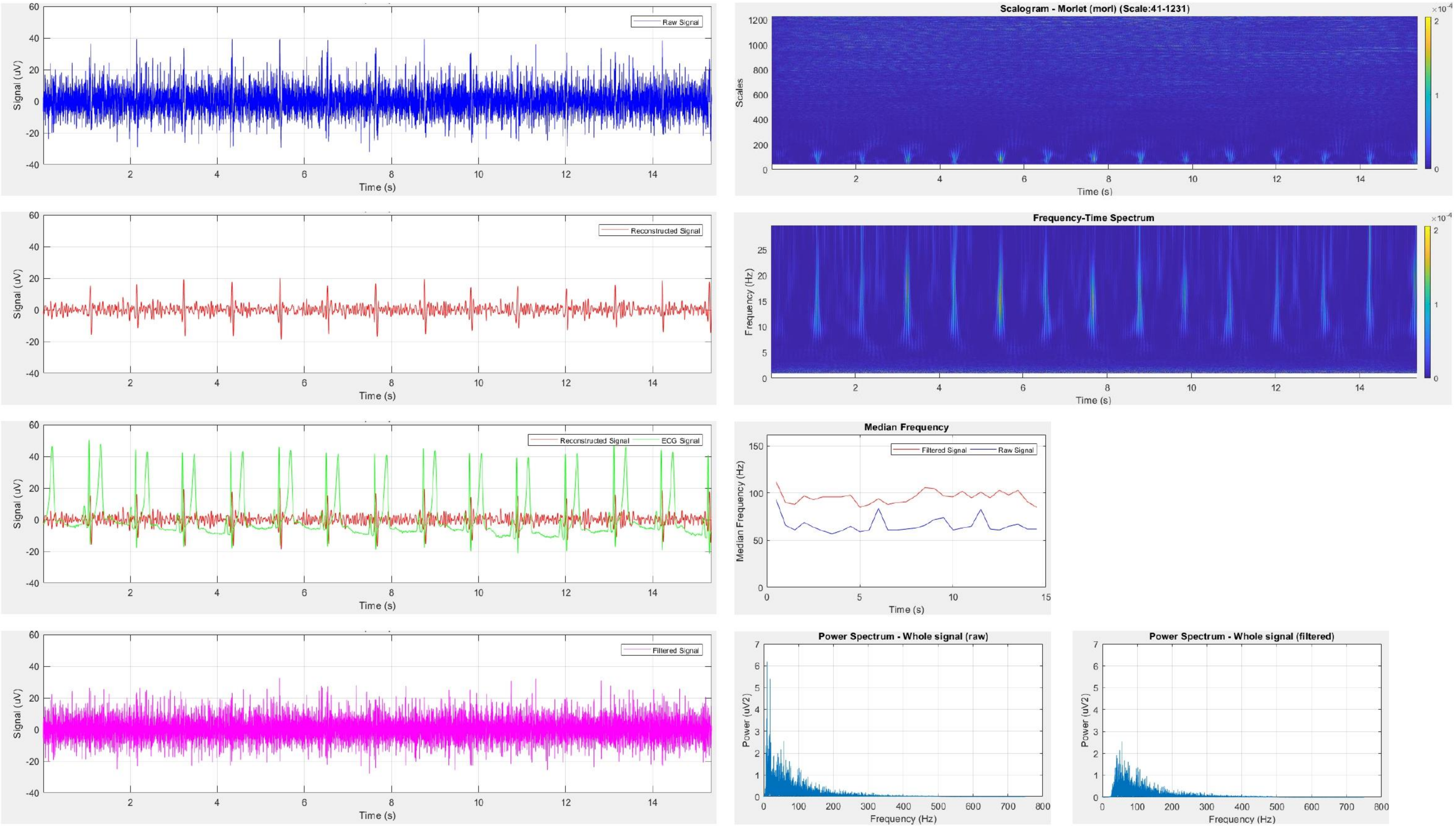

Figure B-21: Participant 5 results 10% MVIC

PARTICIPANT 5: 15% MVIC

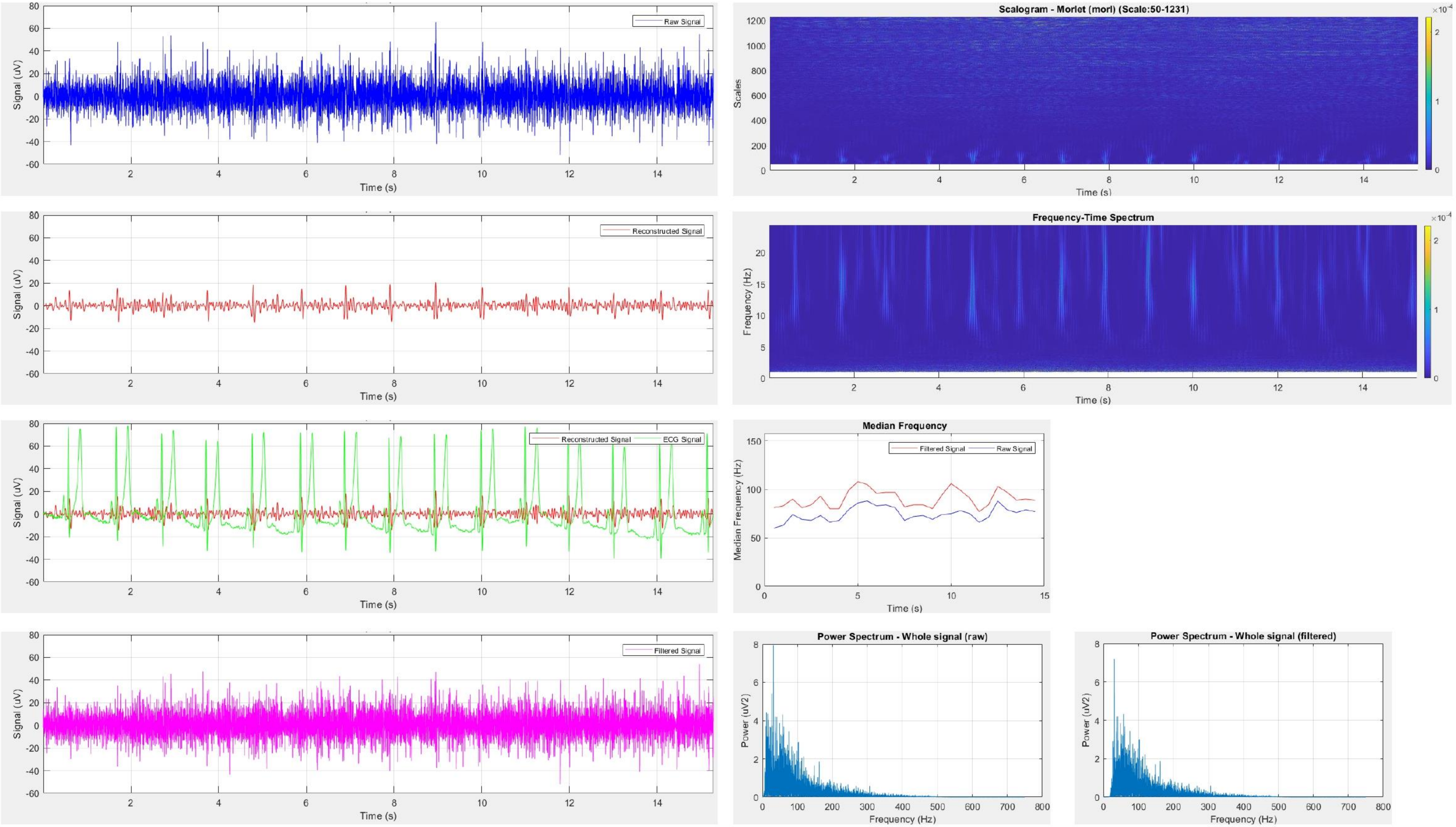

Figure B-22: Participant 5 results 15% MVIC

PARTICIPANT 5: 20% MVIC

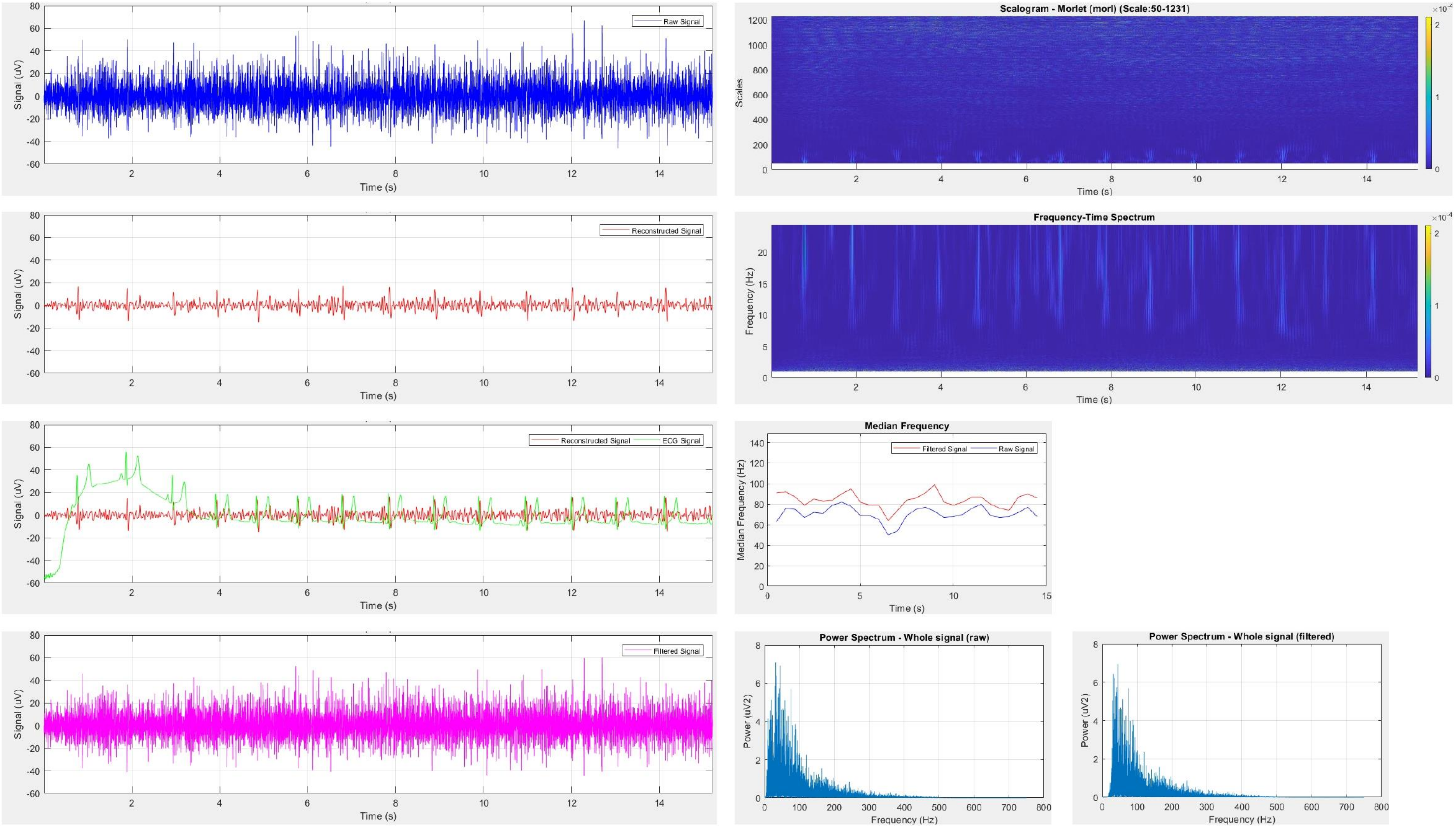

Figure B-23: Participant 5 results 20% MVIC

PARTICIPANT 7: 5% MVIC

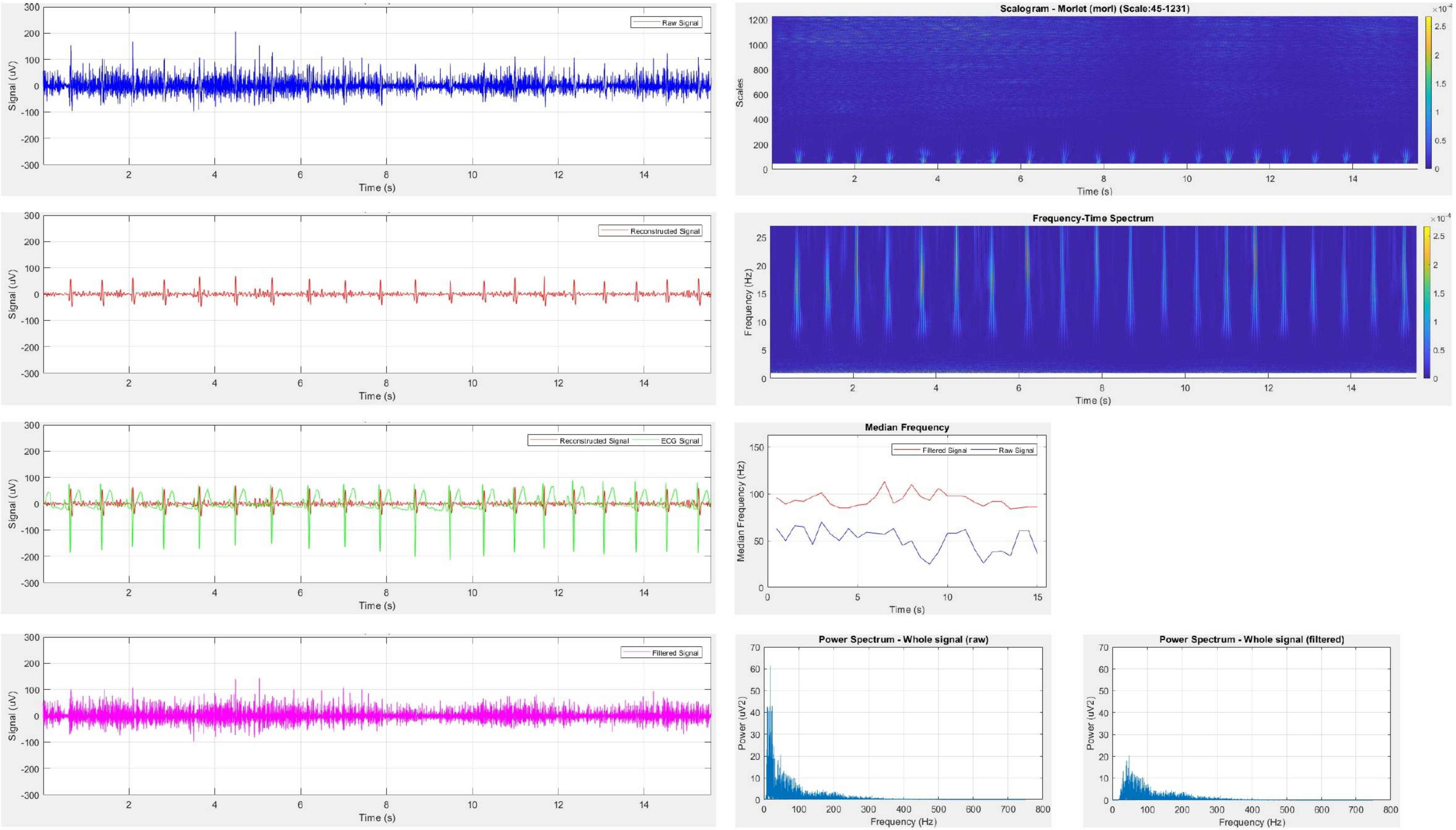

Figure B-24: Participant 7 results 5% MVIC

PARTICIPANT 7: 10% MVIC

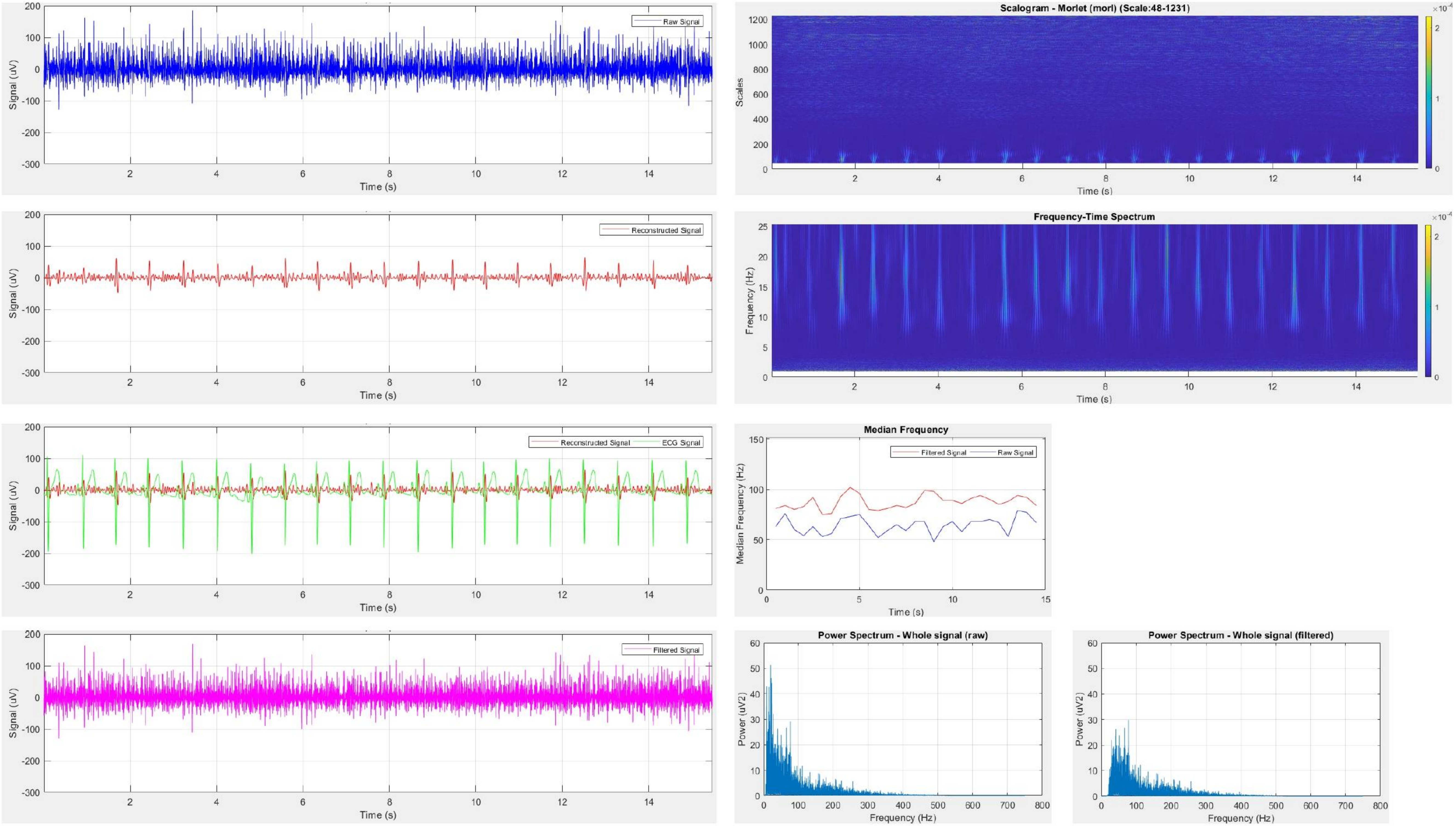

Figure B-25: Participant 7 results 10% MVIC

PARTICIPANT 7: 15% MVIC

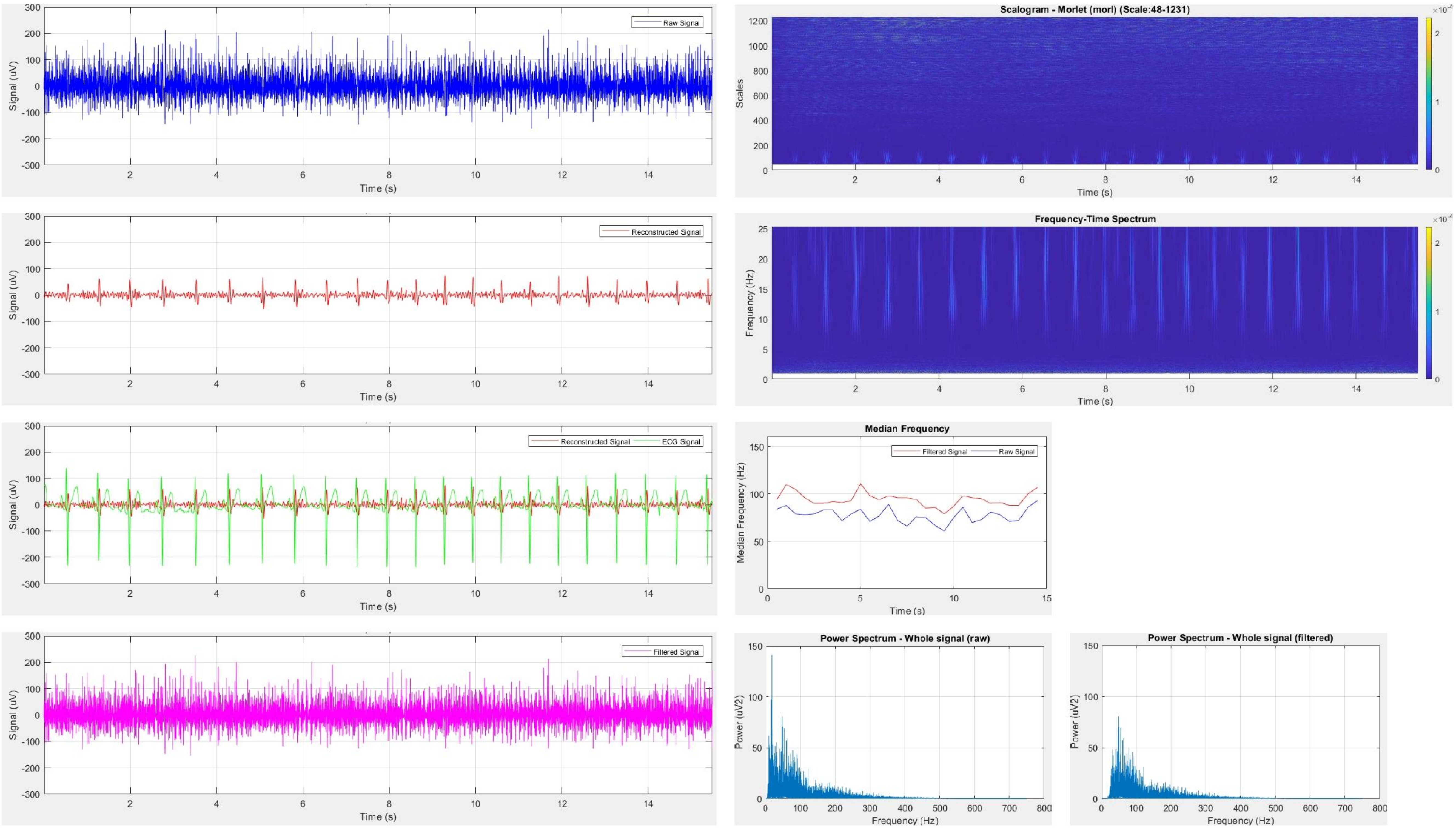

Figure B-26: Participant 7 results 15% MVIC

PARTICIPANT 7: 20% MVIC

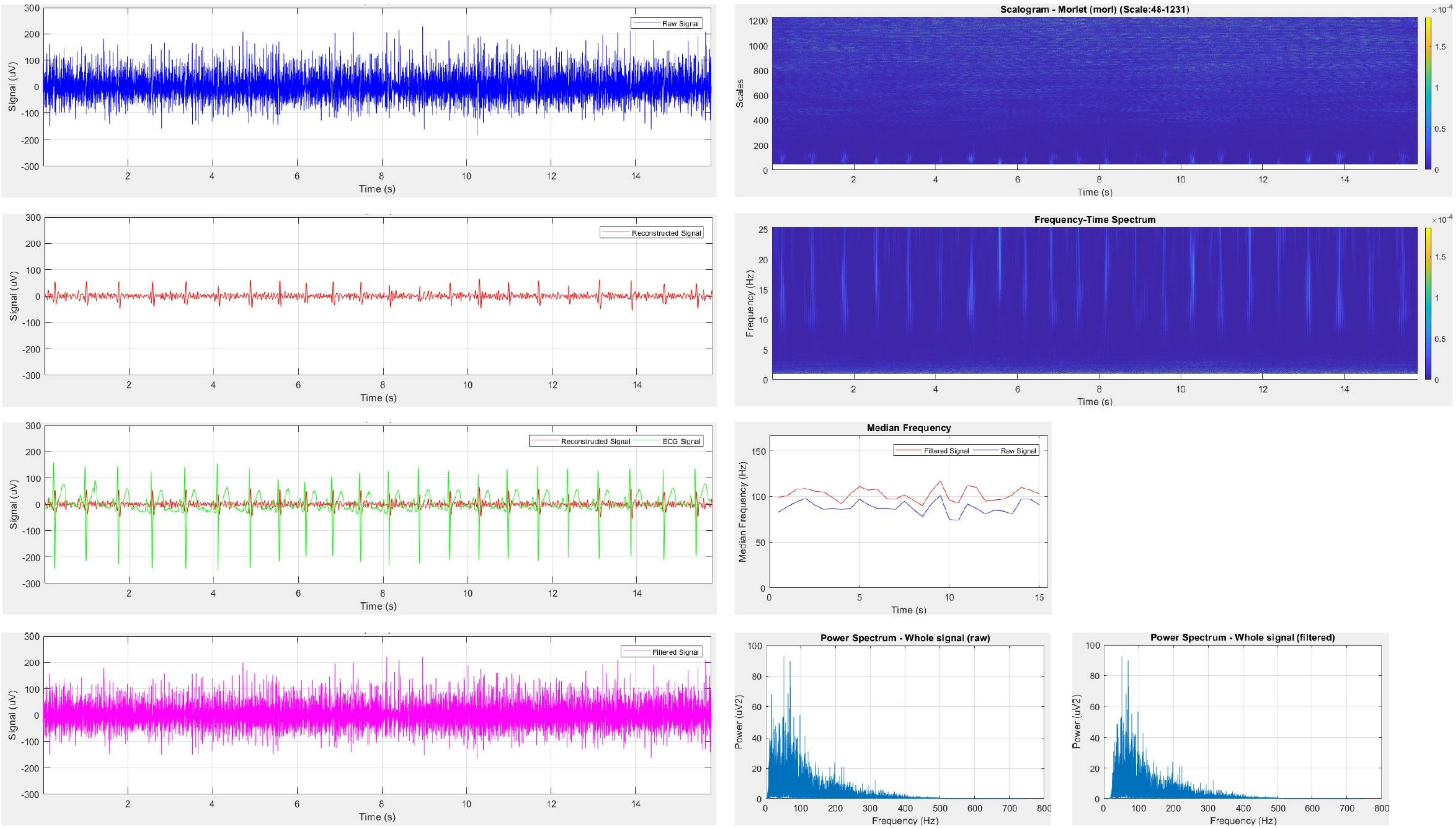

Figure B-27: Participant 7 results 20% MVIC

PARTICIPANT 7: 25% MVIC

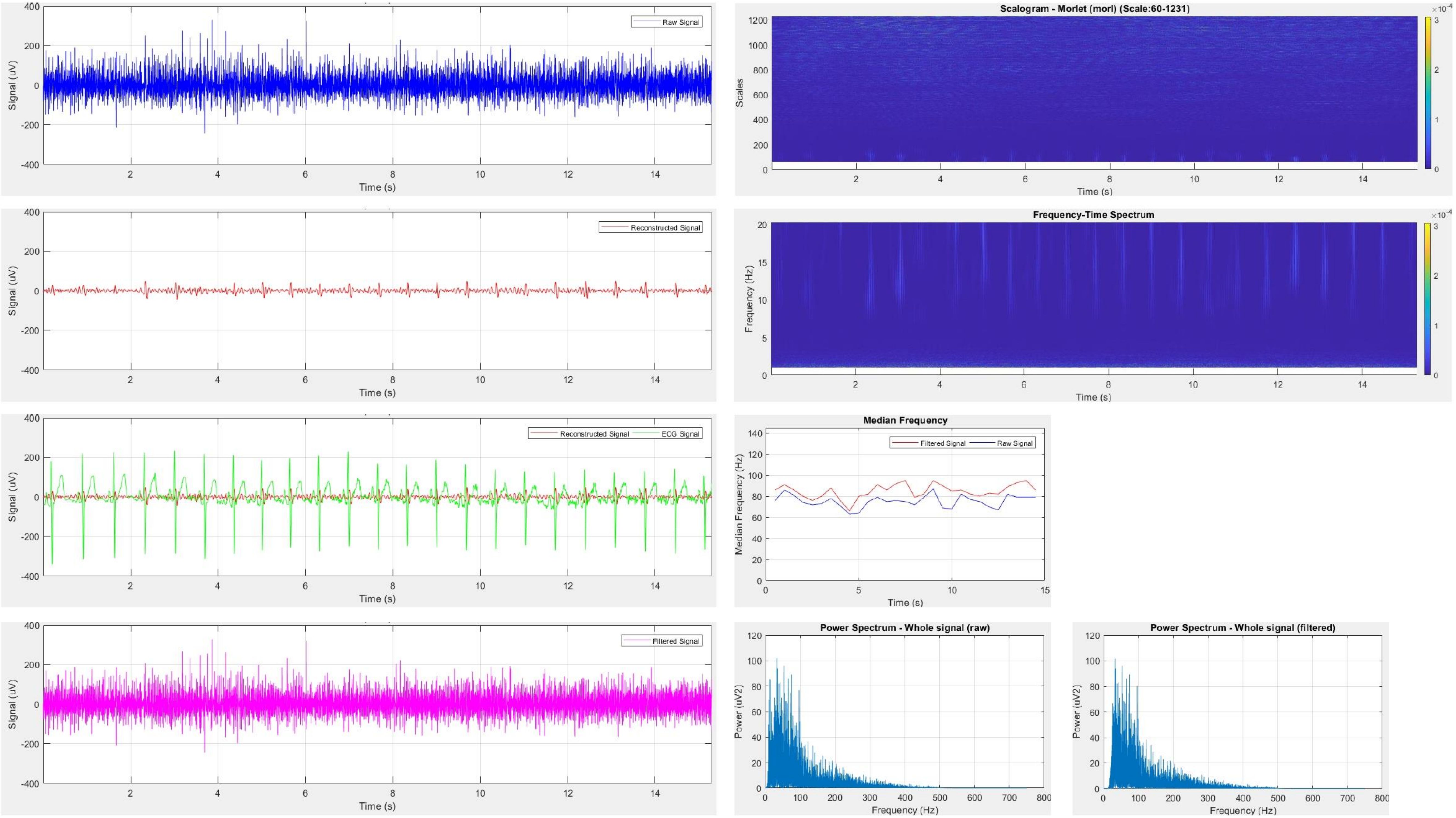

Figure B-28: Participant 7 results 25% MVIC

Appendix C

TE WĀNANGA ARONUI
O TĀMAKI MAKAU RAU

Participant Information Sheet

Date Information Sheet Produced:

22 May 2018

Project Title

Wavelet Techniques for the Decomposition of Surface Electromyography Signals

An Invitation

Kia Ora

I, Anein Deney Simon, a Master of Engineering (ME) student at AUT University in the School of Engineering, am presently conducting a research for completing my qualification. I would like to invite you to participate in my research in signal processing of muscle signals. For any of you who have not had any previous back injuries within the past year or back surgeries, you are welcome to volunteer to be a participant in my research. A part of my research is to collect heart signals and signals from back muscle using electrodes placed on the muscles during a series of set activities. Would you be willing to help me out?

What is the purpose of this research?

The purpose of the research is to find out any useful information regarding heart signals [electrocardiography (ECG)] from muscle signals [electromyography (EMG)]. The research also looks at computing processes to separate the information regarding the heart signals from the muscle signals. The findings of this research may provide important information allowing more accurate measures of how muscles work. This research is conducted towards fulfilment of my Master of Engineering degree.

How was I identified and why am I being invited to participate in this research?

You have been invited to participate in this research upon replying to the advertisement that has been posted at Auckland University of Technology. You will be contacted by the researcher and then you will be screened for inclusion and exclusion criteria. The criteria for being selected for the study is that you will have to be between the age of 18-35 and have not had a back injury within the last year, or any previous back surgeries, and have no brain or nerve injuries, heart disease, or any muscle ailments and are not pregnant. You will also be exempt from participating in this study if you are a student of Dr Jeff Kilby who is my supervisor for this research. If suitable to participate in the study, you will receive verbal explanation of what is involved. Prior to assessment, procedures will be explained to you and time will be given for any remaining questions answered before written consent is obtained.

How do I agree to participate in this research?

Your participation in this research is voluntary (it is your choice) and whether or not you choose to participate will neither advantage nor disadvantage you. You will be required to complete a consent form prior to participating in the research which will be made available to you prior to the data collection at the site. You are able to withdraw from the study at any time. If you choose to withdraw from the study, then you will be offered the choice between having any data that is identifiable as belonging to you removed or allowing it to continue to be used. However, once the findings have been produced, removal of your data may not be possible.

What will happen in this research?

This research will take place in a small gym facility located in the Health and Rehabilitation Research Institute, Physiotherapy Department at the AUT North Shore Campus. Upon arrival, you will be provided with an explanation of procedures, and then asked to complete a consent form. You will then be prepared for placing electrodes that measure the electrical signals of your muscles (EMG) on the skin surfaces covering both the upper (UES in Figure 1) and lower (LES in Figure 1) back muscles. This will involve the shaving of a small area of the skin where the muscle electrode needs to be placed and the cleaning of the shaved area using alcohol wipes. Electrodes that measure the electrical signals of your heart (ECG) electrodes will then be placed on your right (RA) and left (LA) shoulders and left lower chest (LL) (see Figure 1).

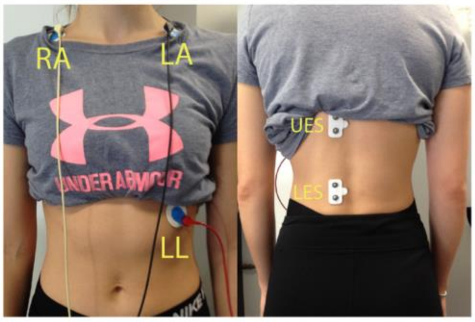

Figure 1. Electrode placement

Following the preparation and placing of the electrodes, you will then perform a 5-minute standardised warm up which will include riding an exercise bike. This will be followed by lifting a box to the beat of a metronome (10-15 lifts per minute) from floor to mid-thigh using a self-selected lifting technique for a period of 2-3 minutes. During the lifting warm-up exercises, the heart and back muscle signals will be recorded.

You will then be positioned in a back device in an upright posture with your pelvis fixated (using quick release harnesses). A quick release chest strap will be attached to you around the upper chest to secure your body to a device that measures force (force gauge) (see Figure 2). This will be attached to a pulley cable with weights attached to it. To familiarise you with the assessment process, you will be required to perform 5 back extensions (pulling backward on cable) at a moderate effort. You will be then required to pull on the cable at maximal effort for 5 seconds. This will be repeated three times.

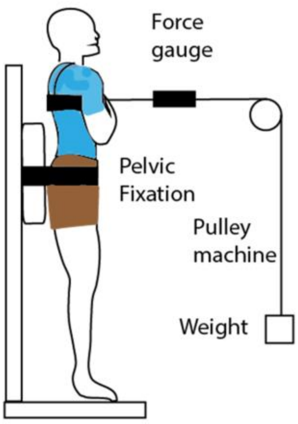

Figure 2. AMT back device and experimental setup.

You will then be required to stand upright, and resist weights loaded at very low to moderate resistance (5-60% of the maximal effort) for 10-15 seconds. Between each of the submaximal efforts, the weights will then be released from the chest harness and you will be able to rest for a period of

2-3 minutes. Following the submaximal tests, you will be asked to perform a back-muscle endurance test. This will involve holding your upright position against a weight of approximately 30-40% of that recorded during your maximal effort for as long as possible. Heart and back muscle signals will be recorded throughout the duration of each task.

Since this research does require the placement of electrodes on your skin, it is advised that you wear something suitable for the procedure. It is recommended that you wear a loose t-shirt, and a sports bra if you are a female participant. For female participants, a female research officer will be present to put on the electrodes and throughout the testing procedures.

What are the discomforts and risks?

There is a possible risk of muscle discomfort during or after the test, but this tends to be short-lived. Undertaking maximum muscle contractions poses a low risk of back muscle strains. Back injury is not expected during the test as previous studies following the same procedure have had no incidences of back injuries. The skin underlying the electrodes will show some redness or mild irritation due to shaving of the skin during preparation. The possible embarrassment will be the requirement of having you to move your shirt for the placement of electrodes and the patches of shaven area of hair on your chest and back, which may be of concern due to the time taken for the hair to grow back.

How will these discomforts and risks be alleviated?

You will be able to terminate testing at any time for any reason. A standardised warmup has been included to reduce any chance of any muscle strain or soreness occurring during the procedure. A mandatory rest period between maximal and sub maximal tasks will also reduce the risk of a muscle strain to occur because of fatigue.

The secondary supervisor for this project (Dr Grant Mawston) is a registered physiotherapist will be present, therefore identify any potential hazardous situation that could occur during testing.

To address the irritation and potential redness, the skin will be cleaned with alcohol swabs before and after electrode placement. Aloe vera cream will be made available to avoid any further skin irritation to develop.

What are the benefits?

You will not have any direct benefit from participating in this research, however you will be acknowledged to have contributed your valuable time and effort towards the research. You will also be provided with a report detailing your individual results against the overall results for the research. This provides you an opportunity to have access to results pertaining to your muscle signals information that aligns with the research.

This research provides the researcher with the knowledge and exposure to further develop the researcher in study of Signal Processing. This research is also required as a prerequisite towards the completion of the primary researcher's Master of Engineering.

This research will provide academic groups within the biomedical sector (not limited to) to facilitate the advancements in research and development involving heart and back muscle signals. This research aims to benefit the Auckland University of Technology School of Engineering and School of Physiotherapy to progress within the area of study involving back muscle signals.

What compensation is available for injury or negligence?

In the unlikely event of a physical injury as a result of your participation in this study, rehabilitation and compensation for injury by accident may be available from the Accident Compensation Corporation, providing the incident details satisfy the requirements of the law and the Corporation's regulations.

How will my privacy be protected?

You will not be personally identifiable during any point of this research. All written consent forms will be scanned and stored on an external electronic storage device in a secured location in Dr Grant Mawston's office (AA116) at AUT University for ten years at AUT University North Shore Campus. The heart and back muscle signals data are to be stored in the external data (electronic) storage devices which will be held in a secured location in Dr Jeff Kilby's office (WZ348) at AUT University for ten years at AUT University City Campus. After ten years they will be destroyed by erasing the data from the external devices. The hard copies of the consent forms will be shredded immediately after being scanned for storage.

What are the costs of participating in this research?

There is no financial cost for you to participate in the research. The only cost to you is the time in attending the testing session which will be no longer than 90 minutes.

What opportunity do I have to consider this invitation?

You will have the opportunity to consider this invitation until the end of August 2018.

Will I receive feedback on the results of this research?

You will be provided with the results obtained from this research by filling the request within the consent form. This will be given in the form of small report to show how your individual results are reflected and compared with the overall results.

What do I do if I have concerns about this research?

You may withdraw from the research at any time.

Any concerns regarding the nature of this project should be notified in the first instance to the Project Supervisor: Dr Jeff Kilby, *jeffrey.kilby@aut.ac.nz,* 09 921 9999 ext 8748.

Concerns regarding the conduct of the research should be notified to the Executive Secretary of AUTEC, Kate O'Connor, *ethics@aut.ac.nz* , 921 9999 ext 6038.

Whom do I contact for further information about this research?

Please keep this Information Sheet and a copy of the Consent Form for your future reference. You are also able to contact the research team as follows:

Researcher Contact Details:

Anein Deney Simon, *qgt9550@aut.ac.nz,* +64210501517.

Project Supervisor Contact Details:

Dr Jeff Kilby, *jeffrey.kilby@aut.ac.nz,* 09 921 9999 ext 8748.

Approved by the Auckland University of Technology Ethics Committee on 21 September 2018, AUTEC Reference number *18/219.*

Auckland University of Technology Ethics Committee (AUTEC)

Auckland University of Technology
D-88, Private Bag 92006, Auckland 1142, NZ
T: +64 9 921 9999 ext. 8316
E: ethics@aut.ac.nz
www.aut.ac.nz/researchethics

6 August 2018

Jeffrey Kilby
Faculty of Health and Environmental Sciences

Dear Jeffrey

Re Ethics Application: **18/219 Wavelet techniques for the decomposition of surface electromyography signals**

Thank you for providing evidence as requested, which satisfies the points raised by the Auckland University of Technology Ethics Committee (AUTEC).

Your ethics application has been approved for three years until 6 August 2021.

Standard Conditions of Approval

1. A progress report is due annually on the anniversary of the approval date, using form EA2, which is available online through http://www.aut.ac.nz/research/researchethics.
2. A final report is due at the expiration of the approval period, or, upon completion of project, using form EA3, which is available online through http://www.aut.ac.nz/research/researchethics.
3. Any amendments to the project must be approved by AUTEC prior to being implemented. Amendments can be requested using the EA2 form: http://www.aut.ac.nz/research/researchethics.
4. Any serious or unexpected adverse events must be reported to AUTEC Secretariat as a matter of priority.
5. Any unforeseen events that might affect continued ethical acceptability of the project should also be reported to the AUTEC Secretariat as a matter of priority.

Please quote the application number and title on all future correspondence related to this project.

AUTEC grants ethical approval only. If you require management approval for access for your research from another institution or organisation then you are responsible for obtaining it. You are reminded that it is your responsibility to ensure that the spelling and grammar of documents being provided to participants or external organisations is of a high standard.

For any enquiries, please contact ethics@aut.ac.nz

Yours sincerely,

K O'Connor

Kate O'Connor
Executive Manager
Auckland University of Technology Ethics Committee

Cc: qgt9550@aut.ac.nz; Grant Mawston

Appendix D

```
%This program creates the interface for the selection of Parameters and the
%signal for analysis
function cwavanalysis
global waveletsel;
global wavelet;
global scales; %higher scale limit
global scales0;%lower scale limit
global ordsc;
global pseufreq;
global pseufreq0;
global Fs;
global Fc;
global window;
global wnn;
global kk;
rr = 0;
N = 0;
rawdata = [];
%creation of initial interface
f = figure('Visible','off');
f.Units = 'normalized';
        val = uicontrol('Style','text','Units','normalized',...
            'FontSize', 8,'Position',[0.05 0.82 0.04 0.022],'Visible', 'off',...
            'HandleVisibility','off');
        val0 = uicontrol('Style','text','Units','normalized',...
            'FontSize', 8,'Position',[0 0.82 0.04 0.022],'Visible', 'off',...
```

```
    'HandleVisibility','off');
  valf = uicontrol('Style','text','Units','normalized',...
    'FontSize', 8,'Position',[0.05 0.8 0.04 0.022],'Visible', 'off',...
    'HandleVisibility','off');
  valf0 = uicontrol('Style','text','Units','normalized',...
    'FontSize', 8,'Position',[0 0.8 0.04 0.022],'Visible', 'off',...
    'HandleVisibility','off');
  val2 = uicontrol('Style','text','Visible', 'off',...
    'HandleVisibility','off','Units','normalized','FontSize', 10,...
    'Position',[0.05 0.015 0.2 0.03]);
  sld0 = uicontrol('Style', 'slider','Units','normalized',...
    'Position', [0.015 0.2 0.008 0.6],'Visible', 'off',...
    'HandleVisibility','off','BackgroundColor', [0 0 0],...
    'Callback', {@sca0,val0,valf0});
  sld = uicontrol('Style', 'slider','Units','normalized',...
    'Position', [0.065 0.2 0.008 0.6],'Visible', 'off',...
    'HandleVisibility','off','BackgroundColor', [0 0 0],...
    'Callback', {@sca,val,valf});
  winerrtxt =  uicontrol('Style','text',...
    'Visible', 'off','HandleVisibility', 'off',...
    'FontSize', 8,'Units','normalized',...
    'Position', [0.005 0.10 0.287 0.022],...
    'HorizontalAlignment','left');
  ordtxt = uicontrol('Style','text',...
    'FontSize', 8,'HandleVisibility', 'off','Units','normalized',...
    'Visible', 'off','Position', [0 0.87 0.057 0.022],...
    'HorizontalAlignment','left','String','Order:');
  popupord = uicontrol('Style', 'popup','Units','normalized',...
    'String', {'Morlet','Mexican Hat',...
    'Coiflets','Biorthogonal','Reverse Biorthogonal',...
```

```
        'Gaussian','Complex Gaussian'},...
        'Position', [0.025 0.9 0.03 0],'Visible', 'off',...
        'HandleVisibility','off');
    popup = uicontrol('Style', 'popup','Units','normalized',...
        'String', {'Morlet','Mexican Hat','Coiflets','Biorthogonal',...
        'Reverse Biorthogonal','Gaussian','Complex Gaussian'},...
        'Position', [0 0.935 0.09 0],'Visible', 'off',...
        'HandleVisibility','off','Callback', {@wav,popupord,ordtxt});
    betartxt = uicontrol('Style','text',...
        'FontSize', 8,'HandleVisibility', 'off','Units','normalized',...
        'Visible', 'off','Position', [0.01 0.125 0.057 0.022],...
        'HorizontalAlignment','left');
    betarval = uicontrol('Style','edit',...
        'FontSize', 8,'Visible', 'off','HandleVisibility', 'off',...
        'Units','normalized','Visible', 'off',...
        'Position', [0.035 0.125 0.04 0.03]);
    popup2 = uicontrol('Style', 'popup','Units','normalized',...
        'String', {'No window','Bartlett','Blackman','Boxcar','Chebyshev',...
        'Hamming','Hanning','Kaiser','Taylor','Triangular'},...
        'Position', [0.01 0.19 0.07 0],'Visible', 'off',...
        'HandleVisibility','off','Callback', {@wind,betartxt,betarval,winerrtxt});
    btn = uicontrol('Style', 'pushbutton','String','Run',...
        'FontName' , 'Georgia','FontSize', 12,'Units','normalized',...
        'Visible', 'off','HandleVisibility','off',...
        'Position', [0.02 0.02 0.05 0.04],...
        'Callback', {@exel,val2,popup2,betarval,winerrtxt});
    fstxt = uicontrol('Style','text',...
       'FontSize', 8,'HandleVisibility', 'off','Units','normalized',...
       'Visible', 'off','Position', [0.004 0.94 0.057 0.022],...
       'HorizontalAlignment','left','String','Sampling Rate:');
```

```
        sampf = uicontrol('Style','edit',...
          'FontSize', 8,'Visible', 'off','HandleVisibility', 'off',...
          'Units','normalized','Visible', 'off',...
          'Position', [0.06 0.938 0.04 0.03]);
        chkbw = uicontrol('Style', 'checkbox', 'Units','normalized',...
          'Visible', 'off','HandleVisibility', 'off',...
          'Position', [0.09 0.91 0.015 0.019],...
          'Callback', {@chboxw,val,val0,valf,valf0,sld0,sld,popup,...
                    btn,popupord,val2,popup2,betartxt,betarval});
        chkb = uicontrol('Style', 'checkbox', 'Units','normalized',...
          'Visible', 'off','HandleVisibility', 'off',...
          'Position', [0.1 0.94 0.015 0.019],...
          'Callback', {@chbox,sampf,val,val0,valf,valf0,sld0,sld,...
                     popup,btn,betartxt,betarval,popup2,popupord,ordtxt,...
                     val2,chkbw,winerrtxt});
        uicontrol('Style', 'pushbutton', 'String', 'Load Signal',...
          'FontName' , 'Georgia', 'FontSize', 10,...
          'HandleVisibility', 'off','Units','normalized',...
          'Position', [0.015 0.97 0.1 0.03],...
          'Callback', {@load,val,val0,valf,valf0,sld0,sld,popup,btn,...
                    fstxt,sampf,chkb,betartxt,betarval,popup2,popupord,...
                    ordtxt,val2,chkbw,winerrtxt});
f.Visible = 'on';
plotwindow();
%Load the signal from file and access to more parameter controls
function load (~,~,val_handle,val0_handle,valf_handle,...
            valf0_handle,sld0_handle,sld_handle,popup_handle,btn_handle,...
            fstxt_handle,sampf_handle,chkb_handle,betartxt_handle,...
            betarval_handle,popup2_handle,popupord_handle,ordtxt_handle,...
            val2_handle,chkbw_handle,winerrtxt_handle)
```

```
clf;
set(val_handle,'Visible','off');
set(val0_handle,'Visible','off');
set(valf_handle,'Visible','off');
set(valf0_handle,'Visible','off');
set(sld0_handle,'Visible','off');
set(sld_handle,'Visible','off');
set(popup_handle,'Visible','off');
set(btn_handle,'Visible','off');
set(fstxt_handle,'Visible','off');
set(sampf_handle,'Visible','off');
set(chkb_handle,'Visible','off');
set(betartxt_handle,'Visible','off');
set(betarval_handle,'Visible','off');
set(popup2_handle,'Visible','off');
set(popupord_handle,'Visible','off');
set(ordtxt_handle,'Visible','off');
set(val2_handle,'Visible','off');
set(chkbw_handle,'Visible','off');
set(winerrtxt_handle,'Visible','off');
%execution of file and data collection subfunctions
[filename,sheets] = excelfile();
if filename == 0
return
end
[sheetx] = selsheet(sheets);
if isempty(sheetx)
return
end
rawdata = sample(filename,sheetx);
```

```
      if rawdata == 0
      return
      end
%computation of scale limit based on the data length
N = length(rawdata);
if N~=0
   m2 = 0;
   while ((2^m2) < (N/2))
      m2 = m2+1;
   end
   max = 2^(m2-1);
   scales0 = 1;
   scales = 1;
      set(sld0_handle,'Min',1,'Max',max,'Value',1,...
        'SliderStep',[(1/(max-1)) (10/(max-1))]);
      set(sld_handle,'Min',1,'Max',max,'Value',1,...
        'SliderStep',[(1/(max-1)) (10/(max-1))]);
      set(fstxt_handle,'Visible', 'on');
      set(sampf_handle,'String','','Enable','on','Visible', 'on');
      set(chkb_handle,'Value',0,'Visible', 'on');
end
end
%Sampling frequency input and error check
function chbox(checkbox,~,sampf_handle,val_handle,val0_handle,valf_handle,...
            valf0_handle,sld0_handle,sld_handle,popup_handle,btn_handle,...
            betartxt_handle,betarval_handle,popup2_handle,popupord_handle,...
            ordtxt_handle,val2_handle,chkbw_handle,winerrtxt_handle)
   aa = checkbox.Value;
   if aa == 1
      set(sampf_handle,'Enable','Off');
```

```
    Fs = str2double(get(sampf_handle,'String'));
clf;
if isnan(Fs) || (Fs<0) || floor(Fs)~=Fs
    uicontrol('Style','text','FontSize', 8,'Units','normalized',...
     'Position', [0.005 0.915 0.3 0.022],'HorizontalAlignment','left',...
     'string','Sampling Frequency incorrect (please enter an integer number greater than 0)');
elseif Fs>N
    uicontrol('Style','text','FontSize', 8,'Units','normalized',...
     'Position', [0.005 0.915 0.287 0.022],'HorizontalAlignment','left',...
     'string','Please load a signal with a sample size of at least 1 second');
else
    waveletsel = 'Morlet';
    wnn = 'morl';
    ordsc = 0;
    kk = 0;
    set(popup_handle,'Value',1,'Visible','on','Enable','on');
    set(popupord_handle,'Enable','On');
    set(chkbw_handle,'Value',0,'Visible','on');
end
else
    clf;
    set(sampf_handle,'Enable','On');
    set(val_handle,'Visible', 'off');
    set(val0_handle,'Visible', 'off');
    set(valf_handle,'Visible', 'off');
    set(valf0_handle,'Visible', 'off');
    set(sld0_handle,'Visible', 'off');
    set(sld_handle,'Visible', 'off');
    set(popup_handle,'Visible', 'off');
    set(btn_handle,'Visible', 'off');
```

```
        set(betartxt_handle,'Visible','off');
        set(betarval_handle,'Visible','off');
        set(popup2_handle,'Visible','off');
        set(popupord_handle,'Visible','off');
        set(ordtxt_handle,'Visible','off');
        set(val2_handle,'Visible','off');
        set(chkbw_handle,'Visible','off');
        set(winerrtxt_handle,'Visible','off');
    end
end

%Window function display for FFT window selection
function wind(source,~,betartxt_handle,betarval_handle,winerrtxt_handle)
        windn = source.String;
        windv = source.Value;
        window = windn{windv};
        clf;
        set(winerrtxt_handle,'Visible','off');
switch window
    case {'No window','Bartlett','Blackman','Boxcar','Hamming',...
          'Hanning','Taylor','Triangular'}
        set(betartxt_handle,'Visible','off');
        set(betarval_handle,'String','','Visible','off','Enable','off');
        rr = 0;
    case 'Chebyshev'
        set(betartxt_handle,'String','Ripple:','Visible','on');
        set(betarval_handle,'Visible','on','Enable','on');
        rr = 1;
    case 'Kaiser'
        set(betartxt_handle,'String','Beta:','Visible','on');
```

```
        set(betarval_handle,'Visible','on','Enable','on');
        rr = 2;
end
end

%Display of wavelet function available for selection
function wav(source,~,popupord_handle,ordtxt_handle)
        wavn = source.String;
        wavv = source.Value;
        waveletsel = wavn{wavv};
        kk = 0;
switch waveletsel
    case 'Morlet'
        ordsc = 0;
        wnn = 'morl';
    case 'Mexican Hat'
        ordsc = 0;
        wnn = 'mexh';
    case 'Coiflets'
        ordsc = 1:5;
        wnn = 'coif';
    case 'Biorthogonal'
        ordsc = [2.2 2.4 2.6...
                 2.8 4.4 5.5 6.8];
        wnn = 'bior';
    case 'Reverse Biorthogonal'
        ordsc = [2.2 2.4 2.6...
                 2.8 4.4 5.5 6.8];
        wnn = 'rbio';
    case 'Gaussian'
```

```
        ordsc = [2 4 6 8];
        wnn = 'gaus';
    case 'Complex Gaussian'
        ordsc = [2 4 6 8];
        wnn = 'cgau';
end
if ordsc ~= 0
        set(popupord_handle,'Visible','On');
        set(ordtxt_handle,'Visible','On');
        set(popupord_handle,'string', cellfun(@num2str,num2cell(ordsc),'UniformOutput',false));
        set(popupord_handle,'value',1);
else
        set(popupord_handle,'Visible','Off');
        set(ordtxt_handle,'Visible','Off');
end
end

%computation of pseudo-frequency for display
function chboxw(checkboxw,~,val_handle,val0_handle,valf_handle,valf0_handle,...
                sld0_handle,sld_handle,popup_handle,btn_handle,popupord_handle,...
                val2_handle,popup2_handle,betartxt_handle,betarval_handle)
    clf;
    ab = checkboxw.Value;
    if ab == 1
        set(popup_handle,'Enable','Off');
        set(popupord_handle,'Enable','Off');
            if ordsc ~=0
                ordn = get(popupord_handle,'String');
                ordv = get(popupord_handle,'Value');
                order = ordn{ordv};
```

```
            wavelet = strcat(wnn,order);
        else
            wavelet = wnn;
        end
        Fc = centfrq(wavelet);
        scales0 = 1;
        scales = 1;
        pseufreq = Fs*(Fc/scales);
        pseufreq0 = Fs*(Fc/scales0);
        set(val_handle,'String',['Max:',num2str(scales)]);
        set(val0_handle,'String',['Min:',num2str(scales0)]);
        set(valf_handle,'String',['f:',(sprintf('%.3f',round(pseufreq,3)))]);
        set(valf0_handle,'String',['f:',(sprintf('%.3f',round(pseufreq0,3)))]);
        set(val_handle,'Visible', 'on');
        set(val0_handle,'Visible', 'on');
        set(valf_handle,'Visible', 'on');
        set(valf0_handle,'Visible', 'on');
        set(sld0_handle,'Value',scales0,'Visible','on');
        set(sld_handle,'Value',scales,'Visible','on');
        set(popup2_handle,'Value',1,'Visible','on');
        set(btn_handle,'Visible','on');
    else
        set(popup_handle,'Enable','On');
        set(popupord_handle,'Enable','On');
        set(val_handle,'Visible', 'off');
        set(val0_handle,'Visible', 'off');
        set(valf_handle,'Visible', 'off');
        set(valf0_handle,'Visible', 'off');
        set(sld0_handle,'Visible', 'off');
        set(sld_handle,'Visible', 'off');
```

```
        set(btn_handle,'Visible','off');
        set(popup2_handle,'Visible','off');
        set(val2_handle,'Visible','off');
        set(betartxt_handle,'Visible','off');
        set(betarval_handle,'Visible','off');
    end
end

%scale display based on the current selection of display
function sca (source,~,val_handle,valf_handle)
    scales = round(source.Value,0);
    pseufreq = Fs*(Fc/scales);
    set(val_handle,'String',['Max:',num2str(scales)]);
    set(valf_handle,'String',['f:',(sprintf('%.3f',round(pseufreq,3)))]);
end
function sca0 (source,~,val0_handle,valf0_handle)
    scales0 = round(source.Value,0);
    pseufreq0 = Fs*(Fc/scales0);
    set(val0_handle,'String',['Min:',num2str(scales0)]);
    set(valf0_handle,'String',['f:',(sprintf('%.3f',round(pseufreq0,3)))]);
end

%Execution of selected parameters and CWT with error catching
function exel(~,~,val2_handle,popup2_handle,betarval_handle,winerrtxt_handle)
    if scales > scales0
        set(winerrtxt_handle,'Visible','off');
        windown = get(popup2_handle,'String');
        windowv = get(popup2_handle,'Value');
        windowx = windown{windowv};
        br = str2double(get(betarval_handle,'String'));
```

```
        if rr == 0
            br = 0;
        elseif (isnan(br) && rr==1) || br<0
            set (val2_handle,'Visible','off');
            set(winerrtxt_handle,'string',...
                'Chebyshev stopband ripple invalid','Visible','on');
            return
        elseif (isnan(br) && rr==2) || br<0
            set (val2_handle,'Visible','off');
            set(winerrtxt_handle,'string',...
                'Kaiser parameter beta invalid','Visible','on');
            return
        end
        tic;
        set (btn,'enable','off');
        pause(0.0000001);
        clf;
        Calculations (waveletsel,wavelet,scales,scales0,N,rawdata,Fs,br,windowx);
        tim = sprintf('%.3f',round(toc,3));
        set (val2_handle,'String',['Runtime: ', tim,'seconds'],'Visible','on');
        set (btn,'enable','on');
    else
        msgbox(sprintf('Error: Minimum scale > Maximum scale'));
    end

end
end
```

```
%This program creates the plot window required for interface
function plotwindow()
warning('off', 'MATLAB:HandleGraphics:ObsoletedProperty:JavaFrame');
pause(0.00001);
frame_h = get(handle(gcf),'JavaFrame');
set(frame_h,'Maximized',1);
end
```

```
%This program includes the implementation of CWT and the display of plots
function [] = Calculations(waveletsel,wavelet,scale,scale0,N,rawdata,Fs,br,windowx)
t = 1/Fs:1/Fs:N/Fs;    % set time scale for plot
freq = 0:Fs/N:Fs/2;     % set frequency scale for plot
%demeaning the sEMG and ECG
rawdat1 = rawdata(:,1);
rawdata1 = rawdat1 - mean(rawdat1);
rawdat2 = rawdata(:,2);
rawdata2 = rawdat2 - mean(rawdat2);
%Implementation of CWT
scales = scale0:scale;
[coeff,pseufreq] = cwt(rawdata1,scales,wavelet,(1/Fs));
%Calculation of threshold value
thresh = [];
coeffx = abs(coeff);
medofdev = mad(coeffx,1,1);
sdev = medofdev/0.6745;
thresh = (sdev*(sqrt(2*log10(Fs))))/(sqrt(Fs));
```

```
%Implementation of threshold function
for rx = 1:N
    for ry = 1:((scale-scale0)+1)
      if coeffx(ry,rx)<thresh(rx)
          coeff(ry,rx) = 0;
      end
    end
end
%Reconstruction of the CWT function
sigwavinv = icwtlin(wavelet,0,coeff,scales,(1/Fs));
sigwavx = transpose(sigwavinv);

maxr = max(rawdata1);
minr = min(rawdata1);
maxr2 = max(rawdata2);
minr2 = min(rawdata2);

graaa2 = [];
var21=[];
var22=[];

for xx = 2:N
    grad2 = (rawdata2(xx)-rawdata2(xx-1))/(1/Fs);
    graaa2 = [graaa2 grad2];
end

%ECG peak detection
[pks2,locs2] = findpeaks(rawdata2); %finding peaks minimse data points to analyse
for ax2 = 1:length (pks2)
    v21 = pks2(ax2);
```

```
v21l = locs2(ax2);
grcount2 = 0;
mm2 = 0;
%detection of the R peak in the ECG signal
for aa2 = v21l:(v21l+ceil(0.02*Fs))
if aa2<N
   vg2 = graaa2(aa2);
   if vg2<0
      grcount2 = grcount2+1;
      if vg2<(10*(minr2-maxr2)) && mm2 == 0
         mm2 = 1;
      end
      if grcount2 < 12 && mm2 == 1
         v21x = v21;
         v21lx = v21l;
      end
      if grcount2 == 12 && mm2 == 1
         if (v21l-v21lx)<(ceil(Fs/300)) && v21x>v21
            var21 = [var21 v21x];
            var22 = [var22 v21lx];
         else
            var21 = [var21 v21];
            var22 = [var22 v21l];
         end
         mm2 = 0;
      end
   else
      grcount2 = 0;
   end
end
```

```
    end
end

%window function to select the window for the FFT of the signal
sigwavxa = rawdata1-sigwavx;
switch windowx
    case 'No window'
        sigxx = sigwavxa;
        rawdata1x = rawdata1;
    case 'Bartlett'
        winx = bartlett(N);
        sigxx = winx.*sigwavxa;
        rawdata1x = winx.*rawdata1;
    case 'Blackman'
        winx = blackman(N);
        sigxx = winx.*sigwavxa;
        rawdata1x = winx.*rawdata1;
    case 'Boxcar'
        winx = rectwin(N);
        sigxx = winx.*sigwavxa;
        rawdata1x = winx.*rawdata1;
    case 'Hamming'
        winx = hamming(N);
        sigxx = winx.*sigwavxa;
        rawdata1x = winx.*rawdata1;
    case 'Hanning'
        winx = hann(N);
        sigxx = winx.*sigwavxa;
        rawdata1x = winx.*rawdata1;
    case 'Taylor'
```

```
        winx = taylorwin(N);
        sigxx = winx.*sigwavxa;
        rawdata1x = winx.*rawdata1;
    case 'Triangular'
        winx = triang(N);
        sigxx = winx.*sigwavxa;
        rawdata1x = winx.*rawdata1;
    case 'Chebyshev'
        winx = chebwin(N,br);
        sigxx = winx.*sigwavxa;
        rawdata1x = winx.*rawdata1;
    case 'Kaiser'
        winx = kaiser(N,br);
        sigxx = winx.*sigwavxa;
        rawdata1x = winx.*rawdata1;
end
%FFT of EMG and ECG signal
xdft = fft(sigxx);      % fft of signal to obtain frequency components
xdft = xdft(1:(floor(N/2)+1));% increments of signal frequency upto nyquist frequency (N/2+1)
psda = (1/(Fs*N));  % obtaining the epoch from the time period and number of samples
psdb = abs(xdft).^2;% squaring the absolute values to obtain power (V^2)
psdx = psda.*psdb;  % total power spectrum
psdx(2:end-1) = 2*psdx(2:end-1);% positive and negative components are enhanced by
                                % multiplying frequencies by a factor of 2, apart
                                % from the Nyquist and 1st frequency values.
xdftr = fft(rawdata1x);      % fft of signal to obtain frequency components
xdftr = xdftr(1:(floor(N/2)+1));% increments of signal frequency upto nyquist frequency (N/2+1)
psdar = (1/(Fs*N));  % obtaining the epoch from the time period and number of samples
psdbr = abs(xdftr).^2;% squaring the absolute values to obtain power (V^2)
psdxr = psdar.*psdbr;  % total power spectrum
```

```
psdxr(2:end-1) = 2*psdxr(2:end-1);% positive and negative components are enhanced by
                                 % multiplying frequencies by a factor of 2, apart
                                 % from the Nyquist and 1st frequency values.
psdxt = sum(psdx);
psdxrt = sum(psdxr);
CC1 = {};
CCf1 = {};
CC2 = {};
CCf2 = {};
%Isolation function to extract windows between consecutive QRS waveforms
for swt = 2:length(var22)
    pkx11 = var22(swt-1)+90;
    pkx12 = var22(swt)-90;
    datpx = [];
    datpx2 = [];
    if pkx12>pkx11
        for nn = pkx11:pkx12
        datp = sigwavxa(nn);
        datpx = [datpx datp];
        datp2 = rawdata1(nn);
        datpx2 = [datpx2 datp2];
        end
        xN = length(datpx);
        xdftk = fft(datpx);      % fft of signal to obtain frequency components
        xdftk = xdftk(1:(floor(xN/2)+1));% increments of signal frequency upto nyquist frequency (N/2+1)
        psdak = (1/(Fs*xN));  % obtaining the epoch from the time period and number of samples
        psdbk = abs(xdftk).^2;% squaring the absolute values to obtain power (V^2)
        psdxk = psdak.*psdbk;  % total power spectrum
        psdxk(2:end-1) = 2*psdxk(2:end-1);% positive and negative components are enhanced by
                                 % multiplying frequencies by a factor of 2, apart
```

```
                        % from the Nyquist and 1st frequency values.
        freqk = 0:Fs/xN:Fs/2;
        CC1 = [CC1;psdxk];
        CCf1 = [CCf1;freqk];

        xN2 = length(datpx2);
        xdftk2 = fft(datpx2);      % fft of signal to obtain frequency components
        xdftk2 = xdftk2(1:(floor(xN2/2)+1));% increments of signal frequency upto nyquist frequency (N/2+1)
        psdak2 = (1/(Fs*xN2));  % obtaining the epoch from the time period and number of samples
        psdbk2 = abs(xdftk2).^2;% squaring the absolute values to obtain power (V^2)
        psdxk2 = psdak2.*psdbk2;  % total power spectrum
        psdxk2(2:end-1) = 2*psdxk2(2:end-1);% positive and negative components are enhanced by
                        % multiplying frequencies by a factor of 2, apart
                        % from the Nyquist and 1st frequency values.
        freqk2 = 0:Fs/xN2:Fs/2;
        CC2 = [CC2;psdxk2];
        CCf2 = [CCf2;freqk2];
    end
end
scff1=[];
scff2=[];
for coecount1 = 1:length(CC1)
    scff1(coecount1,:) = sum (cell2mat(CC1(coecount1,:)));
    scff2(coecount1,:) = sum (cell2mat(CC2(coecount1,:)));
end

coeff2 = abs(coeff).^2;
coeff2 = 100*coeff2./sum(coeff2(:));
rwx = ((maxr-minr)/(maxr2-minr2));
rw2 = rwx*rawdata2;
```

```
%Plot generation with selection for the Raw sEMG signal, Reconstructed ECG
%signal, Filtered EMG signal and Acquired ECG signal
chb1 = 1;
chb2 = 1;
chb3 = 1;
chb4 = 1;
hold on
clf
uicontrol('Style', 'checkbox', 'Units','normalized',...
        'value',1,'Position', [0.44 0.955 0.015 0.019],...
        'Callback',@chv1);
uicontrol('Style', 'checkbox', 'Units','normalized',...
        'value',1,'Position', [0.44 0.935 0.015 0.019],...
        'Callback',@chv2);
uicontrol('Style', 'checkbox', 'Units','normalized',...
        'value',1,'Position', [0.55 0.955 0.015 0.019],...
        'Callback',@chv3);
uicontrol('Style', 'checkbox', 'Units','normalized',...
        'value',1,'Position', [0.55 0.935 0.015 0.019],...
        'Callback',@chv4);
uicontrol('Style','text','FontSize', 8,...
        'Units','normalized','Position', [0.455 0.95 0.09 0.022],...
        'HorizontalAlignment','left','String','Raw Signal');
uicontrol('Style','text','FontSize', 8,...
        'Units','normalized','Position', [0.455 0.93 0.09 0.022],...
        'HorizontalAlignment','left','String','Reconstructed Signal');
uicontrol('Style','text','FontSize', 8,...
        'Units','normalized','Position', [0.565 0.95 0.09 0.022],...
        'HorizontalAlignment','left','String','ECG Signal');
uicontrol('Style','text','FontSize', 8,...
```

```
        'Units','normalized','Position', [0.565 0.93 0.09 0.022],...
        'HorizontalAlignment','left','String','Filtered Signal');
subplot(3,3,[1 2])
plot(t,rawdata1,'b',t,sigwavx,'r',t,rw2,'g',t,sigwavxa,'m');
yaxis = ylim;
legend({'Raw Signal','Reconstructed Signal','ECG Signal',...
      'Filtered Signal'},'Location', 'northeast','FontSize',8,...
      'Orientation','Horizontal')
xlim([min(t) max(t)]);
grid on
title({['EMG Signal: ',waveletsel];['(',wavelet,')']})
xlabel('Time (s)')
ylabel('Signal (uV)')

function chv1(chval1,~)
      chb1 = chval1.Value;
      replot(chb1,chb2,chb3,chb4,yaxis,t,...
            rawdata1,sigwavx,rw2,sigwavxa,waveletsel,wavelet);
end

function chv2(chval2,~)
      chb2 = chval2.Value;
      replot(chb1,chb2,chb3,chb4,yaxis,t,...
            rawdata1,sigwavx,rw2,sigwavxa,waveletsel,wavelet);
end

function chv3(chval3,~)
      chb3 = chval3.Value;
      replot(chb1,chb2,chb3,chb4,yaxis,t,...
            rawdata1,sigwavx,rw2,sigwavxa,waveletsel,wavelet);
```

```
end

function chv4(chval4,~)
        chb4 = chval4.Value;
        replot(chb1,chb2,chb3,chb4,yaxis,t,...
            rawdata1,sigwavx,rw2,sigwavxa,waveletsel,wavelet);
end

%Scalogram plot
subplot(3,3,[4 5])
surf(t,scales,coeff2);
shading interp
view(0,90)
cb1 = colorbar;
cb1.Location = 'manual';
cb1.Position = [0.63 0.41 0.005 0.215];
xlim([min(t) max(t)]);
ylim([0 max(scales)]);
title(['Scalogram - ',waveletsel,' (',wavelet,')',' (Scale:',num2str(scale0),'-',num2str(scale),')'])
xlabel('Time (s)')
ylabel('Scales')

%Frequency-time spectrum plot
sbp = subplot(3,3,[7 8]);
surf(t,pseufreq,coeff2);
shading interp
view(0,90)
cb2 = colorbar;
cb2.Location = 'manual';
cb2.Position = [0.63 0.11 0.005 0.215];
```

```
axis xy;
xlim([min(t) max(t)]);
ylim([0 max(pseufreq)]);
slda = uicontrol('Style', 'slider','Units','normalized',...
        'Min',1,'Max',1000,'Value',1,...
        'SliderStep',[1/1000 10/1000],...
        'Position', [0.08 0.11 0.007 0.215],...
        'BackgroundColor', [0 0 0],...
        'Callback', @zm);
function zm(source,~)
        set(sbp, 'YLim', [0 (max(pseufreq)/source.Value)]);
end
title(['Frequency-Time Spectrum - ',waveletsel,' (',wavelet,')',' (Scale:',num2str(scale0),'-',num2str(scale),')'])
xlabel('Time (s)')
ylabel('Frequency (Hz)')

%Power spectrum of the whole raw sEMG signal
subplot(3,3,9)
plot(freq,psdxr);
uicontrol('Style','text','FontSize', 8,...
         'Units','normalized','Position', [0.92 0.155 0.09 0.022],...
         'HorizontalAlignment','left','String',[' Total Power:',num2str(psdxrt)]);
grid on
title('Power Spectrum - Whole signal (raw)')
xlabel('Frequency (Hz)')
ylabel('Power (uV2)')
yp1 = ylim;
xp1 = xlim;

%Power spectrum of the whole filtered EMG signal
```

```
subplot(3,3,6);
plot(freq,psdx);        % plotting the spectrum
uicontrol('Style','text','FontSize', 8,...
          'Units','normalized','Position', [0.92 0.455 0.09 0.022],...
          'HorizontalAlignment','left','String',[' Total Power:',num2str(psdxt)]);
grid on
title('Power Spectrum - Whole signal (filtered)')
xlabel('Frequency (Hz)')
ylabel('Power (uV2)')
ylim(yp1);
xlim(xp1);

%Selection of QRS-QRS window and display of power spectrum for sEMG and
%filtered EMG signal
windn = length(CC1);
winddd = {'Whole Signal'};
for windnum = 1:windn
    wdn = num2str (windnum);
    windnumb = strcat('Window',wdn);
    winddd = [winddd;windnumb];
end
popupw = uicontrol('Style', 'popup','Units','normalized',...
        'String', winddd,...
        'Position',[0.913 0.253 0.08 0.06],...
        'Callback', @wvv);
    function wvv(Source,~)
        windowv = Source.Value;
        subplot(3,3,9)
        cla
        if windowv == 1
```

```
    plot(freq,psdxr);
    uicontrol('Style','text','FontSize', 8,...
    'Units','normalized','Position', [0.92 0.155 0.09 0.022],...
    'HorizontalAlignment','left','String',[' Total Power:',num2str(psdxrt)]);
    title('Power Spectrum - Whole signal (raw)')
else
   CCx2 = cell2mat(CC2((windowv-1),:));
   CCfx2 = cell2mat(CCf2((windowv-1),:));
   CCx2t = sum(CCx2);
   plot(CCfx2,CCx2);
    uicontrol('Style','text','FontSize', 8,...
    'Units','normalized','Position', [0.92 0.155 0.09 0.022],...
    'HorizontalAlignment','left','String',[' Total Power:',num2str(CCx2t)]);
   title(['Power Spectrum - window ',num2str(windowv-1),' (raw)'])
end
grid on
xlabel('Frequency (Hz)')
ylabel('Power (uV2)')
yp1 = ylim;
xp1 = xlim;

subplot(3,3,6)
cla
if windowv == 1
    plot(freq,psdx);
    uicontrol('Style','text','FontSize', 8,...
    'Units','normalized','Position', [0.92 0.455 0.09 0.022],...
    'HorizontalAlignment','left','String',[' Total Power:',num2str(psdxt)]);
    title('FFT - Whole signal (filtered)')
else
```

```
        CCx1 = cell2mat(CC1((windowv-1),:));
        CCfx1 = cell2mat(CCf1((windowv-1),:));
        CCx1t = sum(CCx1);
        plot(CCfx1,CCx1);
         uicontrol('Style','text','FontSize', 8,...
         'Units','normalized','Position', [0.92 0.455 0.09 0.022],...
         'HorizontalAlignment','left','String',[' Total Power:',num2str(CCx1t)]);
        title(['FFT - window ',num2str(windowv-1),' (filtered)'])
      end
      grid on
      xlabel('Frequency (Hz)')
      ylabel('Power (uV2)')
      ylim(yp1);
      xlim(xp1);

   end
hold off
end
```

```
%This program replots the signal based on selection
function replot(chb1,chb2,chb3,chb4,yaxis,...
        t,rawdata1,sigwavx,rw2,sigwavxa,waveletsel,wavelet)
subplot(3,3,[1 2])
        cla;
        hold on
        leg = strings;
        if chb1 == 1
          plot(t,rawdata1,'b');
          leg = [leg 'Raw Signal'];
        end
        if chb2 == 1
          plot(t,sigwavx,'r');
          leg = [leg 'Reconstructed Signal'];
        end
        if chb3 == 1
          plot(t,rw2,'g');
          leg = [leg 'ECG Signal'];
        end
        if chb4 == 1
          plot(t,sigwavxa,'m');
          leg = [leg 'Filtered Signal'];
        end
        leglen = length(leg);
        lege = leg(2:leglen);
        lgd = legend(lege,'Orientation','Horizontal');
        lgd.FontSize = 8;
        ylim(yaxis);
        xlim([min(t) max(t)]);
        grid on
```

```
        title({['EMG Signal: ',waveletsel];['(',wavelet,')']})
        xlabel('Time (s)')
        ylabel('Signal (uV)')
        hold off
end
```

```
%This program selects the file and checks if the selection is valid
function [filename,sheets] = excelfile()
filechk = 0;
while filechk == 0
  [file,path] = uigetfile({'*.xlsx;*.xls','Excel Files (*.xlsx,*.xls)'},'Select Data File');
  filename = fullfile(path, file);
  [status,sheets] = xlsfinfo(filename);
if file == 0
  filename = false;
  return;
elseif isequal(status,'Microsoft Excel Spreadsheet')
  filechk = 1;
else
  filechk = 0;
end
end
end
```

```
%This program creates a list of excel sheets for selection
function [sheetx] = selsheet(sheets)
[indx,tf] = listdlg('PromptString','Select a sheet:',...
                    'SelectionMode','single',...
                    'ListString',sheets);
if tf == 1
   sheetx = sheets(indx);
else
   sheetx = [];
end
end
```

```
%This program selects the sample for the sEMG and ECG signals and compares for equal selection
function sampl = sample(filename,sheetx)
sheetxx = char(sheetx);
smp = 0;
while smp == 0
   prompt = {'EMG Starting Cell:','EMG Ending Cell:','ECG Starting Cell:','ECG Ending Cell:'};
   dlg_title = 'Data Input';
   num_lines = 1;
   input = inputdlg(prompt,dlg_title,num_lines);
   inpp = isempty(input);
   if inpp == 1
      sampl = 0;
      smp = 1;
   else
```

```
c1 = char(input(1));
c2 = char(input(2));
c3 = char(input(3));
c4 = char(input(4));
try
   st1 = strcat(c1,':',c2);
catch
   st1 = [];
end
try
   st2 = strcat(c3,':',c4);
catch
   st2 = [];
end
try
   sam1 = xlsread(filename,sheetxx,st1);
catch
   sam1 = [];
end
try
   sam2 = xlsread(filename,sheetxx,st2);
catch
   sam2 = [];
end
samp = isempty(sam1) || isscalar(sam1) || ~isfloat(sam1) ||...
      isempty(sam2) || isscalar(sam2) || ~isfloat(sam2);
if samp == 1
   waitfor(msgbox('Please enter a valid data range','Error','modal'));
   smp = 0;
elseif length(sam1) ~= length(sam2)
```

```
        waitfor(msgbox({'Both signal ranges are not equal';...
            'Please make sure the sample sizes of both signals are equal.'}...
            ,'Error','modal'));
        smp = 0;
    else
        [~,sch1] = size(sam1);
        [~,sch2] = size(sam2);
        if sch1>1 || sch2>1
            waitfor(msgbox('Please enter a valid data range','Error','modal'));
            smp = 0;
        else
            sampl(:,1) = sam1;
            sampl(:,2) = sam2;
            smp = 1;
        end
    end
    end
end
end
```